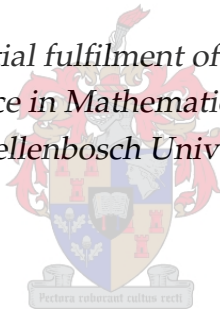


# Calibration and Model Risk in the Pricing of Exotic Options Under Pure-Jump Lévy Dynamics

by

Gael Mboussa Anga

*Thesis presented in partial fulfilment of the requirements for the degree of Master of Science in Mathematics in the Faculty of Science at Stellenbosch University*



Department of Mathematical Sciences,  
University of Stellenbosch,  
Private Bag X1, Matieland 7602, South Africa.

Supervisor: Dr. Peter Ouwehand

December 2015

# Declaration

By submitting this thesis electronically, I declare that the entirety of the work contained therein is my own, original work, that I am the sole author thereof (save to the extent explicitly otherwise stated), that reproduction and publication thereof by Stellenbosch University will not infringe any third party rights and that I have not previously in its entirety or in part submitted it for obtaining any qualification.

December 2015

Copyright © 2015 Stellenbosch University  
All rights reserved.

# Abstract

## Calibration and Model Risk in the Pricing of Exotic Options Under Pure-Jump Lévy Dynamics

Gael Mboussa Anga

*Department of Mathematical Sciences,  
University of Stellenbosch,  
Private Bag X1, Matieland 7602, South Africa.*

Thesis: MSc. (Mathematical Finance)

December 2015

The growing interest in calibration and model risk is a fairly recent development in financial mathematics. This thesis focussing on these issues, particularly in relation to the pricing of vanilla and exotic options, and compare the performance of various Lévy models. A new method to measure model risk is also proposed (Chapter 6). We calibrate only several Lévy models to the log-return of S&P500 index data. Statistical tests and graphs representations both show that pure jump models (VG, NIG and CGMY) the distribution of the proceeds better described as the Black-Scholes model. Then we calibrate these four models to the S&P500 index option data and also to "CGMY-world" data (a simulated world described by the CGMY model) using the root mean square error. Which CGMY model outperform VG, NIG and Black-Scholes models. We observe also a slight difference between the new parameters of CGMY model and its varying parameters, despite the fact that CGMY model is calibrated to the "CGMY-world" data. Barriers and lookback options are then priced, making use of the calibrated parameters for our models. These prices are then compared with the "real" prices (calculated with the true parameters of the "CGMY world), and a significant difference between the model prices and the "real" rates are observed. We end with an attempt to quantization this model risk.

**Key words:** Calibration, Model risk, Exotic options, Black-Scholes model, Normal Inverse Gaussian processes, Variance Gamma processes and CGMY processes.

# Abstract

## Calibration and Model Risk in the Pricing of Exotic Options Under Pure-Jump Lévy Dynamics

Gael Mboussa Anga

*Department of Mathematical Sciences,*

*University of Stellenbosch,*

*Private Bag X1, Matieland 7602, South Africa.*

Thesis: MSc. (Mathematical Finance)

December 2015

Die groeiende belangstelling in kalibrering en modelrisiko is 'n redelik resente ontwikkeling in finansiële wiskunde. Hierdie proefskrif fokusseer op hierdie sake, veral in verband met die prysbepaling van vanielje-en eksotiese opsies, en vergelyk die prestasie van verskeie Lévy modelle. 'n Nuwe metode om modelrisiko te meet word ook voorgestel (hoofstuk 6). Ons kalibreer eers verskeie Lévy modelle aan die log-opbrengs van die S&P500 indeks. Statistiese toetse en grafieke voorstellings toon albei aan dat suiwer sprongmodelle (VG, NIG en CGMY) die verdeling van die opbrengs beter beskryf as die Black-Scholes model. Daarna kalibreer ons hierdie vier modelle aan S&P500 indeks opsie data en ook aan "CGMY-wêreld" data ('n gesimuleerde wêreld wat beskryf word deur die CGMY-model) met behulp van die wortel van gemiddelde kwadraat fout. Die CGMY model vaar beter as die VG, NIG en Black-Scholes modelle. Ons waarneem ook 'n effense verskil tussen die nuwe parameters van CGMY model en sy wisselende parameters, ten spyte van die feit dat CGMY model gekalibreer is aan die "CGMY-wêreld" data. Versperrings-en terugblik opsies word daarna geprys, deur gebruik te maak van die gekalibreerde parameters vir ons modelle. Hierdie pryse word dan vergelyk met die "ware" pryse (bereken met die ware parameters van die "CGMY-wêreld"), en 'n beduidende verskil tussen die modelpryse en die "ware" pryse word waargeneem. Ons eindig met 'n poging om hierdie modelrisiko te kwantiseer

# Acknowledgements

I am grateful to Stellenbosch University (especially the department of mathematical sciences) and African Institute for Mathematical Sciences for providing all the resources that allowed me to complete this study. I would also like to thank my supervisor, Dr. Peter Ouwehand for his enormous contribution to helping me finish this thesis. I am grateful to my family, especially my parents and friends for supporting and motivating me during my research. Last but not least, I would like also thank my God for giving me the strength and keeping me safe while I completed this thesis.

# Dedications

*To my family*

# Contents

<b>Declaration</b>	<b>i</b>
<b>Abstract</b>	<b>ii</b>
<b>Abstract</b>	<b>iii</b>
<b>List of Figures</b>	<b>ix</b>
<b>List of Tables</b>	<b>xiv</b>
<b>1 Introduction</b>	<b>1</b>
1.1 Thesis Structure . . . . .	4
<b>2 Presentation of Lévy Processes</b>	<b>5</b>
2.1 Preliminaries . . . . .	5
2.2 Presentation of Brownian Motion (BM) . . . . .	7
2.2.1 Multivariate Normal Distribution . . . . .	8
2.3 Introduction to Lévy processes . . . . .	9
2.4 Compound Poisson Processes . . . . .	11
2.5 Jump Measure of the Compound Poisson Processes and Lévy result . . . . .	12
2.5.1 Poisson Random Measure . . . . .	13
2.6 Subordinators Representation . . . . .	19
2.7 Construction of a Lévy processes via Brownian subordination . . . . .	21
2.7.1 Subordinating Brownian motion . . . . .	21
<b>3 Pure Jump Lévy Model for Asset Dynamics</b>	<b>23</b>
3.1 Normal Inverse Gaussian Processes (NIG) . . . . .	24
3.2 Variance Gamma processes (VG) . . . . .	26
3.2.1 Gamma Process ( $G(t)$ ) . . . . .	26

3.2.2	VG processes . . . . .	27
3.3	CGMY process . . . . .	29
3.3.1	Properties and characteristic function of CGMY . . . . .	30
3.4	Lévy Market Model . . . . .	36
3.4.1	Equivalent Martingale Measure . . . . .	38
3.5	Density Estimating of S&P 500 time series data . . . . .	38
3.5.1	Autocorrelation function (ACF) . . . . .	39
3.5.2	Model Density Estimation . . . . .	39
3.5.3	Test of the Fitness for the Distribution of the Models . . . . .	41
<b>4</b>	<b>Calibration of Pure Jump Model</b> . . . . .	<b>45</b>
4.1	The Calibration Problem for a Pure Jump Model . . . . .	45
4.2	Calibration Methods . . . . .	47
4.2.1	Method of Maximum Likelihood Estimation (MLE) . . . . .	47
4.2.2	Method of Least Squares Estimation (LSE) . . . . .	48
4.3	Pricing via an Equivalent Martingale Measure . . . . .	49
4.4	Pricing via Fourier Transform . . . . .	50
<b>5</b>	<b>Calibration of Model to Market data</b> . . . . .	<b>54</b>
5.1	Estimation Parameters for the Pure Jump models . . . . .	55
5.1.1	Results of Estimation Parameters for the Lévy models . . . . .	56
5.2	Varying the model parameters for the CGMY model . . . . .	58
5.2.1	Calibration for the CGMY, NIG, VG and Black-Scholes models to the "CGMY-world" data . . . . .	62
5.3	Pricing Call Options . . . . .	66
5.3.1	Models Implied Volatility Surfaces . . . . .	70
<b>6</b>	<b>Pricing Exotic Options and Model Risk</b> . . . . .	<b>75</b>
6.1	Pricing Exotic options . . . . .	75
6.1.1	Pricing Barrier Option . . . . .	76
6.1.2	Pricing the Lookback Fixed Option . . . . .	77
6.1.3	Monte Carlo Method . . . . .	78
6.2	Results and Discussion . . . . .	79
6.3	Model risk . . . . .	81
6.4	Quantifying Model Risk . . . . .	92
6.4.1	Quantifying Model Uncertainty Measure (Cont [26]) . . . . .	92
6.4.2	A Coherent Measure of Model Uncertainty (Rama Cont [26]) . . . . .	94



Contents	viii
6.5 The Results of Model Risk Ratio . . . . .	96
<b>7 Conclusion and Future work</b>	<b>100</b>
<b>A The graphics of hedging performance</b>	<b>i</b>
A.1 Table of S&P 500 indexed . . . . .	i
A.2 The Algorithms for Simulating the Path of the Pure Jump Model . . . . .	i
A.2.1 The Algorithm for Simulating the Path of the VG processes . . . . .	i
A.2.2 The Algorithm for Simulating the Path of NIG processes . . . . .	iv
A.2.3 The Algorithm for Simulating the Path of the CGMY processes . . . . .	iv
A.2.4 Describing the algorithm of CGMY subordinator . . . . .	vii
A.3 Trajectories of pure jump Lévy model via Monte Carlo Method . . . . .	xiii
A.4 Compute the Call Price using the Fast Fourier Transform . . . . .	xiii
<b>Appendix</b>	<b>i</b>
<b>List of references</b>	<b>xvii</b>

# List of Figures

2.1	A sample path of a Poisson process with parameter $\lambda = 0.25$ . . . . .	7
2.2	A sample path of geometric Brownian motion with parameters $\sigma = 0.3, \mu = 0.5$	9
2.3	A sample path of the compound Poisson process with a Gaussian distribution of jumps sizes . . . . .	11
3.1	In the top left is the trajectory of the Normal Inverse Gaussian process with the parameters $\alpha = 45, \beta = -9$ and $\delta = 1$ , the number of simulation $N = 1000$ and the time $T = 1$ . This trajectory is simulated using the algorithm A.2.2. In the top right is the trajectory of Inverse Gaussian process with parameters $b = 3, a = 7$ and the number of simulation $N = 1000$ and $T = 1$ . . .	25
3.2	Ordinary trajectories of Gamma process with parameters $b = 12, a = 27, 20$ and the number of simulation $N = 1000$ and $T = 1$ . . . . .	27
3.3	The ordinary trajectories of the Variance Gamma process with the parameters $\nu = 0.25, 0.05, \sigma = 0.15$ and $\theta = 0.005$ , the number of simulation $N = 1000$ and the time $T = 1$ . This trajectory is simulated using the algorithm A.2.1. .	30
3.4	The ordinary Variance Gamma density with the parameters $C = 3, G = 3$ and $M = 3$ and $C = 5, G = 2$ and $M = 3$ . . . . .	30
3.5	The trajectories of the CGMY process with the parameters $C = 0.0332, G = 0.4614, M = 15.6995, Y = 1.1882$ and $C = 0.0332, G = 0.4614, M = 15.6995, Y = 0.2882$ . These trajectories are simulated using the algorithm A.2.3. . . . .	31
3.6	The trajectories of the CGMY process with the parameters $C = 0.0332, G = 0.4614, M = 15.6995, Y = 1.2882, 1.5882$ and $T = 1$ . This trajectory is simulated using the algorithm A.2.3. . . . .	35
3.7	Autocorrelation for the daily log-return . . . . .	40
3.8	Autocorrelation for square of the daily log-return . . . . .	40
3.9	QQ-plot fitted Normal distribution and NIG distribution to daily log-return .	42
3.10	QQ-plot fitted VG distribution and CGMY distribution to daily log-return . .	42

5.1	The Lévy measure of the CGMY model. The figures summarise the effect of varying the model parameters $C = 0.0332$ and $Y = 1.2882$ on the Lévy measure. Top left, we consider the varying of $(C + \Delta, C - \Delta)$ with $\Delta = 20\%C$ and in the top right $(Y + \Delta, Y - \Delta)$ with the value of $\Delta = 20\%Y$ . . . . .	58
5.2	The Lévy measure of the CGMY model. The figures summarise the effect of varying model parameter $G = 0.4614$ and $M = 15.6995$ on the Lévy measure. In the top left, we consider the varying of $(G + \Delta, G - \Delta)$ with $\Delta = 20\%G$ and in the top right $(M + \Delta, M - \Delta)$ with $\Delta = 20\%M$ . . . . .	59
5.3	The Lévy measure of the CGMY model. Here we summarize the effect of varying the model parameters of $G$ and $M$ on the Lévy measure. In the top left we consider the varying of $(G + \Delta, G - \Delta)$ with the $\Delta = 40\%G$ and in the top right $(M + \Delta, M - \Delta)$ with the $\Delta = 40\%M$ . . . . .	60
5.4	The Lévy measure of the CGMY model. Here we summarize the effect on the Lévy measure of varying the model parameters of $G$ and $M$ . In the top left we consider the vary of $(G + \Delta, G - \Delta)$ with the $\Delta = 60\%G$ and in the top right $(M + \Delta, M - \Delta)$ with the $\Delta = 60\%M$ . . . . .	61
5.5	The Lévy measure of the CGMY model. Here we summarize the effect on the Lévy measure of varying the model parameters of $G$ and $M$ . In the top left we consider the vary of $(G + \Delta, G - \Delta)$ with the $\Delta = 80\%G$ and in the top right $(M + \Delta, M - \Delta)$ with the $\Delta = 80\%M$ . . . . .	61
5.6	Calibration for multiple parameters of Black-Scholes and NIG models to S&P 500 index call options . . . . .	67
5.7	Calibration for multiple parameters of VG and CGMY models to S&P 500 index call options . . . . .	67
5.8	Calibration of single parameter of NIG and BS models to S&P 500 index call options . . . . .	68
5.9	Calibration of single parameters of VG and CGMY models to S&P 500 index call options . . . . .	68
5.10	Comparing the vanilla call prices computed via Fast Fourier transform (FFT) for NIG, VG and CGMY models using their single parameters between those from the S&P 500 index call options for a single maturity from December 2002 (i.e $T = 0.67123$ ) . . . . .	70
5.11	Comparing the vanilla call prices NIG, VG and BS models against the true vanilla call prices computed via the CGMY model with the new parameters $(C, G, M, Y)$ and $(C^-, G, M, Y)$ . We consider the single maturity from December 2002 (i.e $T = 0.67123$ ) . . . . .	70

5.12	Comparing the vanilla call prices obtained with NIG, VG and BS models against the true vanilla call prices computed via the CGMY model with the new model parameters $(C^-, G, M, Y)$ and $(C^+, G, M, Y)$ . We consider the single maturity from December 2002 (i.e $T = 0.67123$ ) . . . . .	71
5.13	Comparison between the values of the vanilla calls computed via FFT for CGMY, VG, NIG and BS models using their multiple and single parameters. In pricing these vanilla calls we consider the single maturity from December 2002 (i.e $T = 0.67123$ ) . . . . .	72
5.14	Comparison between the call prices for all model prices obtained with the model parameters for CGMY model $(C^-, G, M, Y^-)$ and $(C^-, G, M, Y^+)$ . We consider the single maturity from December 2002 (i.e $T = 0.67123$ ) . . . . .	72
5.15	Comparing the vanilla call prices obtained with NIG, VG and BS models against the true vanilla call prices computed via the CGMY model with the new model parameters $(C^+, G, M, Y^-)$ and $(C^+, G, M, Y^+)$ . We consider the single maturity from December 2002 (i.e $T = 0.67123$ ) . . . . .	73
5.16	Comparing the vanilla call prices obtained with NIG, VG and BS models against the true vanilla call prices computed via the CGMY model with the new model parameters $(C, G, M, Y^-)$ and $(C, G, M, Y^+)$ . We consider the single maturity from December 2002 (i.e $T = 0.67123$ ) . . . . .	73
5.17	Implied Volatility Surface for NIG model and S& P500 indexed options . . . . .	74
5.18	Implied Volatility Surface for VG model and CGMY model . . . . .	74
6.1	The vanilla call prices computed with CGMY, NIG and VG models using the Monte Carlo method with the strike price $K = 1130$ , maturity $T = 0.67123$ and the stock price $S_0 = 1124.47$ . . . . .	79
6.2	The figures of up-and-in and up-and-out calls for NIG, VG, CGMY and Black-Scholes models, with the strike price $K = 1130$ , maturity $T = 0.67123$ and the stock price $S_0 = 1124.47$ . The barrier level is range from $(0.5S_0$ to $1.5S_0)$ . . . . .	81
6.3	We computed the prices of the up-and-in and up-and-out options for the NIG, VG, CGMY and BS models obtained with the model parameters calibrated from the vanilla call computed with the model parameters $(C^+, G, M, Y^-)$ , $(C, G, M, Y^-)$ and $(C^+, G, M, Y^+)$ . The barrier level ranges from $1(S_0)$ to $1.5(S_0)$ , the strike price is $K = 110$ , the spot price is equal $S_0 = 100$ , the risk-interest rate $r = 19\%$ , dividend yield at $q = 12\%$ and maturity $T = 1$ . . . . .	83

- 6.4 We computed the prices of the up-and-in and up-and-out options for NIG, VG, CGMY and BS models obtained with the model parameters calibrated from the vanilla call computed with the model parameters  $(C, G, M, Y^+)$  and  $(C^+, G, M, Y)$ . The barrier level ranges from  $1S_0$  to  $1.5S_0$ , the strike price is  $K = 110$ , the spot price is equal  $S_0 = 100$ , the riskless  $r = 19\%$ , dividend yield  $q = 12\%$  and maturity  $T = 1$  . . . . . 84
- 6.5 We computed the prices of the up-and-in and up-and-out options for the NIG, VG, CGMY and BS models obtained with the model parameters calibrated from the vanilla call computed with the model parameters  $(C^-, G, M, Y^-)$ . The barrier level ranges from  $1S_0$  to  $1.5S_0$ , the strike price is  $K = 110$ , the spot price is equal  $S_0 = 100$ , the risk-interest rate  $r = 19\%$ , dividend yield  $q = 12\%$  and maturity  $T = 1$  . . . . . 84
- 6.6 We computed the prices of the up-and-in and up-and-out options for the NIG, VG, CGMY and BS models obtained with the model parameters calibrated from the vanilla call computed with the model parameters  $(C^-, G, M, Y^+)$  and  $(C^-, G, M, Y)$ . The barrier level ranges from  $1S_0$  to  $1.5S_0$ , the strike price is  $K = 110$ , the spot price is equal  $S_0 = 100$ , the risk-interest rate  $r = 19\%$ , dividend  $q = 12\%$  and maturity  $T = 1$  . . . . . 85
- 6.7 We computed the prices of the up-and-in and up-and-out options for the NIG, VG, CGMY and BS models obtained with the model parameters calibrated from vanilla calls computed with the model parameters  $(C, G, M, Y)$ . The barrier level ranges from  $1S_0$  to  $1.5S_0$ , the strike price is  $K = 110$ , the spot price is equal  $S_0 = 100$ , the riskless  $r = 19\%$ , dividend yield  $q = 12\%$  and maturity  $T = 1$  . . . . . 85
- 6.8 We computed the prices of the Up-In and Up-Out for NIG, VG, CGMY and BS models obtain with the model parameters calibrated from the vanilla call computed with the model parameters  $(C, G, M, Y^+)$  and  $(C, G, M, Y^-)$ . The barrier level is ranging from  $1S_0$  to  $1.5S_0$ , the strike price is  $K = 95$ , the spot price is equal  $S_0 = 100$ , the risk-interest rate  $r = 19\%$ , dividend yield  $q = 12\%$  and maturity  $T = 1$  . . . . . 88
- 6.9 We computed the prices of the up-and-in and up-and-out calls for NIG, VG, CGMY and BS models obtained with the model parameters calibrated from the vanilla call computed with the model parameters  $(C^-, G, M, Y^+)$  and  $(C^-, G, M, Y^-)$ . The barrier level ranges from  $1S_0$  to  $1.5S_0$ , the strike price is  $K = 95$ , the spot price is equal  $S_0 = 100$ , the risk-interest rate  $r = 19\%$ , dividend  $q = 12\%$  and maturity  $T = 1$  . . . . . 88

6.10	We computed the prices of the up-and-in and up-and-out calls for NIG, VG, CGMY and BS models obtained with the model parameters calibrated from the vanilla call computed with the model parameters $(C^+, G, M, Y^+)$ and $(C^+, G, M, Y^-)$ , $(C^+, G, M, Y)$ and $(C^-, G, M, Y)$ . The barrier level is ranging from 150 to 1.550, the strike price is $K = 95$ , the spot price is equal $S_0 = 100$ , the risk-interest rate $r = 19\%$ , dividend $q = 12\%$ and maturity $T = 1$ . . . . .	90
6.11	We computed the prices of the up-and-in and up-and-out calls for NIG, VG, CGMY and BS models obtained with the model parameters calibrated from the vanilla call computed with the model parameters $(C, G, M, Y)$ . The barrier level ranges from 150 to 1.550, the strike price is $K = 95$ , the spot price is equal $S_0 = 100$ , the risk-interest rate $r = 19\%$ , dividend $q = 12\%$ and maturity $T = 1$ . . . . .	91
A.1	The Path of VG process with $\nu = 0.0100, \sigma = 0.24, \theta = 0.542$ , the Number of simulation $N = 1000$ , the time $T = 1$ . . . . .	iii
A.2	The Path of NIG process with $\alpha = 12, \beta = 11, \delta = 0.8$ , the Number of simulation $N = 1000$ and the time $T = 1$ . . . . .	v
A.3	The Path of CGMY process with $Y = 1.5$ the Number of simulation $N = 1000$ , the time $T = 1$ . . . . .	xiv
A.4	Trajectories of the CGMY and NIG models . . . . .	xv
A.5	Trajectories of the VG model . . . . .	xv

# List of Tables

3.1	Table of moments of NIG process . . . . .	25
3.2	Table of properties of Gamma(a,b) distribution . . . . .	26
3.3	Table of moments of the VG process . . . . .	29
3.4	Table of moments of the CGMY process . . . . .	34
3.5	Mean-correcting martingale measure for some Lévy models . . . . .	38
3.6	Table of K-S and A-D Statistic value . . . . .	44
5.1	Table of Calibrated Risk-Neutral parameters from S& P 500 indexed options	57
5.2	Here we present the results of 9 sets of the varying parameters of CGMY model obtained by increasing and decreasing the multiple parameters which is given under this form $(C \pm \Delta, G, M, Y \pm \Delta)$ with $(\Delta = 20\%C, 20\%Y)$ . . . .	60
5.3	Results of the new parameters for the CGMY, NIG, VG and Black-Scholes models obtained by fitting these models to the different sets of "CGMY-world" data. . . . .	63
5.4	Results of the new parameters for the CGMY, NIG, VG and Black-Scholes models obtained by fitting these models to the different sets of "CGMY-world" data. . . . .	64
5.5	Results of the new parameters for the CGMY, NIG, VG and Black-Scholes models obtained by fitting these models to the different sets of "CGMY-world" data. . . . .	65
5.6	The values of the vanilla call prices computed via FFT technique for all models using their single parameters, and with one maturity from December 2002 (i.e $T = 0.67123$ ) taken from the S&P 500 index call options . . . . .	69
6.1	Results of the barrier and lookback fixed options for each model price. The barrier level ranges from $(0.5s_0 to 1.5S_0)$ and the strike price $K = 1130$ , maturity $T = 0.67123$ and the stock price $S_0 = 1124.47$ . . . . .	80

6.2	The price values of the lookback options computed with all different model parameters. Strike price $K = 110$ , spot price $S_0 = 100$ , interest rate $r = 19\%$ , dividend yield $q = 12\%$ and $T = 1$ . . . . .	87
6.3	Percentage relative error between the "true" prices of the lookback fixed and the prices obtained with CGMY, NIG, VG and BS models. The strike price $K = 110$ , spot price $S_0 = 100$ , interest rate $r = 19\%$ and dividend $q = 12\%$ and maturity of one year $T = 1$ . . . . .	89
6.4	The price values of the lookback options computed with all different model parameters. Strike price $K = 95$ , spot price $S_0 = 100$ , interest rate $r = 19\%$ , dividend yield $q = 12\%$ and $T = 1$ . . . . .	91
6.5	Percentage relative error between the "true" prices of the lookback fixed and the prices obtained with CGMY, NIG, VG and BS models. The strike price $K = 110$ , spot price $S_0 = 100$ , interest rate $r = 19\%$ and dividend $q = 12\%$ and maturity of one year $T = 1$ . . . . .	92
6.6	The result of model risk for exotic option with model price computed for all set of model estimated from 9 different call vanilla from CGMY model . . . . .	97
6.7	The result model risk for exotic option with model price computed for all set of model estimated from 9 different call vanilla from CGMY model . . . . .	98
6.8	The results of model risk ratio $\mu_{\mathbb{Q}}$ for the lookback call computed with the NIG, VG, CGMY and BS models using their new parameters calibrated to different sets of the "real world" data obtained with the set of the varying parameters of CGMY model. Strike price $K = 95$ , spot price $S_0 = 100$ , interest rate $r = 19\%$ , dividend $q = 12\%$ and $T = 1$ . . . . .	99
6.9	The results of model risk ratio $\mu_{\mathbb{Q}}$ for the lookback calls obtained with the NIG, VG, CGMY and BS models using their new parameters calibrated to different sets of the "real world" data obtained with the set of the varying parameters of CGMY model. Strike price $K = 110$ , spot price $S_0 = 100$ , interest rate $r = 19\%$ , dividend $q = 12\%$ and $T = 1$ . . . . .	99
A.1	Table of 77 call prices of S&P 500 indexed. . . . .	ii



# Chapter 1

## Introduction

Model risk has been well researched in recent years (see Emanuel Derman and Paul Wilmott [32], Joerg Kienitz and Daniel Wetterau [49]). The classical formula for options pricing derived by Merton-Black-Scholes is regarded as an important finding in Mathematical Finance. In order to determine the method to price and hedge vanilla call/put option, Merton-Black-Scholes considered a set of assumptions about the behaviour of the underlying asset price, specifically that the underlying asset price must follow a geometric Brownian motion. However, using this formula in financial markets to hedge or price real financial instruments, leaves one vulnerable to model risk.

Model risk arises in financial markets and in risk management when an inaccurate, or inappropriate model is used to price or hedge real financial instruments. Incorrect calibration or the use of unstable numerical method can also cause model risk. In fact, the prices of any financial markets derived from a particular model is consequently mispriced. Furthermore, any financial condition (or financial position) based on that particular financial model will also be mispriced (.e.i no matter what type of financial market we model or financial model we model use, model risk will cause)

The model risk can also get uncertainty form. In our case, we have considered four Lévy models ( VG, BS, NIG and CGMY ), in order to price the exotic options, where we have the probability of uncertainty modelling. In the case where the Lévy model is identified by a parameter  $\theta$  from some parameter space  $\Theta$ , hence that parameter is considered as uncertainty parameter. By considering an additional probability measure  $P$  on the set of possible model related prices, which quantifies all possibilities that one model is the best choice, therefore we are already in a setting of model risk, which is also known as a special case of model uncertainty [Karl F Bannör and Matthias Scherer. [11], chap:10, pg:287]. Thus, Frank H Knight [50] states, that there is a relationship between

uncertainty and model risk: *"Uncertainty can be considered in a sense radically distinct from the familiar notion of risk, from which it has been never properly separated ... The essential fact is that a "risk" can be taken in some cases as a quantity susceptible of measurement, while at other times it is something distinctly not of this character..."*.

When considering use of a particular financial model it may also be necessary to consider a particular risk measure to obtain the probability of an adverse result. However, in the face of Knightian uncertainty (i.e. an immeasurable risk) our confidence in the true value of model parameters, or, indeed, in the model itself is limited. Model choice is also affected by whether such model is capable of allowing for the actual dynamics of financial markets. There are several reasons why models may not cope with the reality of financial markets. Here, we describe two of them:

### 1 The model price can be inappropriately applied for a certain purpose.

The Black-Scholes model assumes that underlying asset prices follow the Geometric Brownian motion, while in reality the paths of stock prices are discontinuous. The Black-Scholes model also assumes that volatility is a constant, while the time series of the standard deviation of the log returns reveals that stock prices may vary in their volatility at different points during the lifetime of an option, and there is also an autoregressive feature to consider (volatility clustering). The Black-Scholes model cannot capture the different levels of implied surface volatility for market-related variability in maturities and strikes (see Chapter 5). Therefore, we need to use a model with a rich structure such as a pure jump Lévy model, a stochastic volatility model or a local volatility model to allow for surface volatility.

Likewise, not all models allow for interactions between variable. For example, it may not be possible to calibrate a Black-Scholes model to deal with surface volatility and a local volatility model may be needed to correct for this effect. A local volatility model's ability to calibrate for the effect of surface volatility, enables it to reproduce the prices of European options for a given maturity in the manner of self-consistent arbitrage. Moreover, Patrick, Deep, Andrew and Diana [43] stated that: The dynamic behaviour of smiles and skews described by the local volatility model is just the opposite to the behaviour observed in financial market: when the price of underlying asset decreases, local volatility model predict that the smile shifts to higher prices, while the skew shifts to the lower prices when the price of underlying assets increases.

This result implies that a local volatility model may be a worse hedge for the vanilla option than the Black-Scholes model is, despite the fact that such model

calibrates the market data better than the Black-Scholes model. Thus, we can say that not all models are fit for the same purpose. As Joerg Kienitz and Daniel Wetterau [49] stated: "The jump diffusion models (or stochastic volatility models) can capture features of stock price movement which are important for the pricing of exotic options, but they cannot translate them into actionable hedging strategies because markets, by nature are incomplete."

## 2 The calibration issue may also be a cause of the model risk

Precise modelling of the dynamics of the underlying asset prices in financial markets, requires models to have the necessary number of parameters. However, a risk exists that when trying to fit the model to observed market data, it fits it to random noise instead, which does not reflect the actual underlying process

Examples of calibration problem that can also cause model risk are highlighted by Joerg Kienitz and Daniel Wetterau [49]. Joerg Kienitz and Daniel Wetterau [49] discussed the dangers of unstable parameters when a model is calibrated to daily data.

Finally, model risk and Knightian uncertainty may not be limited to hedging and pricing in financial markets. Rama Cont [26] introduced methods to measure model uncertainty in the context of derivative pricing. As model selection or calibration issues may introduce model risk, we may need to consider both a range of different alternative Lévy models (VG, NIG, CGMY and Black-Scholes models) and a range of different parameters calibrated with "CGMY-world" data (market prices computed with the varying parameters of CGMY model as described in Chapter 5). In this study, our aim is to investigate the risk involved in pricing exotic options. The key findings of this research are that: We provide a new formula to measure the model risk in the context of derivative pricing. In order to do this, we modified the model risk formula introduced by Rama Cont [26] by normalizing his formula.

We estimated the risk-neutral parameters for our models from the S&P500 index based on the numerical method RMSE (chapter 4). We observed that calibration errors differ for all models. Furthermore, the prices of the exotic options obtained using different model classes differ significantly (Joerg Kienitz and Daniel Wetterau [49]). We also varied the multiple parameters for the CGMY model and used these risk-neutral parameters to price the vanilla call (see chapter 4). We considered such vanilla calls as our "CGMY-world" data and used this data to estimate new parameters for the CGMY, NIG, VG, and Black-Scholes models. We compared the prices of the barrier and lookback op-

tions computed with all models using their new parameters. Finally, we quantified the model risks of the barrier and lookback options.

## **1.1 Thesis Structure**

The research is structured as follows: In chapter 2 we discuss the fundamental components of Lévy processes. We also discuss some important theorems concerning the Lévy processes and time-changed Brownian motion properties in a no arbitrage market. Chapter 3 focuses on the pure jump Lévy model, namely the VG, NIG, and CGMY models in particular. In chapter 4 we discuss the Fast Fourier method and show how the European call formula for the VG, NIG and CGMY models are derived using this method. We also fit the probability density of our model to the S&P500 time series data using the graphical and statistical tests. Chapter 5 is focused on calibration problems. We estimate the parameters for our model from S&P500 index data using RMSE. We also calibrated CGMY, NIG, VG and Black-Scholes models to the "CGMY-world" data to estimate the new parameters. Finally, in the chapters 6 and 7 we discuss the results and draw conclusions.

## Chapter 2

# Presentation of Lévy Processes

In this chapter we review the basics of Lévy processes. We start by defining *stochastic, càdlàg and adapted processes*. We then discuss certain concepts and results that may help the reader to understand the theory behind this chapter. We discuss Lévy processes in context of the relevant, published literature. We conclude the chapter by giving examples of Lévy processes.

### 2.1 Preliminaries

Here we discuss the concepts behind Lévy processes, including definitions and theorems taken from the books of (Rama Cont and Peter Tankov [29], and Wim Schoutens [72]).

**Definition 2.1.1** (Stochastic processes). *Let  $(\Omega, \mathcal{F}, \mathbb{P}, (\mathcal{F}_t)_{0 \leq t \leq T})$  be a filtered probability space. A stochastic process  $(X_t)_{0 \leq t \leq T}$  on  $(\Omega, \mathcal{F}, \mathbb{P}, (\mathcal{F}_t)_{0 \leq t \leq T})$  is a family of random variables which is indexed by a time parameter  $t$ . The parameter  $t$  can be either discrete or continuous. A trajectory  $X(\omega) : t \rightarrow X_t(\omega)$  at any event  $\omega$  can be viewed as a sample path of the functions and processes, and  $(X_t)_{0 \leq t \leq T}$  can also be said to be a random function.*

**Definition 2.1.2** (càdlàg). *A function.  $g : [0, T] \rightarrow \mathbb{R}^d$  is a càdlàg if it is right-continuous with left limits, i.e. for each  $t \leq T$  the limits*

$$\lim_{r \rightarrow t, r < t} g(r) = g(t-) \quad \text{and} \quad \lim_{r \rightarrow t, r > t} g(r) = g(t+) \quad (2.1.1)$$

*exist and  $g(t) = g(+t)$ .*

**Definition 2.1.3** (Adapted process). Let  $(X_t)_{0 \leq t \leq T}$  be a stochastic process.  $X_t$  is said to be adapted process with respect to the information structure  $\mathcal{F}_t$ -adapted if, for any  $0 \leq t \leq T$ , the random variable  $X_t$  is  $\mathcal{F}_t$ -measurable.

**Definition 2.1.4** (Poisson process). Consider a sequence of independent exponentially distributed random variables  $(\tau_j)_{j \geq 1}$  with parameter  $\lambda$ , and define  $T_n = \sum_{j=1}^n \tau_j$ . The process  $(N_t)_{t \geq 0}$  defined by

$$N_t = \sum_{n \geq 1} \mathbf{1}_{t \geq T_n}. \quad (2.1.2)$$

is called a Poisson process with intensity  $\lambda$

If one regards  $\tau_j$  as a sequence of waiting times between events, then  $T_n$  is the time that the  $n^{\text{th}}$  event occurs. In that case,  $N_t$  is the number of events that have occurred by time  $t$ . Hence, we can say that a Poisson process is a counting process.

**Proposition 2.1.5.** Consider a Poisson process  $(N_t)_{t \geq 0}$ .

- 1 For any  $\omega \in \Omega$ , the sample path  $t \rightarrow N_t(\omega)$  is a piecewise constant and increasing by jumps of unit size.
- 2 For any  $t > 0$ ,  $N_t$  is almost surely finite.
- 3 The sample paths  $t \rightarrow N_t(\omega)$  are càdlàg.
- 4 For any  $t > 0$ ,  $N_{t-} = N_t$  with probability of 1.
- 5 The Poisson process  $(N_t)_{t > 0}$  is continuous in probability:

$$\forall t > 0, \quad N_s \xrightarrow{\mathbb{P}_{s \rightarrow t}} N_t. \quad (2.1.3)$$

- 6 For any  $t > 0$ , the Poisson process  $(N_t)$  is distributed in form of the Poisson distribution with parameter  $\lambda$

$$\forall n \in \mathbb{N}, \quad \mathbb{P}(N_t = n) = e^{-\lambda t} \frac{(\lambda t)^n}{n!}. \quad (2.1.4)$$

- 7 The characteristic function of the Poisson  $(N_t)$  with parameter  $\lambda$  is given as

$$E[e^{ixN_t}] = \exp\{\lambda t(e^{ix} - 1)\}, \forall x \in \mathbb{R}. \quad (2.1.5)$$

- 8 The Poisson process  $(N_t)$  has independent increments.

9 The increments of  $N$  are homogeneous: for any  $t > s$ , the process  $N_t - N_s$  and  $N_{t-s}$  follow the same distribution.

The proof of the above proposition can be found in the book of (Rama Cont and Peter Tankov [29]).

In explaining properties (2), (3) and (4), we can see that, with probability of 1, a sample path of the Poisson process can only move by jumps. We can also observe that at any given point  $t$ , the sample function is continuous with probability of 1. This is because the set  $D_t$  of sample point where  $N$  is discontinuous at time  $t$  has  $\mathbb{P}(D_t) = 0$ , for every  $t$ .

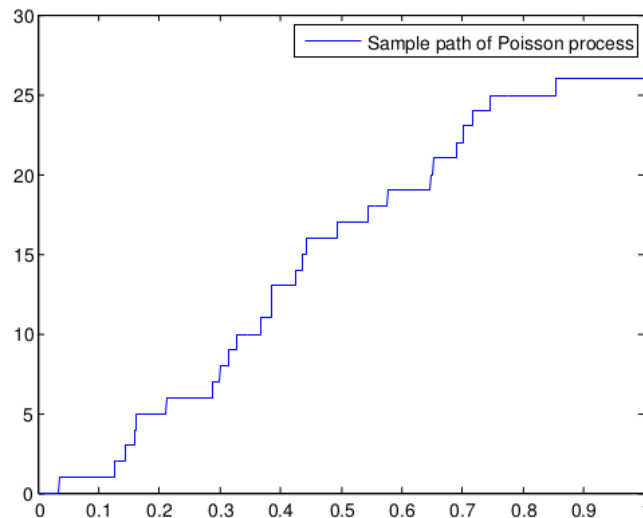


Figure 2.1: A sample path of a Poisson process with parameter  $\lambda = 0.25$

## 2.2 Presentation of Brownian Motion (BM)

The concept of Brownian motion originates from the work of *botanist Robert Brown* in 1828, and was first applied to finance in 1900 by the French mathematician *Louis Bachelier*. In 1905 *Albert Einstein* considered Brownian motion as a model of particles in suspension. Brownian motion is also known as the Wiener process, because its existence was first proved mathematically by *Norbert Wiener* in 1923.

Here, we start by reviewing the multivariate normal distribution before introducing the concept of Brownian motion.

### 2.2.1 Multivariate Normal Distribution

The multivariate normal distribution is a generalization of the one-dimensional (or univariate) normal distribution which the density function (p.d.f) is given by

$$f(y; \mu, \sigma^2) = \frac{1}{\sqrt{2\pi\sigma^2}} \exp\left(-\frac{(y-\mu)^2}{2\sigma^2}\right) \quad y \in \mathbb{R}, \quad -\infty < x < \infty,$$

with variance  $\sigma^2$  and mean  $\mu$ . In  $d$ -dimensions (high dimensions the density becomes [77]):

$$f(y; \mu, \Sigma) = \frac{1}{(2\pi)^{d/2} |\Sigma|^{1/2}} \exp\left(-\frac{(y-\mu)^T \Sigma^{-1} (y-\mu)}{2}\right) \quad y \in \mathbb{R}^d.$$

The mean vector  $\mu$  possesses  $d$  (independent) parameters and the symmetric covariance matrix  $\Sigma$  possesses  $\frac{1}{2}d(d+3)$  independent parameters (Mike Tso [77]).

**Definition 2.2.1** (Brownian motion). *Let  $(\Omega, \mathcal{F}, \mathbb{P})$  be a probability space. A stochastic process  $(B_t)_{t \geq 0}$  is said to be a standard Brownian motion on  $(\Omega, \mathcal{F}, \mathbb{P})$ , if the following properties are satisfied:*

- (a)  $B_0 = 0$ , almost surely,
- (b) The process  $(B_t)_{t \geq 0}$  has stationary increments: This means that the distribution of the increments  $B_{t+h} - B_t$ , (for  $h > 0, t < \infty$ ) is dependent only on  $h$ ,
- (c)  $B$  has independent increments: This means for  $t_1, t_2, \dots, t_n \in \mathbb{R}$  with

$$0 < t_1 < t_2 < \dots < t_n < \infty,$$

the increments

$$B_{t_1}, B_{t_2} - B_{t_1}, \dots, B_{t_n} - B_{t_{n-1}},$$

are independent random variables.

- The increment  $B_{t+h} - B_t$  follows the normal distribution with mean 0 and variance  $h > 0$ :  $B_{t+h} - B_t \sim N(0, h)$ .

If a filtration is not mentioned, the natural filtration is implied. Thus, it is easy to see that the expression of geometric Brownian motion is not defined in term of a filtration  $\mathcal{F}_t$ .



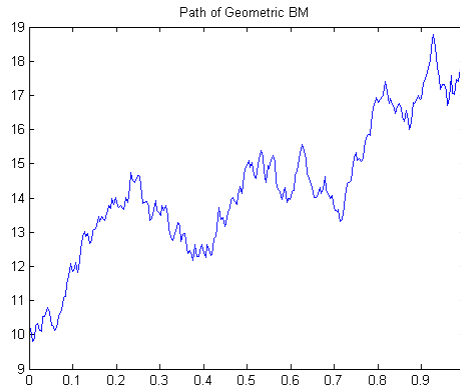


**Figure 2.2:** A sample path of geometric Brownian motion with parameters  $\sigma = 0.3, \mu = 0.5$

## 2.3 Introduction to Lévy processes

Lévy processes are comprehensively discussed by Jean Bertoin [13], Andreas Kyprianou [52], and Ken-Iti Sato [71]. Lévy processes were first studied by French mathematician Paul Lévy in the 1930s, and focused on the sum of independent variables and their limited distributions (David Applebaum [9]). Lévy processes have become popular in mathematical finance, because they described the real financial markets, more than the Black-Scholes model does. In fact, Lévy processes can describe observed financial markets in both the **real** and **risk-neutral** world (Antonis Papapantoleon [63]). Lévy processes also play a crucial role in other fields of science. In economics, they are used to study continuous time-series models, while in actuarial science, they are used to calculate insurance and re-insurance risk. In engineering and physics, they are used to study networks, queues and dams, turbulence, laser cooling and quantum field theory, see David Applebaum [9], Bandoff-Nielsen [10], Rama Cont and Peter Tankov [29], Kyprianou, Wim Schoutens [72], Narahari U Prabhu [65] and Ken-Iti Sato [71] for description of Lévy processes and how they apply to other sciences. Here, we start by introducing Lévy processes and describing some of their important properties, including the Lévy Itô decomposition and the Lévy-Khinchin presentation.

**Definition 2.3.1** (Lévy processes). *Let  $(\Omega, \mathcal{F}, \mathbb{P})$  be a probability space. A càdlàg stochastic process  $(X_t)_{t \geq 0}$  with values in  $\mathbb{R}^n$ , and with  $X_0 = 0$ , is called Lévy process if the following conditions are satisfied:*

- i Independent Increments: Whenever  $0 < t_0 < t_1 < \dots < t_n$ , the random variables  $X_{t_0}, X_{t_1} - X_{t_0}, \dots, X_{t_n} - X_{t_{n-1}}$  are independent.*

ii *Stationary increments:* The law of  $X_{t+s} - X_t$  does not depend on  $t$ .

iii *Stochastic continuity:*  $\forall \epsilon > 0, \lim_{s \rightarrow 0} \mathbb{P}(|X_{t+s} - X_t| \geq \epsilon) = 0$ .

Proposition 2.1.5 states that the sample paths of Poisson process are discontinuous, thus stochastic continuity does not imply continuity of the sample paths of a process.

**Definition 2.3.2** (Infinitely divisible distribution). *Let  $F$  be a probability distribution on  $\mathbb{R}^d$ . Then,  $F$  is said to be infinitely divisible distribution if for any given integer  $n \geq 2$ , there exists  $n$  i.i.d. random variables  $V_1, \dots, V_n$  such that  $V_1 + \dots + V_n$  has distribution  $F$ .*

A strong relationship exists between infinite divisibility and Lévy processes, it is explained by [Sato [71], pg:35] as: if  $(X_t)_{t \geq 0}$  is a Lévy process in law on  $\mathbb{R}^d$ , then, for any given time  $t = 0, 1, 2, \dots$ ,  $F^t = P_{X_t}$  (setting  $F = P_{X_1}$ ) is infinitely divisible distribution. Conversely, if  $F$  is an infinitely divisible distribution on  $\mathbb{R}^d$ , then there is a Lévy process  $(X_t)_{t \geq 0}$  such that  $F = P_{X_1}$ .

Let us define the characteristic function of  $X_t$ :

$$\phi_t(\theta) \equiv \phi_{X_t}(\theta) \equiv E[e^{i\theta \cdot X_t}], \quad \theta \in \mathbb{R}^n.$$

For any given  $t > s$ , we can write  $X_{t+s} = X_s + (X_{t+s} - X_s)$  and using the fact that  $X_{t+s} - X_s$  does not depend of  $X_s$ , we obtain that  $t \mapsto \phi_t(\theta)$  is a multiplicative function Rama Cont and Peter Tankov [29]:

$$\begin{aligned} \phi_{t+s}(\theta) &= \phi_{X_{t+s}}(\theta) = \phi_{X_s}(\theta) \phi_{X_{t+s} - X_s}(\theta) \\ &= \phi_{X_s}(\theta) \phi_{X_t}(\theta) = \phi_s \phi_t. \end{aligned}$$

If  $s \rightarrow t$  then the stochastic continuity of  $t \mapsto X_t$  implies in particular that  $X_t \rightarrow X_s$ . This also means that if  $s \rightarrow t$  the map  $t \mapsto \phi_t(\theta)$  is continuous. Using the multiplicative property of  $\phi_{t+s}(y) = \phi_s \phi_t$  this implies that  $t \mapsto \phi_t(y)$  is an exponential function Rama Cont and Peter Tankov [29].

From the discussion above we can deduce the characteristic function of Lévy process as the following proposition:

**Proposition 2.3.3** (Characteristic function of a Lévy process). *Suppose  $(X_t)_{t \geq 0}$  is a Lévy process on  $\mathbb{R}^d$ . There exists a continuous function  $\psi : \mathbb{R}^d \rightarrow \mathbb{R}$  called characteristic exponent of  $X$ , such that:*

$$\mathbb{E}[e^{i\theta \cdot X_t}] = e^{t\psi(\theta)}, \quad \theta \in \mathbb{R}^d. \quad (2.3.1)$$

## 2.4 Compound Poisson Processes

Compound Poisson processes are simple to study, yet very important for the introduction of such theoretical tools as the Lévy–Khinchin formula (which is key to the distribution properties of Lévy processes) and the Lévy–Itô decomposition (which describes the structure of the sample paths of Lévy processes) Rama Cont and Peter Tankov [29].

**Definition 2.4.1** (Compound Poisson Processes). *Let  $(X_t)_{t \geq 0}$  be a stochastic process. We say that  $(X_t)_{t \geq 0}$  is a compound Poisson process with intensity  $\lambda > 0$  and jump size distribution  $F$  if*

$$X_t = \sum_{j=1}^{N_t} Z_j,$$

where jump sizes  $Z_j$  are independent identically distributed with distribution  $F$  and  $(N_t)$  is a Poisson process with intensity  $\lambda$  which is independent of  $(Z_j)_{j \geq 1}$ .

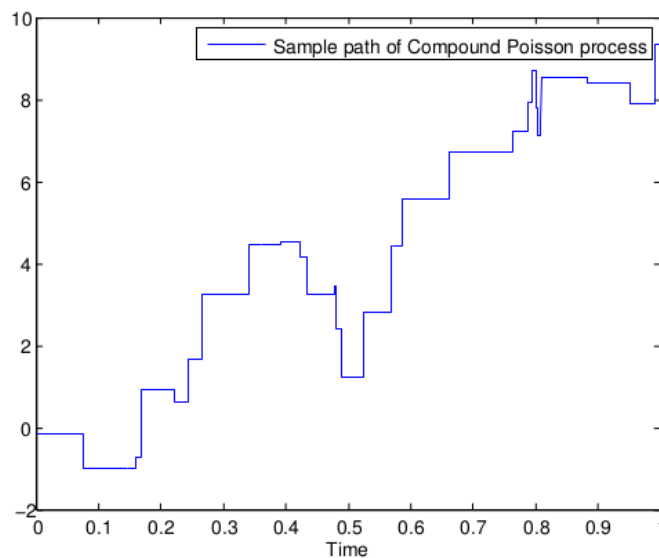


**Figure 2.3:** A sample path of the compound Poisson process with a Gaussian distribution of jumps sizes

From the above definition we can deduce the following properties:

- The jump sizes  $(Z_j)_{j \geq 1}$  are i.i.d. with distribution  $F$ .
- The sample paths of  $X$  are càdlàg piecewise constant functions.

- $X_t$  and  $N_t$  have identical jump times.

**Theorem 2.4.2** (Characteristic function of a compound Poisson Processes). *The Characteristic function of a compound Poisson process  $(X_t)_{t \geq 0}$  on  $\mathbb{R}^d$  with intensity  $\lambda$  and jump distribution  $F$  is represented as follows*

$$\mathbb{E}[e^{iy \cdot X_t}] = \exp \left\{ t\lambda \int_{\mathbb{R}^d} (e^{iy \cdot x} - 1)F(dy) \right\}, \quad \forall y \in \mathbb{R}^d. \quad (2.4.1)$$

*Proof.* Conditioning on  $N_t$ , we obtain

$$\begin{aligned} \mathbb{E}[e^{iy \cdot X_t}] &= \mathbb{E}[\mathbb{E}[e^{iy \cdot X_t} | N_t]], \\ &= \sum_{n \geq 0} \mathbb{E}[e^{iy \cdot \sum_{i=1}^{N_t} Z_i} | N_t = n] \mathbb{P}(N_t = n), \\ &= \sum_{n \geq 0} \mathbb{E}[e^{iy \cdot \sum_{i=1}^n Z_i}] \mathbb{P}(N_t = n), \end{aligned}$$

with  $(Z_i)_{i \geq 0}$  are independent identically distributed with distribution  $F$ .

In proposition 2.1.4, we have  $\mathbb{P}(N_t = n) = e^{-\lambda t} \frac{(\lambda t)^n}{n!}$ , yields

$$\mathbb{E}[e^{iy \cdot X_t}] = \sum_{n=0}^{\infty} e^{-\lambda t} \frac{(\lambda t)^n}{n!} \mathbb{E}[e^{iy \cdot \sum_{i=1}^n Z_i}],$$

then

$$\begin{aligned} \mathbb{E}[e^{iy \cdot X_t}] &= \sum_{n=0}^{\infty} e^{-\lambda t} \frac{(\lambda t)^n}{n!} \left( \mathbb{E}[e^{iy \cdot Z}] \right)^n, \\ &= \sum_{n=0}^{\infty} e^{-\lambda t} \frac{(\lambda t)^n}{n!} \left( \int_{\mathbb{R}^d} e^{ix \cdot y} F(dy) \right)^n, \\ &= \exp \left\{ t\lambda \int_{\mathbb{R}^d} (e^{ix \cdot y} - 1)F(dy) \right\}. \end{aligned}$$

□

## 2.5 Jump Measure of the Compound Poisson Processes and Lévy result

Usually the paths of a Lévy process are discontinuous, an exception being Brownian motion with drift Rama Cont and Peter Tankov [29]. To understand the jump structure of a Lévy process, we first need to understand the concept of a Lévy measure, which requires the explanation of a random measure, and the jump measure of a compound Poisson process.

### 2.5.1 Poisson Random Measure

A Poisson random measure is a fundamental part of the theory of Lévy processes, it characterises the paths of a Lévy process. We start by defining random measures, and then Poisson random measures.

**Definition 2.5.1** (Random Measure). *Consider a probability space  $(\Omega, \mathbb{P}, \mathcal{F})$  and a measurable space  $(E, \xi)$ . A map*

$$\begin{aligned} N : \Omega \times \xi &\rightarrow \mathbb{R} \\ (\omega, B) &\mapsto N(\omega, B), \end{aligned}$$

is called a random measure iff:

1. There exists a partition  $\{B_i, i = 1, 2, \dots\} \in \xi$  of  $E$ , such that  $N(B_i) < \infty$  for all  $i$ .
2. For every  $\omega \in \Omega$ ,  $N(\omega, \cdot)$  is a measure on  $\xi$ .
3. For every  $B \in \xi$ ,  $N(\cdot, B) = N(B)$  is  $f$  measurable.

We say that the random measure  $N$  has independent increments iff  $N(B_i)$  are independent when  $B_i$  are disjoint. We can now define the concept of Poisson random measures.

**Definition 2.5.2** (Poisson random measure). *Consider a probability space  $(\Omega, \mathbb{P}, \mathcal{F})$  with a measurable space  $(E, \xi)$  where  $E \subset \mathbb{R}^d$ , and  $\nu$  is a positive measure on  $(E, \xi)$ . A Poisson random measure on  $E$  with its intensity measure  $\nu$ , is an integer valued random measure:*

$$\begin{aligned} N : \Omega \times \xi &\rightarrow \mathbb{N}, \\ (\omega, B) &\mapsto N(\omega, B), \end{aligned}$$

satisfying the following properties:

- For all  $\omega \in \Omega$ , the  $N(\omega, \cdot)$  is an integer valued measure on  $E$ : This means, for any  $B$  (with  $B$  is bounded),  $N(\omega, B) < \infty$  is an integer valued random variable.
- For each measurable set  $B \subset E$ ,  $N(B)$  is a Poisson random variable with parameter  $\nu(B)$ :

$$\forall k \in \mathbb{N}, \quad \mathbb{P}(N(B) = k) = e^{-\nu(B)} \frac{(\nu(B))^k}{k!}.$$

- For given disjoint measurable sets  $B_1, \dots, B_n \in \xi$ , the variable  $N(B_1), \dots, N(B_n)$  are independent.

A Poisson random measure can be constructed as the counting measure of random scattered points (Rama Cont and Peter Tankov [29]). Another important process we need to consider is the jump measure of a compound Poisson process. Given a compound Poisson process  $(X_t)_{t \in [0, T]}$  on  $\mathbb{R}^d$ , we define the jump measure  $J_X$  of  $X$  on  $[0, t] \times \mathbb{R}^d$  as follows: If  $B \subset \mathbb{R}^d \times [0, \infty]$  is a Borel set, then:

$$J_X(B) = \#\{t : \Delta X_t \neq 0 \text{ and } (t, \Delta X_t) \in B\}. \quad (2.5.1)$$

where  $\Delta X_t = X_t - X_{t-}$ . We can also define  $J_X([t_1, t_2] \times B)$  where  $B \subset \mathbb{R}^d$  as the number of jumps of  $X$  in interval  $[t_1, t_2]$  with jump size in  $B$ . Let us introduce the following proposition in order to show that  $J_X$  is a Poisson random measure in a form of Definition 2.5.2.

**Proposition 2.5.3** (Jump measure of a compound Poisson process (Rama Cont and Peter Tankov [29])). *Given a compound Poisson process  $(Y_t)_{t \geq 0}$  with intensity  $\lambda$  and jump size distribution  $f$ . The jump measure  $J_Y$  is a Poisson random measure on  $\mathbb{R}^d \times [0, \infty)$  with intensity measure  $\nu(dy \times dt) = \nu(dy)dt = \lambda f(dy)dt$ .*

The above proposition suggests another way to interpret the Lévy measure of a compound Poisson process is as the average number of jumps per unit time (Rama Cont and Peter Tankov [29]). This proposition is not only helpful for the interpretation of a Lévy measure of a compound Poisson process, but it is also useful for the definition of a Lévy measure for all Lévy processes (Rama Cont and Peter Tankov [29]). Thus, we state the definition of a Lévy measure:

**Definition 2.5.4** (Lévy measure). *Given a Lévy process  $\{X_t\}_{t \geq 0}$  on  $\mathbb{R}^d$ . The measure  $\nu$  on  $\mathbb{R}^d$ , defined by*

$$\nu(B) = \mathbb{E}\{\#[t \in [0, 1] : \Delta X(t) \neq 0, \Delta X(t) \in B]\}, \quad B \in \mathcal{B}(\mathbb{R}^d). \quad (2.5.2)$$

*is called the Lévy measure of  $X$ . The Lévy measure  $\nu(B)$  can be interpreted as the expected number, per unit time, of jumps whose the size belongs to  $B$  (Rama Cont and Peter Tankov [29]).*

The Lévy measure  $\nu$  is a positive measure on  $\mathbb{R}^d$  and satisfies the integrability condition (Rama Cont and Peter Tankov [29]):

$$\int (x^2 \wedge 1) \nu(dx) < \infty \quad \text{and} \quad \nu(\{0\}) = 0. \quad (2.5.3)$$

The Lévy measure can describe the expected number of jumps of a certain height in any given time interval, and has no mass at the origin, but singularities (infinitely many jumps) can occur around the origin (Rama Cont and Peter Tankov [29]).

Using Lévy measure, we can represent every compound Poisson process as :

$$X_t^1 = \sum_{r \in [0, t]} \Delta X_r = \int_{[0, t] \times \mathbb{R}^d} x J_X(dr \times dx), \quad (2.5.4)$$

where  $J_X$  represents a Poisson random measure with intensity  $\nu(dx)dt$ . Thus, we can see that  $X$  is rewritten as the sum of its jumps. Let  $\gamma t + W_t$  be a Brownian motion with drift and independent of  $X$ . We can define another Lévy process  $X_t$  in the following way:

$$X_t = \gamma t + W_t + X_t^1. \quad (2.5.5)$$

Substituting  $X^1$  in (4.1.4), follows:

$$\begin{aligned} X_t &= \gamma t + W_t + \sum_{r \in [0, t]} \Delta X_r \\ &= \gamma t + W_t + \int_{[0, t] \times \mathbb{R}^d} x J_X(dr \times dx), \end{aligned} \quad (2.5.6)$$

where  $J_X$  is a Poisson random measure on  $[0, t] \times \mathbb{R}^d$  with intensity measure given by  $\nu(dx)dt$ . Looking at this form (2.5.6) of the Lévy process, raises a major question. Can all Lévy processes be represented in this form? In order to answer this question, we need to discuss an important aspect of the Lévy process, the Lévy-Itô decomposition.

**Theorem 2.5.5** (The Lévy-Itô decomposition (Rama Cont and Peter Tankov [29])). *Given a Lévy process  $(X_t)_{t \geq 0}$  on  $\mathbb{R}^d$  and its Lévy measure  $\nu$ , defined in 2.5.4 as :*

1 *The measure  $\nu$  on  $\mathbb{R}^d$  verifies the following condition:*

$$\int_{|x| \leq 1} |x|^2 \nu(dx) < \infty \quad \text{and} \quad \int_{|x| \geq 1} \nu(dx) < \infty \quad (2.5.7)$$

$$(2.5.8)$$

2 *The jump measure of  $X$ , denoted by  $J_X$ , is a Poisson random measure on  $[0, \infty[ \times \mathbb{R}^d$  with  $\nu(dx)dt$  its intensity measure.*

3 There exists a constant vector  $\gamma$  and a  $d$ -dimensional Brownian motion  $(B_t)_{t \geq 0}$ , such that

$$X_t = \gamma t + B_t + X_t^l + \lim_{\epsilon \rightarrow 0} \tilde{X}_t^\epsilon \quad (2.5.9)$$

where

$$X_t^l = \int_{|x| \geq 1, r \in [0, t]} x J_X(dr \times dx) \quad (2.5.10)$$

and

$$\begin{aligned} \tilde{X}_t^\epsilon &= \int_{\epsilon \leq |x| < 1, r \in [0, t]} x \{J_X(dr \times dx) - \nu(dx)dr\} \\ &= \int_{\epsilon \leq |x| < 1, r \in [0, t]} x \{J_X(dr \times dx) - \nu(dr \times dx)\} \\ &= \int_{\epsilon \leq |x| < 1, r \in [0, t]} x \{J_X - \nu\}(dr \times dx) \\ &\equiv \int_{\epsilon \leq |x| < 1, r \in [0, t]} x \tilde{J}_X(dr \times dx) \end{aligned} \quad (2.5.11)$$

where

$$\tilde{J}_X = J_X - \nu$$

All terms in (2.5.9) are independent, and the convergence in the last term  $\tilde{X}_t^\epsilon$  is almost sure and also uniform in  $t$  on  $[0, T]$ .

We can see that the above theorem implies the existence of a triplet  $(\nu, B, \gamma)$ , which is also called the Lévy triplet or characteristic triplet of the process  $X_t$ . Here  $\gamma$  is a constant vector,  $B$  is a positive definite matrix and  $\nu$  is a positive measure.

Given the importance of this result, let us explain each term in (2.5.9). The first term denoted by  $\gamma t + A_t$  is called a continuous Gaussian Lévy process. Every Gaussian Lévy process is a continuous process and can be written in this form. The parameter  $\gamma$  is a drift part and  $A_t$  is a Brownian motion with a covariance matrix  $B$  (Rama Cont and Peter Tankov [29]).

The last two terms in (2.5.9) are not continuous and incorporate the jumps of  $X_t$ . The condition  $\int_{|x| \leq 1} \nu(dx) < \infty$  can be explained as follows: For any  $t > 0$ ,  $\#\{\Delta X_r : |\Delta X_r| \geq 1, r < t\}$  is finite. Thus, we can define  $X_t^l$  as a finite number of terms and it is given as:

$$X_t^l = \sum_{0 \leq r \leq t}^{\Delta X_r \geq 1} \Delta X_r.$$

$X_t^l$  is a compound Poisson process. The  $\tilde{X}_t^\epsilon$  are not compound Poisson processes, since they are not piecewise constant, but are compensated for drift. The Lévy-Itô decomposition implies that every Lévy process can be approximated as a sum of Brownian



motion with drift and a compound Poisson process. In fact, this theory is very useful for the simulation of Lévy processes.

The Lévy-Itô decomposition was first discovered by Paul Lévy [55] using a direct analysis of the paths of Lévy processes. Subsequently it was completed by Andrew G Haldane and Vasileios Madouros [44].

Next, we want to consider a fundamental result which describes the characteristic exponent of a Lévy process in terms of its Lévy triplet  $(B, \nu, \gamma)$ . Let us discuss the following theorem.

**Theorem 2.5.6** (Lévy-Khinchin representation Rama Cont and Peter Tankov [29]). *Given a Lévy process  $\{X_t\}_{t \geq 0}$  on  $\mathbb{R}^d$  and  $(B, \nu, \gamma)$  its characteristic triplet, we can express the characteristic function of Lévy processes using the Theorem 2.3.3 :*

$$\mathbb{E}[e^{iy \cdot X_t}] = \Phi_t(y) = e^{t\psi(y)}, \quad \text{for } y \in \mathbb{R}^d \quad t > 0. \quad (2.5.12)$$

Where the characteristic exponent  $\psi(y)$  is expressed by

$$\psi(y) = -\frac{1}{2}y \cdot By + i\gamma \cdot y + \int_{\mathbb{R}^d} (e^{iy \cdot x} - 1 - iy \cdot x 1_{|x| \leq 1}) \nu(dx), \quad (2.5.13)$$

and is also called a Lévy exponent.

We can also rewrite a Lévy-Khinchin representation (2.5.13) by truncating the large jumps: For all  $\epsilon > 0$ ,

$$\begin{aligned} \psi(y) &= -\frac{1}{2}y \cdot By + i\gamma \cdot y + \int_{\mathbb{R}^d} (e^{iy \cdot x} - 1 - iy \cdot x 1_{|x| \leq 1}) \nu(dx) \\ &= -\frac{1}{2}y \cdot By + i\gamma \cdot y + \int_{\mathbb{R}^d} (e^{iy \cdot x} - 1 + iy \cdot x 1_{|x| \leq \epsilon} - iy \cdot x 1_{|x| \leq \epsilon} - iy \cdot x 1_{|x| \leq 1}) \nu(dx) \\ &= -\frac{1}{2}y \cdot By + i\gamma \cdot y + iy \int_{\mathbb{R}^d} x (1_{\epsilon < |x| \leq 1}) \nu(dx) + \int_{\mathbb{R}^d} (e^{iy \cdot x} - 1 - iy \cdot x 1_{|x| \leq \epsilon}) \nu(dx), \end{aligned} \quad (2.5.14)$$

We then obtain

$$\begin{aligned} \psi(y) &= -\frac{1}{2}y \cdot By + i\gamma^\epsilon \cdot y + \int_{\mathbb{R}^d} (e^{iy \cdot x} - 1 - iy \cdot x 1_{|x| \leq \epsilon}) \nu(dx) \quad (2.5.15) \\ \text{with } \gamma^\epsilon &= \gamma + \int_{\mathbb{R}^d} x (1_{|x| \leq \epsilon} - 1_{|x| \leq 1}) \nu(dx). \end{aligned}$$

We can generalise 2.5.15, for every bounded measurable function  $h : \mathbb{R}^d \rightarrow \mathbb{R}$  which satisfies the following properties:  $h(y) = O(1/|x|)$  for  $x \rightarrow \infty$  and  $h(x) = 1 + o(|x|)$

for  $x \rightarrow 0$ , the general form of  $\psi(x)$  with the truncation function  $h$  can be expressed as follows:

$$\psi(y) = -\frac{1}{2}y \cdot By + i\gamma^h \cdot y + \int_{\mathbb{R}^d} (e^{iy \cdot x} - 1 - iy \cdot xh(x))\nu(dx), \quad (2.5.16)$$

with  $h$  represents the truncate function and  $(B, \nu, \gamma^h)$  a characteristic triplet with respect to  $h$ . Rama Cont and Peter Tankov [29] stated that the different choices of truncation function  $h$  do not affect the intrinsic parameters of Lévy process which are  $B$  and  $\nu$ . However, it may have an affect on  $\gamma$  since it depends on the choice of  $h$ . Therefore, we should avoid calling  $\gamma$  "drift " of the process Rama Cont and Peter Tankov [29]. Numerous choices of the truncation function have been used in the literature. For example  $h(y) = \frac{1}{1+|y|^2}$  was used by Paul Lévy, whereas most newer texts use  $h(y) = 1_{|y| \leq 1}$ . When a Lévy measure satisfies the additional condition  $\int_{|x| \geq 1} |x|\nu(dx) < \infty$ , we do not need to truncate the large jumps, and we can use this simple form:

$$\begin{aligned} \psi(y) &= -\frac{1}{2}y \cdot By + i\gamma^e \cdot y + \int_{\mathbb{R}^d} (e^{iy \cdot x} - 1 - iy \cdot x)\nu(dx) \\ \text{with } \gamma^e &= \gamma + \int_{|x| \geq 1} xv(dx). \end{aligned} \quad (2.5.17)$$

In fact, Rama Cont and Peter Tankov [29] shown that  $\mathbb{E}[X_t] = \gamma^e t$  and with  $\gamma^e$  is called the center of process  $(X_t)$ . The details for the proof of the theorem can be found in [Rama Cont and Peter Tankov [29], pg:96 and Iosif Il'ich Gikhman and Anatolii Skorokhod [40]].

We also have to consider the property of a finite variation Lévy process. Recall that the total variation of a function  $g : [a, b] \rightarrow \mathbb{R}^d$  is given as

$$TV(f) = \sup_{\mathcal{P}} \sum_{j=1}^n |g(t_j) - g(t_{j-1})|. \quad (2.5.18)$$

where  $\mathcal{P}$  is the set of all partitions. The supremum is taken over by all partitions  $a = t_0 < t_1 < \dots < t_{n-1} < t_n = b$  of the interval  $[a, b]$  (see Rama Cont and Peter Tankov [29]). If the Lévy triplet  $(B, \gamma, \nu)$  satisfies the conditions, then the Lévy process is of finite variation. Hence, the following corollary shows that both Lévy results, the Lévy-Khinchin representation and the Lévy-Itô decomposition, can be simplified in the case of finite variation :

**Corollary 2.5.7** (Rama Cont and Peter Tankov [29]). *Consider a Lévy process  $(X_t)_{t \geq 0}$  of finite variation, and let be  $(0, \gamma, \nu)$  its Lévy triplet. We can express  $X$  as the sum of a linear drift*

term and its jumps:

$$\begin{aligned} X_t &= at + \int_{[0,t] \times \mathbb{R}^d} x J_X(dr \times dt) \\ &= at + \sum_{\substack{\Delta X_r \neq 0 \\ r \in [0,t]}} \Delta X_s \end{aligned} \quad (2.5.19)$$

with the characteristic function given by :

$$\begin{aligned} \mathbb{E}[e^{iy \cdot X_t}] &= \exp \left( t \left\{ ia \cdot y + \int_{\mathbb{R}^d} (e^{iz \cdot y} - 1) \nu(dx) \right\} \right), \\ \text{and } a &= \gamma - \int_{|x| \leq 1} x \nu(dx). \end{aligned} \quad (2.5.20)$$

## 2.6 Subordinators Representation

Subordinators are processes with positive increments. They are an important component for models driven by Lévy processes. Many *pure jump Lévy models* can be easily simulated via a subordinator. Subordinators are important for our project, because all Lévy models that we use will be simulated via a subordinator (see Chapter 3). Let us define a subordinator.

**Definition 2.6.1** (Subordinators (see Steven [54])). *A real-valued Lévy process  $(S_t)_{t \geq 0}$  on  $\mathbb{R}$  is called a subordinator if it has nondecreasing sample paths. A stable process is a real-valued Lévy process  $(X_t)_{t \geq 0}$  with initial value  $S_0 = 0$  that satisfies the self-similarity property*

$$S_t/t^{1/\alpha} \stackrel{\mathcal{D}}{=} S_1 \quad \forall t > 0. \quad (2.6.1)$$

The parameter  $\alpha$  is called exponent of the process or index of stability thus the stable distributions with index  $\alpha$  are referred to as  $\alpha$ -stable distributions. Given the above Definition 2.6.1, we can next discuss the following proposition.

**Proposition 2.6.2** (Subordination Rama Cont and Peter Tankov [29]). *A Lévy process  $(S_t)_{t \geq 0}$  on  $\mathbb{R}$  is called a subordinator if it satisfies one of the following equivalent conditions:*

- $S_t \geq 0$  a.s. for some  $t > 0$ .
- $S_t \geq 0$  a.s. for every  $t > 0$ .
- Sample paths of  $S_t$  are almost surely increasing: i.e.  $t \geq s \implies S_t \geq S_s$ .

- $B$  Lévy triplet  $(\nu, A, \gamma)$  of  $S_t$  satisfies the following properties

$$\begin{aligned} A &= 0, \quad \nu((-\infty, 0]) = 0, \\ \int_0^\infty (x \wedge 1) \nu(dx) &< \infty \quad \text{and} \quad b > 0. \end{aligned} \quad (2.6.2)$$

There exists no diffusion component in  $S_t$ , only positive drift and positive jumps of finite variation.

The above equivalent condition implies that the trajectories of  $S_t$  are almost surely increasing. Considering the fact that  $S_t$  is a positive random variable for all  $t$ , we can describe the trajectories of  $S_t$  using Laplace transform rather than Fourier transform Rama Cont and Peter Tankov [29]. Given a characteristic triplet  $(0, \rho, b)$  of  $S$ , then we can represent the moment generating function of  $S_T$  (Rama Cont and Peter Tankov [29]) :

$$E[e^{vS_t}] = e^{tL(v)} \quad \forall v \leq 0 \quad (2.6.3)$$

and

$$L(v) = bv + \int_0^\infty (e^{vx} - 1) \rho(dx). \quad (2.6.4)$$

$L(v)$  is called the Laplace exponent of  $S$ . Considering that the process  $S$  is nondecreasing, it can be explained as a "time deformation" and used to "time-change" other Lévy processes Rama Cont and Peter Tankov [29], as shown by the following theorem:

**Theorem 2.6.3.** *Subordinator Representation (Rama Cont and Peter Tankov [29])*

Let  $(\Omega, \mathcal{F}, \mathbb{P})$  be a probability space. Let  $(X_t)$  be a Lévy process on  $\mathbb{R}^d$  with characteristic triplet  $(\nu, A, \gamma)$  and characteristic exponent  $\Psi(v)$ . Let  $S_t$  be a subordinator with Laplace exponent  $L(v)$  and characteristic triplet  $(0, \rho, b)$ . Let  $(Y_t)_{t \geq 0}$  be a process defined by  $Y(t, \omega) := X(S(t, \omega), \omega)$  for every  $\omega \in \Omega$ . Then  $(Y_t)$  is a Lévy process, with characteristic function given by:

$$\mathbb{E}[e^{ivY_t}] = e^{itL(\Psi(v))}. \quad (2.6.5)$$

We can see that to obtain the characteristic exponent of  $Y$  we have to compose the characteristic exponent of  $X$  with the Laplace exponent of  $S$ . Hence its characteristic triplet  $(A^Y, \gamma^Y, \nu^Y)$  is given by:

$$\begin{aligned} A^Y &= bA, \\ \nu^Y(B) &= b\nu(B) + \int_0^\infty p_s^X(B) \rho(ds), \quad \forall B \in \mathcal{B}(\mathbb{R}), \\ \gamma^Y &= b\gamma + \int_0^\infty \rho(ds) \int_{|x| \leq 1} x p_s^X(dx) \end{aligned}$$

where  $p_t^X$  is the probability density function of  $X_t$  and  $(Y_t)_{t \geq 0}$  is a subordinate of the processes  $(X_t)_{t \geq 0}$ .

## 2.7 Construction of a Lévy processes via Brownian subordination

In this section we show how to build Lévy models with Brownian subordination. This section is important because the three Lévy models that we focus on in this research are written in terms of subordinated Brownian motion.

### 2.7.1 Subordinating Brownian motion

Suppose  $(S_t)_{t \geq 0}$  is a subordinator with Laplace exponent  $L(u)$  and  $(W_t)_{t \geq 0}$  a Brownian motion independent from  $S$ . A new Lévy process  $X_t$  can be obtained by subordinating a Brownian motion with drift  $\mu$  by the process  $S$ . Thus,  $X_t$  can be written as  $X_t = \sigma W(S_t) + \mu S_t$ . We observe that the process  $X_t$  can be seen as a Brownian motion if it is observed on a new time scale, which is a stochastic time scale given by  $S_t$  (Rama Cont and Peter Tankov [29]). Geman et al. [39] stated that the process  $S_t$  (time scale) has an important financial interpretation of business time, which is the integrated rate of information arrival (see Rama Cont and Peter Tankov [29]). This interpretation helps the understanding of the models based on subordinated Brownian motion rather than the general Lévy models. Let us characterise a Lévy measure with subordinated Brownian motion and drift by using the following proposition:

**Theorem 2.7.1.** *Subordinating Brownian motion (Rama Cont and Peter Tankov [29])*

Let  $(X_t)_{t \geq 0}$  be a Lévy process with a Lévy measure  $\nu$  on  $\mathbb{R}$  and  $\mu \in \mathbb{R}$ . A Lévy process  $X_t$  can be expressed as  $X_t = W(Z_t) + \mu(Z_t)$  where  $(Z_t)_{t \geq 0}$  is some subordinator and  $(W_t)_{t \geq 0}$  some Brownian motion independent of  $Z$  if and only if the following conditions are satisfied:

- i)  $\nu(x)e^{-\mu x} = \nu(-x)e^{\mu x}$  for all  $x$ .
- ii)  $\nu$  is absolutely continuous with density  $\nu(x)$ .
- iii)  $\nu(\sqrt{u})e^{-\nu\sqrt{u}}$  is a completely monotonic function on  $(0, \infty)$ . This means all derivatives of  $\nu(\sqrt{u})e^{-\nu\sqrt{u}}$  exist and  $(-1)^k \frac{d^k(\nu(\sqrt{u})e^{-\nu\sqrt{u}})}{du^k} > 0$  for all  $k \geq 1$ .

**Proposition 2.7.2.** *Brownian Subordinator (see [? ])*

Given an increasing Lévy process  $\{Y_t\}_{0 \leq t \leq 1}$  with a Lévy measure  $\mu(dy)$ , and a standard Brownian motion  $\{W_t\}_{0 \leq t \leq 1}$ . Let  $(Z_t)_{T \geq 0}$  be a process defined by:

$$Z_t := \theta Y_t + W(Y_t). \quad (2.7.1)$$

Then  $Z_t$  will have the following Lévy measure:

$$\nu(dx) = dx \int_0^\infty \frac{\exp\left(-\frac{(y-\theta z)^2}{2z}\right)}{\sqrt{2\pi z}} \mu(dz). \quad (2.7.2)$$

The outline of the proof can be found in (Dilip B Madan and Marc Yor [57] , and Ken-Iti Sato [71],Theorem.30.1).

## Chapter 3

# Pure Jump Lévy Model for Asset Dynamics

In this chapter, we discuss in detail the three Lévy models that are the focus of this research, namely the Variance Gamma model, the Normal Inverse Gaussian (NIG) model and the CGMY model. The reason why these models are preferred over the Black-Scholes model is that they have advantages over the Black-Scholes model, hence their wide usage in mathematical finance. We can easily simulate these processes, since their underlying theory is often simpler to understand than the other models and they are more efficient (Peter Carr and Dilip Madan [24]). In fact, they have a specific characteristic functions which make them easy to use for the calculation of European option pricing formulas using the Fast Fourier method (Peter Carr and Dilip Madan [24]). Here, we concentrate on the properties of Lévy processes, and Lévy triplets and their characteristic functions. We do not discuss Lévy densities here, since we price European call options using their characteristic functions via the Fast Fourier method. We also focus on variance, skewness and kurtosis in this chapter.

The procedures to simulate those processes are discussed in the Appendix A. We conclude the chapter by fitting the historical returns of S&P 500 time series data to these models. The densities are fitted via the method of FFT using its characteristic functions.

We conduct these analysis to illustrate why these models are the preferred ones for modelling asset return dynamics. In next section, we describe the models used.

### 3.1 Normal Inverse Gaussian Processes (NIG)

The NIG distribution is type of generalized hyperbolic distribution, and was first introduced by (Ole Barndorff-Nielsen [12]). Tina Hviid Rydberg [69] and [68] used the NIG model in financial modelling by fitting it to the time series of daily stock returns via a maximum likelihood method. The NIG model was fitted to the historical return data by matching its first four moments of the return process (Erik Bølviken and Fred Espen Benth [14]).

The NIG process is a pure jump model which is characterised by an Inverse Gaussian (IG) component associated with the distribution part. The IG distribution describes the distribution of the time a standard Brownian motion with a positive drift  $b > 0$  takes to reach the level of  $a$  ([6]). The time that Brownian motion distribution takes must be positive, so we define a density function with support on  $\mathbb{R}^+$  (Wim Schoutens [72]):

$$f^{IG}(x, a, b) = \frac{ae^{ab}}{\sqrt{2\pi}} x^{-3/2} \exp\left(-\frac{1}{2}\left(\frac{a^2}{x} + b^2x\right)\right), \quad x > 0$$

Its characteristic function is given by:

$$\phi^{IG}(v, a, b) = \exp\left\{-a(\sqrt{-2iv + b^2} - b)\right\}. \quad (3.1.1)$$

Ole Barndorff-Nielsen [12] defined the characteristic function of Normal Inverse Gaussian(NIG) distribution (with the parameter  $-\alpha < \beta < \alpha$  represents the skewness,  $\alpha > 0$  the tail,  $\delta > 0$  the scale), NIG( $\beta, \alpha, \delta$ ) as follows:

$$\phi_{NIG}(v, \beta, \alpha, \delta) = \exp\left\{-\delta(\sqrt{\alpha^2 - (\beta + iv)^2} - \sqrt{\alpha^2 - \beta^2})\right\}. \quad (3.1.2)$$

The above characteristic function (3.1.2) of a NIG distribution is infinitely divisible. Thus, we can define a NIG process :

$$X^{NIG} = \{X_t^{NIG}, t \geq 0\},$$

which follows the law of NIG distributed. Thus, we can rewrite above characteristic function (3.1.2) as :

$$\begin{aligned} \mathbb{E}\{e^{i\langle v, X_t^{NIG} \rangle}\} &= \phi_{NIG}(v, \beta, \alpha, t\delta) \\ &= \exp\left\{-\delta t(\sqrt{\alpha^2 - (\beta + iv)^2} - \sqrt{\alpha^2 - \beta^2})\right\}. \end{aligned} \quad (3.1.3)$$



According to Wim Schoutens [72], NIG process can be obtained as a time-changed Brownian motion  $(W_t)_{t \geq 0}$  with subordinate  $\{(IG)_t\}_{t \geq 0}$ . With the parameters  $a = 1$  and  $b = \delta\sqrt{\alpha^2 - \beta^2}$ :

$$Y_t = \mu + \beta\delta^2((IG)_t) + \delta W((IG)_t). \quad (3.1.4)$$

If a random variable  $X$  follows the  $\text{NIG}(\alpha, \beta, \delta)$  distribution, then  $-X$  follows a  $\text{NIG}(\alpha, -\beta, \delta)$  distribution. We list the central moments of the NIG distribution in the following table:

**Table 3.1:** Table of moments of NIG process

The Moments of NIG process	
Mean	$(\delta t \beta) / \sqrt{\alpha^2 - \beta^2}$
Variance	$(\alpha^2 \delta t) (\alpha^2 - \beta^2)^{-3/2}$
Skewness	$3\beta\alpha^{-1} (\delta t)^{-1/2} (\alpha^2 - \beta^2)^{-1/4}$
Kurtosis	$3 \left( 1 + \frac{\alpha^2 + 4\beta^2}{\alpha^2 + \delta t \sqrt{\alpha^2 - \beta^2}} \right)$

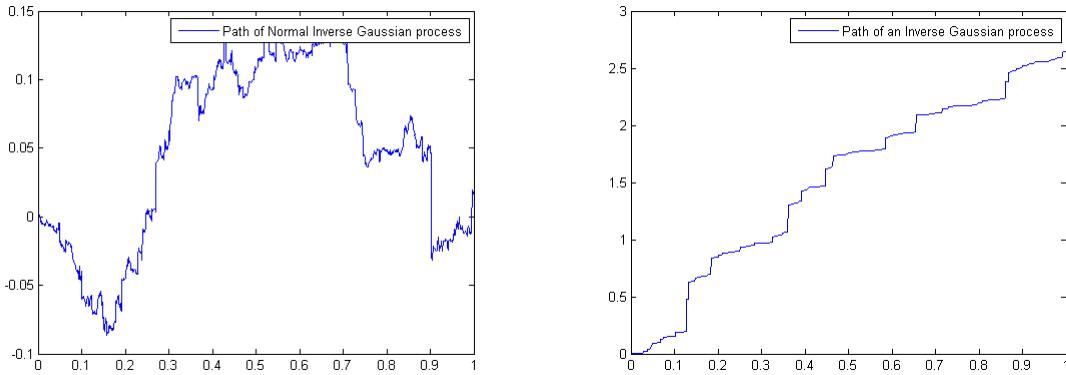


**Figure 3.1:** In the top left is the trajectory of the Normal Inverse Gaussian process with the parameters  $\alpha = 45, \beta = -9$  and  $\delta = 1$ , the number of simulation  $N = 1000$  and the time  $T = 1$ . This trajectory is simulated using the algorithm A.2.2. In the top right is the trajectory of Inverse Gaussian process with parameters  $b = 3, a = 7$  and the number of simulation  $N = 1000$  and  $T = 1$ .

## 3.2 Variance Gamma processes (VG)

### 3.2.1 Gamma Process ( $G(t)$ )

**Definition 3.2.1.** Let  $f_{\Gamma}(x; a, b)$  be the density function of Gamma distribution  $\text{Gamma}(a, b)$  with the parameters  $b > 0$  and  $a > 0$ , given by (Wim Schoutens [72]):

$$f_{\Gamma}(x; a, b) = \frac{b^a}{\Gamma(a)} x^{a-1} \exp(-bx), \quad x > 0. \quad (3.2.1)$$

The characteristic function of Gamma distribution with parameters  $b > 0$  and  $a > 0$  is given by:

$$\phi_{\Gamma}(a, v, b) = \left(1 - \frac{iv}{b}\right)^{-a} \quad v \in \mathbb{R} \quad (3.2.2)$$

We clearly see that the above characteristics function 3.2.2 is infinitely divisible (Wim Schoutens [72]). A stochastic process  $G = \{G(t), t \geq 0\}$  with parameters  $b > 0$  and  $a > 0$  is Gamma process if it starts at zeros and has a stationary and independent Gamma distributed increments.

The Lévy triplet of the Gamma process is given by (Wim Schoutens [72])

$$[a(1 - \exp(-b))/b, 0, a \exp(-bx)x^{-1}1_{x>0}dx]$$

#### 3.2.1.1 Properties of Gamma Distribution

Schoutens[72] derived the following properties of  $\text{Gamma}(a, b)$  distribution using the density function (3.2.1): Also note that if  $X$  is  $\text{Gamma}(a, b)$  and for any  $e > 0$ ,  $eX$  is a

**Table 3.2:** Table of properties of  $\text{Gamma}(a, b)$  distribution

Name	$\text{Gamma}(a, b)$
Means	$\frac{a}{b}$
Variance	$\frac{a}{b^2}$
Skewness	$2a^{-1/2}$
Kurtosis	$3(1 + 2a^{-1})$

$\text{Gamma}(a, b/e)$ .

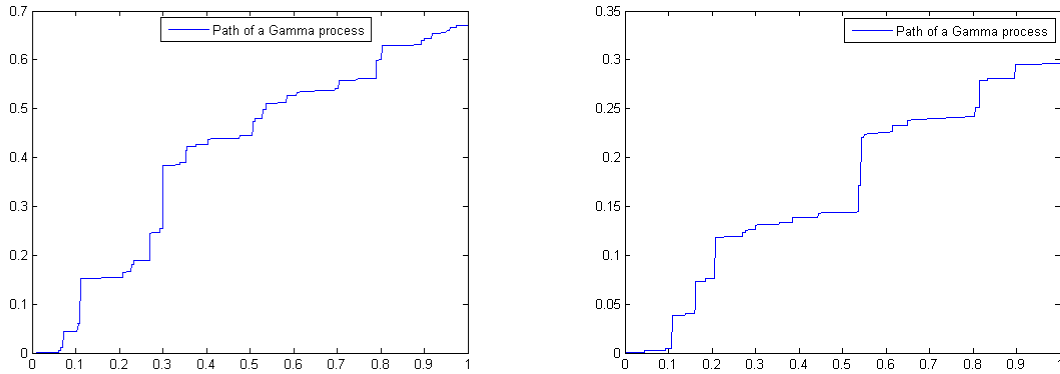


**Figure 3.2:** Ordinary trajectories of Gamma process with parameters  $b = 12$ ,  $a = 27, 20$  and the number of simulation  $N = 1000$  and  $T = 1$ .

### 3.2.2 VG processes

The Variance Gamma process has three parameters  $(\sigma, \theta, \nu)$  introduced by Dilip B Madan, Peter P Carr, and Eric C Chang [56]. Here the parameter  $\sigma$  is volatility,  $\theta$  is a drift of arithmetic Brownian motion and  $\nu$  a variance which controls the fat tails. The VG model was introduced in financial modelling to provide a good model for stock market returns, and gives an analytic solution for European-types option prices (Dilip B Madan, Peter P Carr, and Eric C Chang [56]). Let  $B_t(\sigma, \theta)$  be a Brownian motion with drift  $\theta$  and  $\sigma$  volatility:

$$dB_t(\sigma, \theta) = \theta dt + \sigma dW_t,$$

where  $W_t$  is a standard Brownian motion. The VG process is obtained by subordinating the Brownian motion  $B_t(\sigma, \theta)$  with a Gamma process  $G(t)$  :

$$\begin{aligned} X(t, \sigma, \nu, \theta) &= B_t(G(t), \sigma, \theta) \\ &= \theta G(t) + \sigma W(G(t)), \end{aligned}$$

According to Hélyette Geman [38], the probability density of VG is defined:

$$f(v) = \frac{v^{\frac{t}{\nu}-1} e^{-\frac{v}{\nu}}}{\nu^{\frac{t}{\nu}} \Gamma\left(\frac{t}{\nu}\right)} \quad (3.2.3)$$

where  $\Gamma(y)$  represents the gamma function and  $\nu$  a variance. We can then obtain the characteristic function of the VG( $\sigma, \nu, \theta$ ) distribution :

$$\phi^{VG}(v; \sigma, \nu, \theta) = \left(1 - iv\theta\nu + \frac{1}{2}\sigma^2\nu v^2\right)^{-\frac{1}{\nu}}. \quad (3.2.4)$$

The above characteristic function 3.2.4 of a VG distribution is infinitely divisible. Thus, we can define a VG process :

$$X = \{X_t^{VG}, t \geq 0\},$$

as the process which starts at zero, and has independent and stationary increments (Wim Schoutens [72]). The increment  $X_{t+z} - X_z$  follows a VG ( $\sigma\sqrt{t}, \frac{\nu}{t}, t\theta$ ) law over interval  $[z, t+z]$ . The characteristic function of a VG process is given by the equation (3.2.4) :

$$\begin{aligned} \mathbb{E}\{e^{i\langle v, X_t^{VG} \rangle}\} &= \phi^{VG}(v; \sigma\sqrt{t}, \frac{\nu}{t}, t\theta) \\ &= (\phi^{VG}(v; \sigma, \nu, \theta))^t \\ &= \left(1 - iv\theta\nu + \frac{1}{2}\sigma^2\nu v^2\right)^{-\frac{t}{\nu}}. \end{aligned} \quad (3.2.5)$$

Hélyette Geman [38] also shows that the VG process can be expressed as the difference of two independent gamma processes:

$$X(t) = G_+(t) - G_-(t),$$

where  $G_+(t)$  can be seen as the price change resulting from "positive" shocks and  $G_-(t)$  "negative" shocks. Hélyette Geman [38] rewritten the equation (3.2.4) as follows :

$$\left(1 - iv\theta\nu + 0.5\sigma^2\nu v^2\right)^{-1} = \left(1 - iv\chi_+\right)^{-1} \left(1 + iv\chi_-\right)^{-1}.$$

where

$$\chi_+ - \chi_- = \theta\nu; \quad \text{and} \quad \chi_+\chi_- = \frac{\sigma^2\nu}{2}. \quad (3.2.6)$$

The terms (3.2.6) can also be written by :

$$\chi_+ = \left(\sqrt{\frac{1}{4}\theta^2\nu^2 + \frac{1}{2}\sigma^2\nu} - \frac{1}{2}\theta\nu\right)^{-1} > 0 \quad (3.2.7)$$

$$\chi_- = \left(\sqrt{\frac{1}{4}\theta^2\nu^2 + \frac{1}{2}\sigma^2\nu} + \frac{1}{2}\theta\nu\right)^{-1} > 0. \quad (3.2.8)$$

The fact that the VG process can be expressed as the difference of two independent gamma process  $\chi_-$  and  $\chi_+$  implies that the VG process is a finite variation processes (Hélyette Geman [38]). However, the process  $\chi_-$  and  $\chi_+$  being negative and positive allow the determination of the VG density which is given in the following form:

$$\nu_{VG}(y) = \begin{cases} C \frac{\exp(-My)}{y} & y > 0 \\ C \frac{\exp(-G|y|)}{|y|} & y < 0 \end{cases}$$

where

$$C = \frac{1}{\nu}; G = \frac{1}{\chi_-}; M = \frac{1}{\chi_+}.$$

When we look at the moments of the VG model written in table (3.2.2), we observe that the parameter  $\theta$  has an influence on skewness. A negative value of  $\theta$  leads to a lower value of  $G$ , as well as negative skewness. If  $\theta = 0$  and  $G = M$ , the distribution of the VG model is symmetric [Hélyette Geman [38],pg:18]. The parameter  $\nu$  controls the kurtosis which is equal to  $3(1 + \nu)$  if  $\theta = 0$  (in the absence of a skew).

**Table 3.3:** Table of moments of the VG process

Name	Moments of the VG( $\sigma, \theta, \nu$ ) model	Moments of the VG( $C, G, M$ ) model
Means	$\theta t$	$Ct(G - M) / MG$
Variance	$\sigma^2 t + \theta^2 \nu t$	$Ct(G^2 + M^2) / (MG)^2$
Skewness	$\theta \nu (3\sigma^2 + 2\nu\theta^2) / (\sigma^2 + \nu\theta^2)^{3/2}$	$2C^{-1/2}(G^3 - M^3) / (G^2 + M^2)^{3/2}$
Kurtosis	$3(1 + 2\nu - \nu\sigma^4(\sigma^2 + \nu\theta^2)^{-2})$	$3(1 + 2C^{-1}(G^4 + M^4) / (M^2 + G^2)^2)$

### 3.3 CGMY process

In section 3.2.2 and 3.2 we saw that the VG process is of infinite activity and finite variation, while the NIG process is of infinite activity and infinite variation. In order to represent the full spectrum of different values of the parameters set, Carr,P, Hélyette Geman, Madan.Dilip B, and Marc Yor [25] introduced the following Lévy density:

$$\nu_{CGMY}(x) = \begin{cases} C \frac{\exp(-G|x|)}{|x|^{1+Y}} & x < 0 \\ C \frac{\exp(-Mx)}{x^{1+Y}} & x > 0 \end{cases}$$

The parameter  $Y$  determines the structure of the process for CGMY model and also the characterisation of its Lévy density. When  $Y < 0$ , the integral of the Lévy density

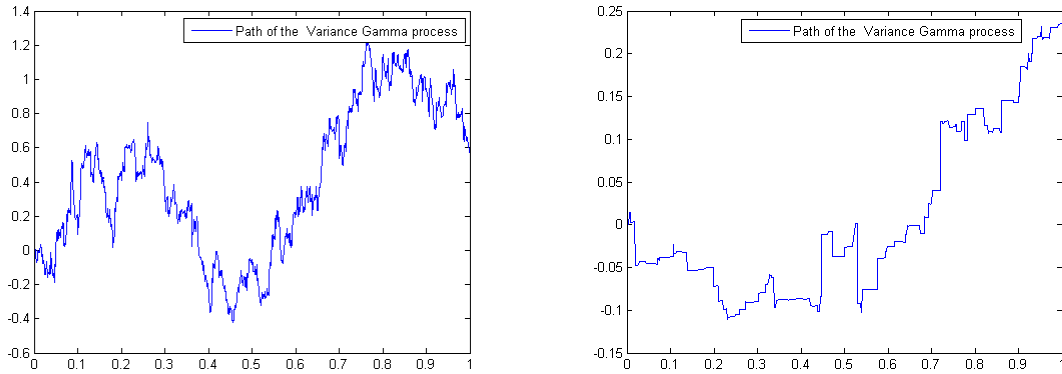


**Figure 3.3:** The ordinary trajectories of the Variance Gamma process with the parameters  $\nu = 0.25, 0.05, \sigma = 0.15$  and  $\theta = 0.005$ , the number of simulation  $N = 1000$  and the time  $T = 1$ . This trajectory is simulated using the algorithm A.2.1.

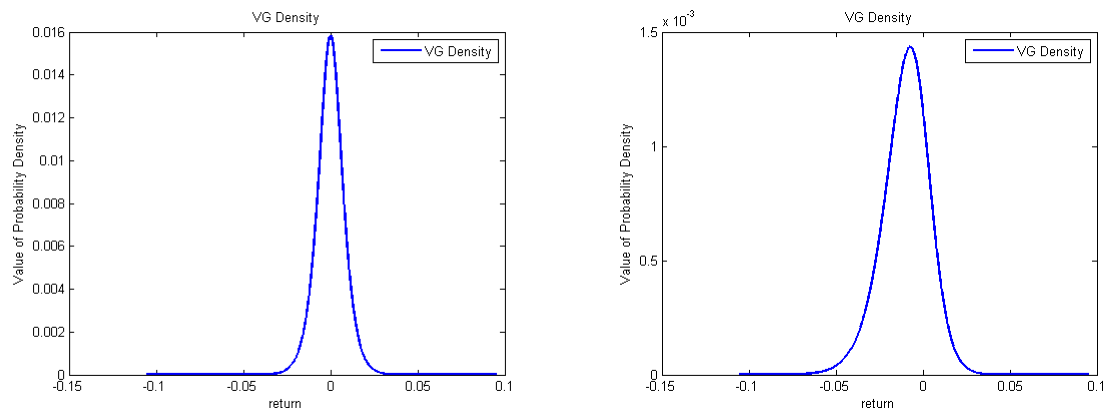


**Figure 3.4:** The ordinary Variance Gamma density with the parameters  $C = 3, G = 3$  and  $M = 3$  and  $C = 5, G = 2$  and  $M = 3$

over the interval is finite. Concurrently, the product of the Lévy density and integral of  $|x|$  is also finite, and implies that the CGMY model has finite activity, like a compound Poisson process (see Hélyette Geman [38]). For  $Y = 0$ , we obtain the VG process. For  $Y \in (0, 1)$  we obtain a process of finite variation and infinite activity. If  $Y \in (1, 2)$  we have a process of infinity activity and infinite variation like an NIG process.

### 3.3.1 Properties and characteristic function of CGMY

In this subsection we discuss how to determine the characteristic function of a CGMY model. To determine the characteristic function of a CGMY model, we need to give

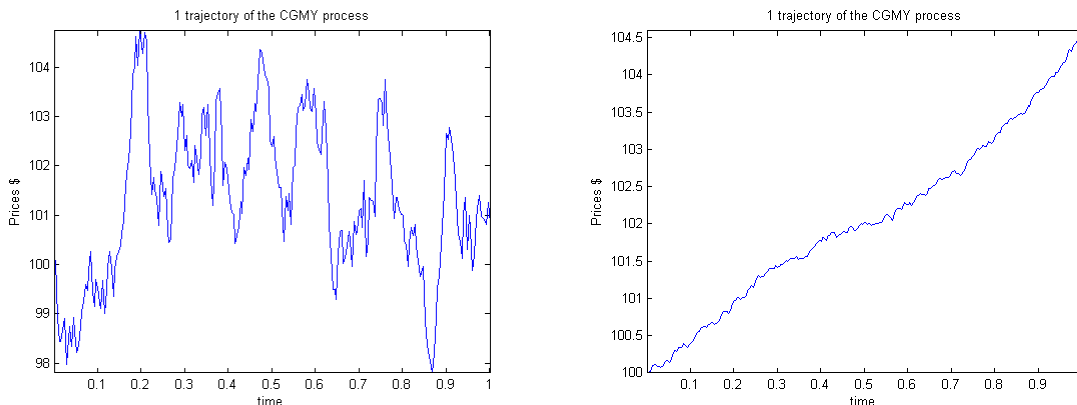


**Figure 3.5:** The trajectories of the CGMY process with the parameters  $C = 0.0332$ ,  $G = 0.4614$ ,  $M = 15.6995$ ,  $Y = 1.1882$  and  $C = 0.0332$ ,  $G = 0.4614$ ,  $M = 15.6995$ ,  $Y = 0.2882$ . These trajectories are simulated using the algorithm A.2.3.

some conditions to the parameter of  $Y$ . Let us integrate the Lévy density under finite value: This means for  $Y \in (0, 1)$  we have:

$$\int_{(\infty, 0) \cup (0, -\infty)} v_{CGMY}(dx) = C \left\{ \int_{x>0} \frac{e^{-Mx}}{x^{1+Y}} dx + \int_{x<0} \frac{e^{Gx}}{(-x)^{1+Y}} dx \right\}, \quad (3.3.1)$$

by taking  $t = Mx$  and  $r = -Gx$ , the equation (3.3.1) becomes

$$\int_{\mathbb{R} \setminus \{0\}} v_{CGMY}(dx) = C \left\{ \int_{t>0} \frac{e^{-t} M^Y}{t^{1+Y}} dt + \int_{r>0} \frac{e^{-r} G^Y}{r^{1+Y}} dr \right\}. \quad (3.3.2)$$

By using the definition of Gamma function with positive real parts, the equation (3.3.2) reduces at:

$$\int_{\mathbb{R} \setminus \{0\}} v_{CGMY}(dx) = C \Gamma(-Y) (M^Y + G^Y). \quad (3.3.3)$$

This implies that the process has a finite number of aggregate arrival rate (jumps of all sizes). Consequently, the process also has a finite activity and finite variation when  $Y < 0$ . Furthermore, if the value of  $Y$  exceeds zero and the integral (3.3.1) diverges in the region of zero, we obtain the number of infinite small jumps. Moreover, when we consider the case where  $Y < 1$  we may expect that the sum of all jumps can be finite since

$$\int_{\mathbb{R} \setminus \{0\}} |x| v_{CGMY}(dx) = C \Gamma(-Y + 1) (M^{Y-1} + G^{Y-1}) < \infty. \quad (3.3.4)$$

When  $Y > 1$  thus, we have a process of finite quadratic variation but an infinite total variation Carr.P, Hélyette Geman, Madan.Dilip B, and Marc Yor [25]:

$$\int_{\mathbb{R} \setminus \{0\}} x^2 v_{CGMY}(dx) = C\Gamma(-Y+2)(M^{Y-2} + G^{Y-2}) < \infty. \quad (3.3.5)$$

Hence, the parameter  $Y$  must be smaller than two ( $Y < 2$ ) so that the Lévy density can be integrated  $|x^2|$  in the region of zero. Carr.P, Hélyette Geman, Madan.Dilip B, and Marc Yor [25] assumed that both the parameters  $C$  and  $Y$  may not change for an equivalent measure change. Therefore, we can compute the characteristic function of CGMY model under the parameters  $(C, G, M, Y)$  using the Lévy-Kinchin presentation with a truncate function  $h(x) = 1$  (2.5.6):

$$\begin{aligned} \phi_{CGMY}(v, t, C, G, M, Y) &= \exp \left[ i\gamma y + t \int_{\mathbb{R}/0} \left( e^{iyx} - 1 - iyx \right) v_{CGMY}(dx) \right] \\ &= \exp \left[ i\gamma y + tC \int_{\mathbb{R}/0} \left( e^{iyx} - 1 - iyx \right) \left( \frac{e^{-Mx}}{x^{1+Y}} 1_{x>0} + \right. \right. \\ &\quad \left. \left. \frac{e^{Gx}}{|x|^{1+Y}} 1_{x<0} \right) (dx) \right]. \end{aligned} \quad (3.3.6)$$

If we expend the exponential

$$e^{iyx} = \sum_{n=0}^{\infty} \frac{(iyx)^n}{n!} = 1 + iyx + \sum_{n=2}^{\infty} \frac{(iyx)^n}{n!}.$$

We can rewrite the above expression (3.3.6) as follows:

$$\begin{aligned} \phi_{CGMY}(v, t, C, G, M, Y) &= \exp \left[ i\gamma y + tC \sum_{n=2}^{\infty} \frac{(iy)^n}{n!} \left( \int_0^{+\infty} e^{-Mx} x^{n-1-Y} dx + \right. \right. \\ &\quad \left. \left. \int_{-\infty}^0 (-1)^n e^{Gx} x^{n-1-Y} dx \right) \right] \end{aligned}$$

Taking  $u = -xG$  and  $v = xM$ :



$$\begin{aligned}
\phi_{CGMY}(v, t, C, G, M, Y) &= \exp \left[ i\gamma y + tC \sum_{n=2}^{\infty} \frac{(iy)^n}{n!} M^{Y-n} \left( \int_0^{+\infty} e^{-v} v^{n-1-Y} dv \right. \right. \\
&\quad \left. \left. + (-1)^n G^{Y-n} \int_0^{+\infty} e^{-u} u^{n-1-Y} du \right) \right] \\
&= \exp \left[ i\gamma y + tC \left( \sum_{n=2}^{\infty} \frac{(iy)^n}{n!} M^{Y-n} \Gamma(n-Y) + \right. \right. \\
&\quad \left. \left. \sum_{n=2}^{\infty} \frac{(iy)^n}{n!} (-1)^n G^{Y-n} \Gamma(n-Y) \right) \right] \\
&= \exp \left[ i\gamma y + tC \left( M^Y \sum_{n=2}^{\infty} \frac{(iy/M)^n}{n!} \Gamma(n-Y) + \right. \right. \\
&\quad \left. \left. G^Y \sum_{n=2}^{\infty} \frac{(iy/G)^n}{n!} (-1)^n \Gamma(n-Y) \right) \right], \tag{3.3.7}
\end{aligned}$$

we can write this sum  $\sum_{n=2}^{\infty} \frac{(iy/M)^n}{n!} \Gamma(n-Y)$  by using the following form:

$$\begin{aligned}
\sum_{n=2}^{\infty} \frac{(iy/M)^n}{n!} \Gamma(n-Y) &= \frac{1}{2!} \left( \frac{iy}{M} \right)^2 \Gamma(2-Y) + \frac{1}{3!} \left( \frac{iy}{M} \right)^3 \Gamma(3-Y) + \\
&\quad \frac{1}{4!} \left( \frac{iy}{M} \right)^4 \Gamma(4-Y) + \dots \\
&= \Gamma(2-Y) \left[ \frac{1}{2!} \left( \frac{iy}{M} \right)^2 + \frac{1}{3!} (2-Y) \left( \frac{iy}{M} \right)^3 + \right. \\
&\quad \left. \frac{1}{4!} (2-Y)(3-Y) \left( \frac{iy}{M} \right)^4 + \dots \right]. \tag{3.3.8}
\end{aligned}$$

Using the property that the  $\Gamma(n+1) = n\Gamma(n)$ , we can then transform

$\Gamma(2-Y) = Y(Y-1)\Gamma(-Y)$  since  $Y < 2$ . Therefore we can write the above expression (3.3.8) as follows

$$\begin{aligned}
\sum_{n=2}^{\infty} \frac{(iy/M)^n}{n!} \Gamma(n-Y) &= \Gamma(-Y) \left[ Y(Y-1) \frac{1}{2!} \left( -\frac{iy}{M} \right)^2 + \frac{1}{3!} Y(Y-1)(Y-2) \left( -\frac{iy}{M} \right)^3 + \right. \\
&\quad \left. \frac{1}{4!} Y(Y-1)(Y-2)(Y-3) \left( -\frac{iy}{M} \right)^4 + \dots \right]. \tag{3.3.9}
\end{aligned}$$

The power series can be written as :

$$(1 + y)^n = 1 + ny + ny(y - 1) \frac{1}{2!} y^2 + \dots$$

Thus, the expression (4.1.1) can be written again

$$\sum_{n=2}^{\infty} \frac{(iy/M)^n}{n!} \Gamma(n - Y) = \Gamma(-Y) \left[ \left(1 - \frac{iy}{M}\right)^Y - 1 + \frac{iyY}{M} \right]. \quad (3.3.10)$$

Using the same method for the sum  $\sum_{n=2}^{\infty} \frac{(iy/G)^n}{n!} (-1)^n \Gamma(n - Y)$  and if we substitute the two sums in (3.3.7) we get :

$$\begin{aligned} \phi_{CGMY}(v, t, C, G, M, Y) &= \exp \left[ i\gamma y + tC \left( M^Y \Gamma(-Y) \left( \left(1 - \frac{iy}{M}\right)^Y - 1 + \frac{iyY}{M} \right) \right. \right. \\ &\quad \left. \left. + G^Y \Gamma(-Y) \left( \left(1 - \frac{iy}{G}\right)^Y - 1 + \frac{iyY}{G} \right) \right) \right] \\ &= \exp \left[ i\gamma y + tC \Gamma(-Y) \left( (M - iy)^Y + (G + iy)^Y - G^Y - M^Y \right. \right. \\ &\quad \left. \left. + iyY(-G^{Y-1} + M^{Y-1}) \right) \right] \end{aligned} \quad (3.3.11)$$

Taking  $\gamma = -tCY\Gamma(-Y)(-G^{Y-1} + M^{Y-1})$ , it follows the characteristic function

$$\phi_{CGMY}(v, t, C, G, M, Y) = \exp[tC\Gamma(-Y)((M - iv)^Y - M^Y + (G + iv)^Y - G^Y)]. \quad (3.3.12)$$

Using the characteristic function  $\phi_{CGMY}$  and the gamma relation  $\Gamma(n + 1) = n\Gamma(n)$  results in the following cumulant properties:

**Table 3.4:** Table of moments of the CGMY process

Name of features	Moments of CGMY model
CGMY characteristic	$\exp[tC\Gamma(-Y)((M - iv)^Y - M^Y + (G + iv)^Y - G^Y)]$
Lévy density	$C(e^{Ax-B x })/ x ^{1+Y}$ with $A = (G - M)/2, B = (G + M)/2$
Mean	$Ct(M^{Y-1} - G^{Y-1})\Gamma(1 - Y)$
Variance	$Ct(M^{Y-2} - G^{Y-2})\Gamma(2 - Y)$
Skewness	$(Ct(M^{Y-3} - G^{Y-3})\Gamma(3 - Y))/[C(M^{Y-2} + G^{Y-2})\Gamma(2 - Y)]^{\frac{3}{2}}$
Kurtosis	$3 + (Ct(M^{Y-4} - G^{Y-4})\Gamma(4 - Y))/[C(M^{Y-2} + G^{Y-2})\Gamma(2 - Y)]^{2t}$

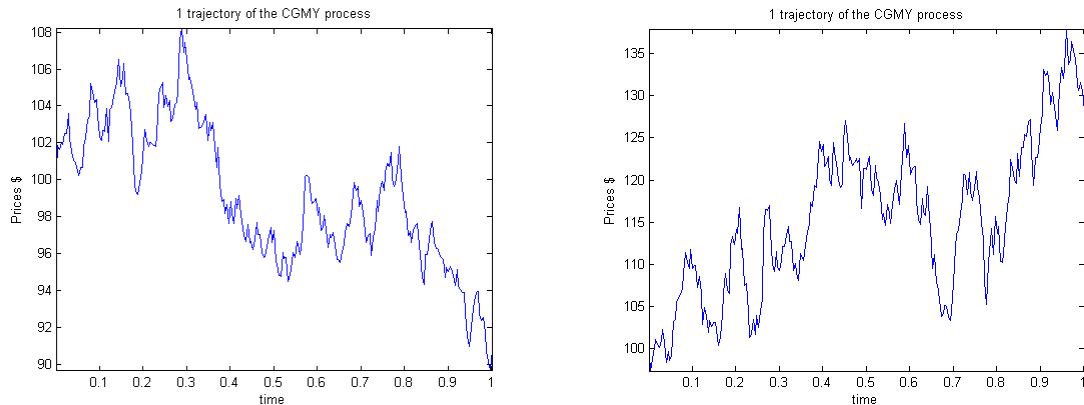


**Figure 3.6:** The trajectories of the CGMY process with the parameters  $C = 0.0332$ ,  $G = 0.4614$ ,  $M = 15.6995$ ,  $\gamma = 1.2882, 1.5882$  and  $T = 1$ . This trajectory is simulated using the algorithm A.2.3.

### 3.3.1.1 Remark and origin

Carr, P., Hélyette Geman, Madan, Dilip B., and Marc Yor [25] introduced the CGMY process (which has the properties of infinite activity, finite activity and infinite variation) to analyse the stochastic properties of asset returns, and to obtain a model which is more flexible than VG process. Thus, they added an additional parameter  $\gamma$  to the VG model (Wim Schoutens [72]). The four parameters discussed above were studied by Carr et al [25] and were generalized by six-parameters in Carr, P., Hélyette Geman, Madan, Dilip B., and Marc Yor [23]. They split the two parameters,  $C$  and  $\gamma$ , into two negative parts  $C_n$  and  $\gamma_n$  which correspond to the negative part of Lévy measure, and also two positive parts  $\gamma_p$  and  $C_p$  which correspond to the positive part of a Lévy measure.

The following authors Ismo Koponen [51] and Svetlana I Boyarchenko and SZ Levendorskii [20]; Jean-Philippe Bouchaud and Marc Potters [15], Rama Cont, Marc Potters, and Jean-Philippe Bouchaud [28], Andrew Matacz [58], and Svetlana I Boyarchenko and SERGEI Z LEVENDORSKII [18] and [19] refer to the family of a CGMY distribution models by Kobol (Wim Schoutens [72]), which was originally called a truncated Lévy process (TLP), but Shiryaev changed the name given by Kobol to avoid confusion (Wim Schoutens [72]).

### 3.4 Lévy Market Model

In the Black-Scholes framework the path of the underlying asset price follows an exponential Brownian motion with drift  $\mu$ , and is given by:

$$S_t = S_0 \exp\left(\left(\mu - \frac{1}{2}\sigma^2\right)t + \sigma W_t\right) \quad (3.4.1)$$

where  $S_0 > 0$  is an initial price and  $W_t$  a standard Brownian motion. Here, we assume that the underlying asset follows an exponential Lévy model

$$S_t = S_0 \exp(X_t) \quad (3.4.2)$$

where  $(X_t)$  is a Lévy process.

We can see that the log-return of the underlying asset is modelled by NIG, VG and CGMY distributions instead of the normal distribution (Wim Schoutens [73], pg:31):

$$\log S_{t+h} - \log S_t = X_{t+h} - X_t \sim (NIG(\alpha, \beta, \delta), VG(\sigma, \theta, \nu), CGMY(C, G, M, Y)). \quad (3.4.3)$$

Note that under the Black-Scholes framework, the log-return of an underlying asset is given by:

$$\log S_{t+1} - \log S_t \sim Normal\left(\mu - \frac{1}{2}\sigma^2, \sigma^2\right). \quad (3.4.4)$$

The expression (3.4.4) shows that the Black-Scholes framework moves easily from the historical world to the risk neutral by substituting the drift  $\mu$  by the difference between an interest rate  $r$  and a dividend note  $q$  (Wim Schoutens [73], pg:31):

$$S_t = S_0 \exp\left(\left(r - q - \frac{1}{2}\sigma^2\right)t + \sigma W_t\right). \quad (3.4.5)$$

It is difficult to shift between the historical world and the risk-neutral world when using more advanced models, such as the VG, NIG and CGMY, because there are an infinite number of possible measure changes (Wim Schoutens [73], pg:31). For example, the mean-correcting change measure is an easy transformation where the pure jump models (VG, NIG and CGMY model) are shifted in order to find the martingale (Wim Schoutens [73], pg:31):

$$S_t = S_0 \exp\left((r - q - \omega)t + X_t\right) \quad t \geq 0,$$

where (3.4.6)

$$\omega = \ln \phi^{(VG, CGMY, NIG)}(-i). \quad (3.4.7)$$

Wim Schoutens [72] defined a mean-correcting martingale measure as  $m_{new} = r - q - \omega$  and it is chosen such that the discount stock prices  $\exp(-(r - q)t)S$  is a martingale (Wim Schoutens [72], pg:79). For the pure jump models (VG,NIG and CGMY models) the mean-correcting martingale measure can be obtained as follows:

$$m_{new} = r - q - \ln \phi^{(VG,CGMY,NIG)}(-i), \quad (3.4.8)$$

where  $\phi^{VG,CGMY,NIG}$  are the characteristic functions of the VG, NIG and CGMY models(see 3.3.12,3.2.5 and 3.1.2) discussed in the previous sections. Let us compute the values of mean-correcting martingale measure for our Lévy models using the equation 3.4.8: For a VG process is given as follows:

$$\begin{aligned} m_{new}^{VG} &= (r - q) - \ln[\phi^{VG}(v; \sigma, \nu, t\theta)(-i)], \\ &= (r - q) - \ln \left( 1 - v\theta\nu + \frac{1}{2}\sigma^2\nu v^2 \right)^{-\frac{1}{\nu}} \\ &= (r - q) + \frac{1}{\nu} \ln \left( 1 - v\theta\nu + \frac{1}{2}\sigma^2\nu v^2 \right). \end{aligned} \quad (3.4.9)$$

We also compute for a NIG process as follows:

$$\begin{aligned} m_{new}^{NIG} &= (r - q) - \ln \phi_{NIG}(v, \beta, \alpha, \delta)(-i) \\ &= (r - q) - \ln \left[ \exp \left\{ -\delta(\sqrt{\alpha^2 - (\beta + v)^2} - \sqrt{\alpha^2 - \beta^2}) \right\} \right] \\ &= (r - q) + \delta(\sqrt{\alpha^2 - (\beta + v)^2} - \sqrt{\alpha^2 - \beta^2}). \end{aligned} \quad (3.4.10)$$

And for the CGMY process is given as follows:

$$\begin{aligned} m_{new}^{CGMY} &= (r - q) - \ln \phi_{CGMY}(v, C, G, M, Y)(-i) \\ &= (r - q) - \ln \exp[\text{C}\Gamma(-Y)((M - iv)^Y - M^Y + (G + iv)^Y - G^Y)] \\ &= (r - q) - \text{C}\Gamma(-Y)((M - v)^Y - M^Y + (G + v)^Y - G^Y). \end{aligned} \quad (3.4.11)$$

The table below presents the values of mean-correcting martingale measure for our Lévy models.

In order to price derivative assets, the models need to satisfy the no-arbitrage condition. In order to avoid models with arbitrage, one needs to obtain an equivalent martingale measure. Next, we discuss the fundamental properties of asset prices.

**Table 3.5:** Mean-correcting martingale measure for some Lévy models

Model	$m_{new}$
CGMY	$(r - q) - \text{CT}(-Y)((M - v)^Y - M^Y + (G + v)^Y - G^Y)$
VG	$(r - q) + \frac{1}{v} \ln \left( 1 - v\theta v + \frac{1}{2}\sigma^2 v^2 \right)$
NIG	$(r - q) + \delta(\sqrt{\alpha^2 - (\beta + v)^2} - \sqrt{\alpha^2 - \beta^2})$

### 3.4.1 Equivalent Martingale Measure

An arbitrage is strategy with zero initial cost, zero probability of loss, and strictly positive probability of profit. In the case of arbitrage-free, the price of a financial asset is given by an expectation under an appropriate risk-neutral measure (probability measure). To explain arbitrage-free, we need to discuss the following theorem:

**Theorem 3.4.1** (Fundamental Theorem of Asset Pricing (Rama Cont and Peter Tankov [29])). *The market model defined by  $(\Omega, \mathcal{F}, (\mathcal{F}_t), \mathbb{P})$  and asset prices  $(S_t)_{t \in [0, T]}$  is only arbitrage-free if there exists a probability measure  $\mathbb{Q} \sim \mathbb{P}$  such that the discounted assets  $(\hat{S}_t)_{t \in [0, T]}$  are martingale with respect to  $\mathbb{Q}$ .*

Given the above theorem, the existence of an equivalent martingale measure implies the non existence of arbitrage in the models. This raises the question as to the best way of choosing an equivalent martingale measure. Choosing an equivalent martingale measure is discussed extensively by the following authors Rama Cont and Peter Tankov [29], Wim Schoutens [72] and will not be explained here. We limit our focus to an easy method for obtaining an equivalent measure, the mean-correcting martingale measure (EMM) discussed previously.

Empirical research suggests that the Black-Scholes model poorly explains the statistical properties of financial time series. For instance, the different levels of implied volatility for varying maturities and strikes cannot be incorporated into the Black-Scholes model (Rama Cont and Peter Tankov [29]). Thus, we need a model with a rich structure to incorporate such features. In the next section, we estimate the density of a historic time series data set using the pure jump model to show why this model is preferred to the Black-Scholes model as a density estimator.

## 3.5 Density Estimating of S&P 500 time series data

In this section we consider the adjusted daily closing prices of S&P500 time series data closing from 3/01/1930 to 3/03/2008 taken from yahoo finance, and we discuss the

fitting of the daily log-return of the S&P500 time series data to a specific distribution. First, we compute the autocorrelation function, and the *log*-return of the S&P500 time series data and then we fit the log-returns to the distribution of the VG, CGMY and NIG models and also to the normal distribution. Below we show how to compute an autocorrelation function and we also estimate the density of the NIG, VG and CGMY distributions.

### 3.5.1 Autocorrelation function (ACF)

The autocorrelation function is used to check the randomness in a data set. This randomness can be verified by computing the autocorrelation of the empirical data at any time lag (George EP Box, Gwilym M Jenkins, and Gregory C Reinsel [17]). We define the ACF as follows:

Given a stationary time series  $\{X_t\}$ . The autocorrelation function of  $\{X_t\}$  at lag  $h$  is given:

$$\rho_X(h) = \frac{\gamma_X(h)}{\gamma_X(0)} = \text{Corr}(X_{t+h}, X_t), \quad (3.5.1)$$

where  $\gamma_X(h) = \text{Cov}(X_{t+h}, X_t)$  is the auto-covariance function of  $\{X_t\}$  at lag  $h$ . Further details of this method can be found in (Peter J Brockwell and Richard A Davis [22]).

We plotted the sample autocorrelation function of the daily log-return and the square daily log –return for the S&P500 time series data. Figure 3.7 shows that the ACF of the daily log –return is uncorrelated, while figure 3.8 shows that the ACF of the square daily log –return for S&P500 time series data rapidly declines as the lag increases. That means the square daily log-return for S&P500 time series data are correlated, they are not independent, and cannot be modelled by a process with independent increments. However, we can consider using the pure jump Lévy models to model the empirical daily log –return of S&P500 time series data, since the skewness and kurtosis of this data are  $-0.3531$  and  $22.4401$ , which differs from the values  $0$  and  $3$  of the skewness and kurtosis of the Gaussian distribution.

### 3.5.2 Model Density Estimation

Before estimating the model densities for our models, we need to know if the density function of the distribution and their parameters are known. In some cases, the density function of the distribution for the models either does not exist or has a very complex form, as was the case of the models used in this chapter. Thus, we needed to use a nu-

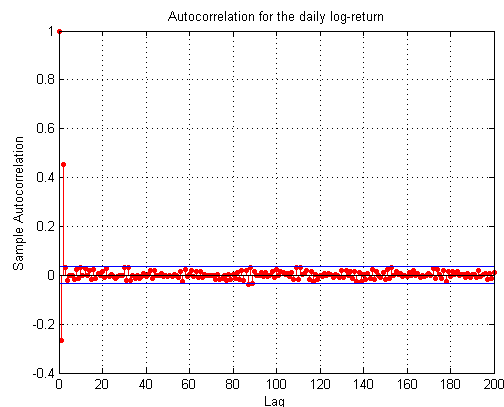


**Figure 3.7:** Autocorrelation for the daily log-return

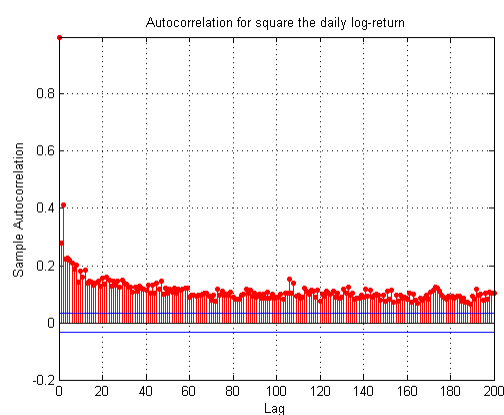


**Figure 3.8:** Autocorrelation for square of the daily log-return

merical approach, where the characteristic function of our models are used to estimate the model densities. The outline of the procedure is given as follows:

- i) The Fast Fourier transform introduced by Peter Carr and Dilip Madan [24] (discussed in Chapter 4), is used to invert the characteristic functions of the NIG, VG and CGMY models to determine their density functions.
- ii) The density functions are then fitted to the daily log-returns of the S&P500 time series data using maximum likelihood estimation (MLE) to obtain the values of our model parameters. The (MLE) procedure is discussed in Chapter 4. We also note that to obtain the good values for our parameters using the optimisation procedure, we needed to estimate the initial optimisation parameters from historical data (Rama Cont and Peter Tankov [29]).



- iii) After computing the values of the model parameters by MLE, they need to be plugged back into the characteristic function for each model price using the FFT technique, and then the density function graphs are plotted for each model with historical data using QQ-plots.

### 3.5.3 Test of the Fitness for the Distribution of the Models

In this section, we tested the performance of the model density for each model. To do this, we first assessed the fitness of the model density graphically (QQ-plots), and then used Kolmogorov-Smirnov ( $K - S$ ) and Anderson and Darling ( $A - D$ ) tests (explained later in subsection 3.5.3.3); to verify the results.

#### 3.5.3.1 Graphical Test

Graphical tools fulfil an important role in statistical analyses. There are numerous graphical tools that can be used in statistical analysis to test the fit of model density to the S&P500 time series data. A popular graphical test is the Quantile-Quantile plot (QQ-plot). Let  $G$  be a cumulative distribution function and  $X_{1,m}, \dots, X_{m,m}$  a sequence of i.i.d random variable rank in order  $X_{1,m} \leq \dots \leq X_{m,m}$ . We can define the QQ-plot as a simple graphical method for comparing two sets of sample quantiles, and given in the following set (Sergio M Focardi and Frank J Fabozzi [37] and Albyn Jones [47]):

$$\left\{ X_{j,m}, G^{\leftarrow} \left( \frac{m-j+1}{m+1} \right) : j = 1, \dots, m \right\}. \quad (3.5.2)$$

where  $G^{\leftarrow}$  is an inverse of the cumulative distribution function,  $X_{j,m}$  the sequence of i.i.d random variable.

In other part, the Glivenko-Cantelli theorem (Sergio M Focardi and Frank J Fabozzi [37], pg : 370) states that: " if the sample  $X_{1,m}, \dots, X_{m,m}$  are independent draws from for the distribution function  $G(\cdot; \theta)$ , then the empirical distribution  $G_m$  tends to  $G$  for  $m \rightarrow \infty$  as":

$$\Delta_m = \sup_{x \in \mathbb{R}} |G_m(x) - G(x)| \xrightarrow{a.s.} 0, \quad \text{for } m \rightarrow \infty.$$

The above Glivenko-Cantelli theorem and quantile transform allow us to conclude that the QQ-plot must be approximately linear (Sergio M Focardi and Frank J Fabozzi [37], pg : 374). The QQ-plot allows a verification of the statistical hypotheses by confirming the approximate linearity of the plot (Sergio M Focardi and Frank J Fabozzi [37]).

Figures 3.9, and 3.10 represent the QQ-plot of the log-return of S&P500 time series data with the probability density of the VG, NIG, CGMY models and the normal distribution. Studying these plots; confirms that our model densities fit the daily log-return of

S&P500 time series data better than a normal distribution. However, apart from justifying how well the model densities fit the empirical data, we also need to run a statistical test on those model densities, and this is the objective of the next section.

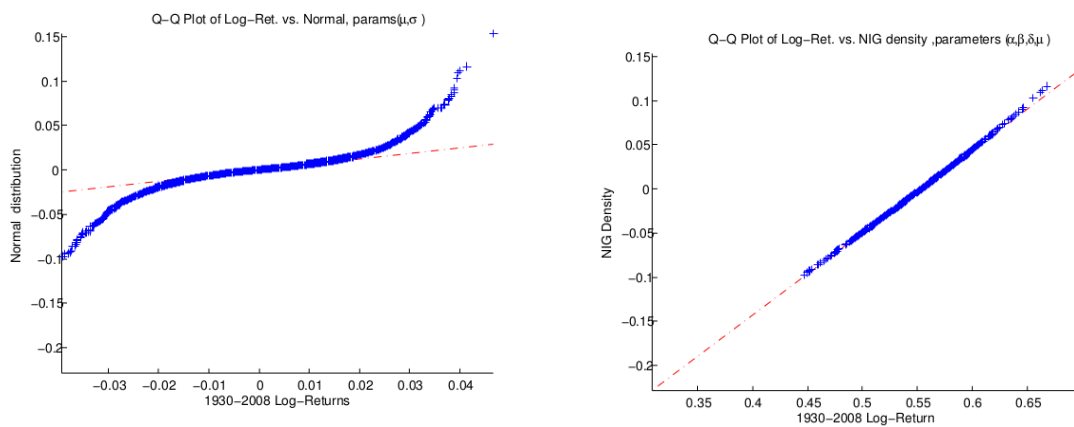


Figure 3.9: QQ-plot fitted Normal distribution and NIG distribution to daily log-return

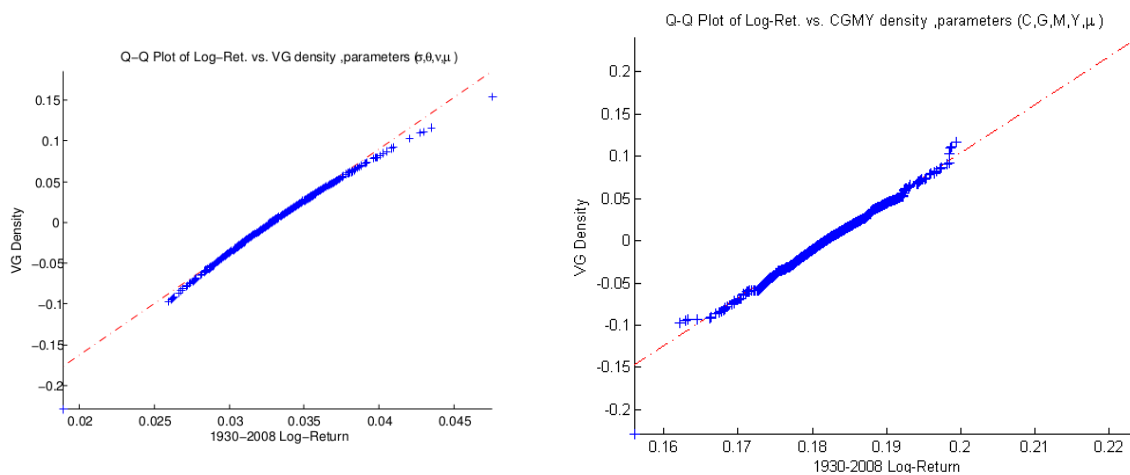


Figure 3.10: QQ-plot fitted VG distribution and CGMY distribution to daily log-return

### 3.5.3.2 Statistical test

In this thesis we focus on two statistical tests, namely the Kolmogorov-Smirnov test (K-S) and the Anderson & Darling statistics (A-D).

### 3.5.3.3 Kolmogorov-Smirnov test (K-S)

The Kolmogorov-Smirnov test is a non-parametric test which can be used to compare two distributions. This test is based on comparison between two distances, the fitted distribution and empirical distribution of a log-return data set. Let  $Z_1, \dots, Z_n$  be an i.i.d. sample data and  $\mathbb{P}$  an unknown distribution, and we would like to test the hypothesis that  $\mathbb{P}$  is equal to a particular distribution  $\mathbb{P}_0$  [3]. We can represent this as follows:

$$H_0 : \mathbb{P} = \mathbb{P}_0, \quad H_1 : \mathbb{P} \neq \mathbb{P}_0.$$

To test this hypothesis, we need to obtain the value of the Kolmogorov-Smirnov test. Let  $F_{fit}$  be a fitted distribution and  $F_m$  an empirical distribution of a data set. We can define the Kolmogorov-Smirnov test as the largest vertical difference between  $F_{fit}$  and  $F_m$  [4]. It is described as follows:

$$KS = \sup_{z \in \mathbb{R}} |F_m(z) - F_{fit}(z)|.$$

where the  $\sup Z$  is a supremum of  $Z$ .

The expression of the empirical distribution of a data set  $F_m$  with  $m$  i.i.d observation  $Z_j$  is given by :

$$F_m(z) = \frac{1}{m} \sum_{j=1}^m I_{Z_j \leq z}$$

where the values  $Z_1, Z_2, \dots, Z_m$  are i.i.d. The function  $I_{Z_j \leq z}$  is a an indicator function which is equal to 1 if  $Z_j \leq z$  or zero otherwise. An important characteristic of K-S test is that its distribution does not in itself depend on the underlying cumulative distribution function that is being tested. Additionally, the Kolmogorov-Smirnov test performs better with a large range of distributional assumptions.

### 3.5.3.4 Anderson and Darling Test (A-D)

Theodore W Anderson and Donald A Darling [8] introduced the Anderson & Darling test (A-D); which is a general test used to compare two distribution functions. This test is based on comparing the fit of an observed cumulative distribution functions to an

expected cumulative distribution function [4]. Let  $F_{fit}$  be a fitted cumulative distribution function and  $F_n$  an expected cumulative distribution function. According to Theodore W Anderson and Donald A Darling [8], the A-D test is defined by:

$$AD = \sup_{z \in \mathbb{R}} \frac{|F_n(z) - F_{fit}(z)|}{\sqrt{F_{fit}(z)(1 - F_{fit}(z))}}.$$

The A-D test focuses on the fit in the tails by amplifying the deviation as compared to the K-S test. First, we test the density function of the distribution of our models to check if these results correspond with ones obtained with graphical tests.

Table 3.6 reports the results of the statistical tests. It gives the values of the distributions of the NIG, VG and CGMY model obtained with the K-S and A-D tests which are smaller than the one obtained with a normal distribution. These results correspond with those on the graphs. Therefore, we can conclude that the pure jumps models (VG, NIG and CGMY models) fit our empirical data better than their Gaussian counterpart, while CGMY model provides the best fit for the empirical data.

**Table 3.6:** Table of K-S and A-D Statistic value

Model distributions	K-S statistic	A-D statistic
Normal Distribution	0.0239	0.0749
NIG	0.0180	0.0485
VG	0.0179	0.0358
CGMY	0.0164	0.0328

## Chapter 4

# Calibration of Pure Jump Model

In this chapter we discuss the procedure for estimating the risk-neutral parameters for each of the models described in Chapter 3. In calibrating a model to market prices, we seek the "best" parameters, i.e. those parameters which yield model prices that are as close as possible to the observed market prices. To perform a calibration, you need to input the observed market prices, which can be time series data or quoted option prices (Joerg Kienitz and Daniel Wetterau [49]). Here we used the S&P500 index from 18 April 2002 to December 2003 (see Wim Schoutens [72]), as our market prices. The calibration method produces estimates of the model parameters. A set of model parameters is considered optimal when the model prices best fit the observed market prices in term of an error measure (Rama Cont, Peter Tankov, et al [30]). The purpose of the calibration is to find the model parameters that are needed to value exotic options, whose prices are not quoted on the open market.

### 4.1 The Calibration Problem for a Pure Jump Model

The calibration problem is stated as follows: Let  $\{C_0(T_j, K_j), j = 1 \dots n\}$  be a set of observed market prices for a set of liquid call options at  $t = 0$ , with  $(K_j)$  a range of different strikes and  $(T_j)$  a range of maturities. And let  $S_t = \exp X_t$  be an exponential Lévy models where  $X_t$  is a Lévy process defined by the characteristic function  $(\sigma, \nu)$  "The calibration problem consists of obtaining a Lévy measure  $\nu$  and a constant  $\sigma > 0$  from a set of  $C_0(T_j, K_j)$  such that the option prices obtained with the exponential Lévy models driven by  $X$  coincide with the observed market call prices  $C_0(T_j, K_j)$  "(Rama Cont, Peter Tankov, et al[30]):

$$C_0(T_j, K_j) = C^{\sigma, \nu}(T_j, K_j), \quad \forall j \in J, \quad (4.1.1)$$

where  $C^{\sigma,\nu}(T_j, K_j)$  is the option price calculated for the Lévy process with Lévy triplet  $(\sigma, \nu, \gamma(\sigma, \nu))$ . Rama Cont, Peter Tankov, et al [30] stated that, the index set  $J$  in the most general formation need not be finite. In fact, if one know the market prices for one maturity and all strikes, one might determine a Lévy measure  $\nu$  and volatility  $\sigma$  as follows (Rama Cont, Peter Tankov, et al [30]):

- Calculate the risk-neutral  $q_T$  distribution of log price based on the formula of (Douglas and Robert [21]):

$$q_T(k) = e^{-k} \{C''(k) - C'(k)\} \quad \text{with } k = \ln K. \quad (4.1.2)$$

- Taking the Fourier transform of  $q_T$ , we may compute the characteristic function of the stock price.
- Determine a Lévy measure  $\nu$  and a volatility  $\sigma$  from the characteristic function  $\Phi_T$  (2.5.12) (Rama Cont, Peter Tankov, et al [30]). Ken-Iti Sato [71] shows that the volatility  $\sigma$  of the Gaussian component may be found in the following way:

$$\sigma^2 = - \lim_{x \rightarrow \infty} \frac{2 \log \Phi_T(x)}{Tx^2}. \quad (4.1.3)$$

We now denote  $\Theta(x) = \frac{2 \log \Phi_T(x)}{T} + \frac{\sigma^2 x^2}{2}$  which can be obtained (Ken-Iti Sato [71], equation (8.10)) by:

$$\int_1^{-1} (\Theta(x) - \Theta(x+y)) dz = 2 \int_{\mathbb{R}} e^{iuy} \left(1 - \frac{\sin y}{y}\right) \nu(dy). \quad (4.1.4)$$

The right-hand side of equation (4.1.4) is exactly the Fourier transform of the measure  $(2 - 2 \sin y/y) \nu(dy)$ . This means that a Lévy measure  $\nu$  may be obtained through the Fourier transform of  $\Theta$  (Ken-Iti Sato [71]).

If we knew the precise set of observed market prices for one maturity and all strikes, we may then deduce the model parameters for each our model, and thus we can compute the option prices for other maturities (Rama Cont, Peter Tankov, et al [30]). In this case, the option prices for any other maturity cannot give us any additional information but can only contradict the ones that we already have (Rama Cont, Peter Tankov, et al [30]). Moreover, the above procedure is similar to the Bruno Dupire [34] procedure. This procedure cannot be applied in practice for the following reasons:

- Call option prices are only available for a finite number of strikes, and this finite number may be very small. In this case, the limits and derivatives for the equations

(4.1.4) and (4.1.2) are in fact interpolation and extrapolation of the call option prices data. Thus our calibration problem (or inverse problem) is largely indeterminate (Rama Cont, Peter Tankov, et al [30]).

- When all maturities are present in the data, our calibration problem with equality constraint may not have a solution due to the model specification error. Then, the Lévy processes often fail to reproduce the term structure of implied volatility because of the stationary or homogeneous nature of these increments (Rama Cont, Peter Tankov, et al [30]).
- The presence of bid-ask spreads in market price data can also cause another difficulty. In taking the derivative of observations, like in equation (4.1.3) we can obtain the errors, and these errors can destabilise the results of the calculation.

Rama Cont, Peter Tankov, et al [30] states that by considering all these facts, it is necessary to reformulate the calibration problem as an *approximation problem*.

The rest of the chapter is organised as follows: First, we describe two calibration methods used here to obtain our model parameters. Second, we discuss the pricing formula of European option via an equivalent martingale measure. Finally, we discuss the method of the Fast Fourier transform.

## 4.2 Calibration Methods

A calibration method allows us to determine the "best" parameters (i.e. those parameters which yield model prices that are as close as possible to the observed market prices), initially from a guess, by minimizing the quadratic error between the option market prices and model prices. There are various calibration methods, but here we will focus on two: Maximum likelihood estimation and least squares estimation.

### 4.2.1 Method of Maximum Likelihood Estimation (MLE)

John Aldrich et al [7] introduced the maximum likelihood estimation between 1912 and 1922. The main purpose of MLE is to find the model parameters by maximizing the likelihood of the sample data. In fact, MLE focuses on knowing the density function for any given distribution which leads to estimating the parameters (Wim Schoutens [72]).

Given a density function  $g(x; \theta)$  where  $\theta$  is the set of the model parameters which must be calculated, and let  $x_1, x_2, \dots, x_n$  be a set of  $n$  independent observations of a random variable  $X$  (e.g the log returns of underlying asset). We can use these observations

to deduce a reasonable estimate for a set of the model parameter  $\theta$ . We may express the likelihood function as follows:

$$L_g(x_1, x_2, \dots, x_n | \theta) = L_g = \prod_{j=1}^n g(x_j; \theta). \quad (4.2.1)$$

We note that sometimes it is more straightforward to maximize the logarithm of the function, instead the function itself (Wim Schoutens [72]). Therefore, we take the logarithm of the likelihood function (log-likelihood function) which is denoted by:

$$\log L_g = \sum_{j=1}^n \log g(x_j; \theta). \quad (4.2.2)$$

If we want to maximize the logarithm of  $L_g$ , then we can rely on numerical procedures; however; in few cases these estimator can be computed explicitly (Wim Schoutens [72]).

### Remark

In Chapter 3 we used this method when we fitted density distribution for our models of log-return data. Note that when the density functions are either not known or complex (as with the CGMY model when probability density is not known), one needs to use the discrete Fourier transform presented in this chapter (Section 4.4) in order to approximate the density from the characteristic function. More details about this method can be found in (Wim Schoutens [72], and In Jae Myung [60]).

### 4.2.2 Method of Least Squares Estimation (LSE)

The method of LSE allows us to determine the unknown parameters (optimal parameters) of models by minimizing the quadratic pricing error between the model prices and observed market prices. The LSE method may be expressed as a linear or non-linear method. In the case of the non-linear method, a closed form solution is not usually available (Rama Cont, Peter Tankov, et al [30]), while it is available for the linear case. We need to guess a start value (initial value) for optimal parameters, and then determine the model parameters by successive approximation.

Let assume that  $C^*(t = 0, T_j, K_j)$  is the  $t = 0$  a market price of an option with strike  $K_j$  and maturity  $T_j$ , and let  $C^{\sigma, \nu}(t = 0, S_0, T_j, K_j)$  be an option price obtained via the calculation of a Lévy exponential, with a Lévy triplet  $(B, \sigma, \nu)$ . To determine the model parameters for any given model, we wish to perform a least squares estimation using



the following formula:

$$LSE = \arg \inf_{(\sigma, \nu)} \sum_{j=1}^N \omega_j |C^{\sigma, \nu}(t=0, S_0, T_j, K_j) - C^*(t=0, T_j, K_j)|^2, \quad (4.2.3)$$

where  $T_j, j = 1 \dots N$  is a range of maturities,  $K_j, j = 1 \dots N$  is a range of strikes and  $S_0$  a spot price.

LSE was introduced by Carl Friedrich Gauss [62]. Wim Schoutens [72], and Peter Carr, Hélyette Geman, Dilip B Madan, and Marc Yor [23] also used this method to compute the parameters of a number of models. They used the root-mean-squared error to minimize the error between the market prices and the model prices. This method was also used by Rama Cont and Peter Tankov [29], who proposed a regularisation method based on relative entropy minimization to enforce stability of the numerical solution of the calibration problem (Rama Cont, Peter Tankov, et al [30]). This method was also used by Rama Cont, Peter Tankov, et al [31], Wim Schoutens, Erwin Simons, and Jurgen Tistaert [75], and Andreas Kyprianou, Wim Schoutens, and Paul Wilmott [53].

We have discussed the calibration problem and also how to solve it, and maximum likelihood estimation (MLE) was used in Chapter 3 to fit the density distribution of our models to the log-return S&P500 time series data. Next we estimate the model parameters of the NIG, BS, VG and CGMY models by fitting these models to the observed market prices data. These models parameters will then used to value exotic options, specially barrier and lookback options. To do this, we first need to discuss the Lévy market model from which we will be calculating both the model vanilla prices (during our calibration procedure) and the exotic option prices (in Chapter 6). We refer the reader to section 3.4 for the discussion of this framework. Below we discuss pricing via an equivalent martingale measure (pricing formula for European option), which is a useful measure because it helps the computation of our models during the calibration procedure.

### 4.3 Pricing via an Equivalent Martingale Measure

According to the fundamental theorem of asset pricing, the price of an asset can be expressed as the risk-neutral expectation of its payoff  $H_T$  (Michael Harrison and Stanley R Pliska [45], and Wim Schoutens [73]):

$$C(K, T) = \mathbb{E}_{\mathbb{Q}}[e^{-r(T-t)} H_T | \mathcal{F}_t], \quad (4.3.1)$$

where  $C(K, T)$  represents the price of an European call option,  $K$  a strike and  $T$  a maturity. The payoff  $H_T$  can be expressed as  $H_T = \max(S_T - K, 0)$  for a call option and

$H_T = \max(K - S_T, 0)$  for a put option. In this case of the underlying asset follows an exponential Lévy process, we can rewrite this expression (4.3.1) as follows:

$$C(S_T, K, \Delta t) = e^{-r(\Delta t)} \mathbb{E}_{\mathbb{Q}}[(S e^{r(\Delta t) + X_{\Delta t}} - K)^+ | S_t = S], \quad (4.3.2)$$

where the expectation is taken under the risk-neutral martingale measure  $\mathbb{Q}$ , and  $\Delta t = T - t$ .

Wim Schoutens [72] shows that when we know the density function of the underlying asset, we can use numerical methods to compute the vanilla option prices as discounted expected values of the payoffs. Although the density function of underlying asset is not always known, we may have access to the characteristic function of underlying asset in a risk neutral world (Wim Schoutens [72]).

There are several different methods for computing the vanilla option prices (4.3.2). For example, Yoshio Miyahara [59] uses the Esscher transform to derive two kinds of Esscher transformed martingale measures. While, Antonis Papapantoleon [63] derives the vanilla option formula by solving a partial differential integral equation using the boundary conditions taken from a Lévy triplet. Here, we consider the method introduced by Peter Carr and Dilip Madan [24] which derives the vanilla option formula using the characteristic function of models, and applies the fast Fourier transform (FFT). The FFT can only be used if the characteristic functions of underlying asset prices are known. In the next section, we discuss the procedure for computing a European call/put option price using the FFT method.

## 4.4 Pricing via Fourier Transform

In this section, we discuss the procedure for pricing the vanilla options using the theory of the characteristic functions and the FFT. The FFT method is useful in the context of pure jump Lévy models (VG, CGMY and NIG models) where the closed-form solution for the vanilla options are unknown. By understanding this technique, we can obtain the vanilla call formula for the pure jump Lévy models. The advantage of using the FFT is that we only need to know the characteristic functions OF of the models, the parameters, the range of strikes and the terminal maturities to compute the vanilla options prices using the algorithm (Wim Schoutens [73]). Since the characteristic functions of the models are known, we can easily compute the prices of European call and put using this method. The FFT method can also be applied to more general options whose payoffs depend solely on the stock price at a terminal time.

The Lévy processes are defined by the Lévy measures, which makes it difficult to express the probability density in closed form. Therefore, it may not be possible to

compute the price of underlying asset using equation (4.3.1):

$$C(S_T, K, \Delta t) = e^{-r\Delta t} \int_0^\infty C_T(S) \mathcal{Q}_{(T)}(S) dS, \quad (4.4.1)$$

where  $\mathcal{Q}_{(T)}(S)$  is a risk neutral density for underlying asset in  $[0, T]$  and  $(C_t(S_T, K))_{t \in [0, T]}$  its contingent claim.

However, we have shown in Section 3.4 that the characteristic function of Lévy processes can be expressed analytically using the Lévy-Khinchin representation. Hence, we can use the Fourier transform to determine the pricing formula of the vanilla option in terms of the characteristic functions of the underlying asset.

Let  $K$  be a strike price, and set  $k = \log(K)$ . Let  $s_T = \log(S_T)$  and let  $q_T$  be a risk neutral density of  $s_T$ . We define the characteristic function of  $s_T$  as follows:

$$\phi(T, v) = \mathbb{E}_{\mathbb{Q}}[\exp(ivs_T)]. \quad (4.4.2)$$

We can also define the characteristic function of this density as follows:

$$\phi(T, v) = \int_{\mathbb{R}} e^{ivs} q_T(s) ds, \quad (4.4.3)$$

We can now express the formula of vanilla call option in terms of  $k$  and  $s$  using equation (4.3.1) :

$$C(k; T) = e^{-rT} \int_{\mathbb{R}} (e^s - e^k)^+ q_T(s) ds, \quad (4.4.4)$$

where  $s$  is a dummy variable ranging over  $\mathbb{R}$ . When  $k \rightarrow -\infty$ , the value of  $C(k, T)$  tends to  $S_0$  (Wim Schoutens [73]). That means the call price function (4.4.4) is not a square integrable (because the integral of the square of the call price function (4.4.4) over  $\mathbb{R}$  is not finite). Thus, we cannot use Fourier theory, and in order to obtain a square integrable we must modify the call price function as follows (Wim Schoutens [73]):

$$c(k; T) = \exp(\alpha k) C(k; T). \quad (4.4.5)$$

where  $\alpha$  is a positive value (i.e.  $\alpha > 0$ ). We need an appropriate method for choosing a parameter  $\alpha$ . However, Wim Schoutens [73] states that if we have an appropriate range of positive values of  $\alpha$ , we may expect that the modified call price  $c(k; T)$  can be a square integrable in  $k$  over the entire real line. More details about choosing  $\alpha$  can be found in [Peter Carr and Dilip Madan [24], pg.64 ].

In the following expression we use the Fourier transform of the modified call price (4.4.5) to obtain an analytic expression of the characteristic function of the underlying asset :

$$\psi(c, v) = \int_{-\infty}^{\infty} e^{ivk} c(k; T) dk. \quad (4.4.6)$$

Combining the equations (4.4.5) and (4.4.4) in equation (4.4.6), it follows that

$$\psi(c, v) = e^{-rT} \int_{-\infty}^{\infty} e^{ivk} e^{\alpha k} \int_{\mathbb{R}} (e^s - e^k) q_T(s) ds dk \quad (4.4.7)$$

By changing the order of integration, it follows that

$$\begin{aligned} \psi(T, v) &= e^{-rT} \int_{-\infty}^{\infty} q_T(s) \int_{\mathbb{R}} e^{(\alpha+iv)k} (e^s - e^k) dk ds \\ &= e^{-rT} \int_{-\infty}^{\infty} q_T(s) \left( \int_{-\infty}^s e^{(\alpha+iv)k} (e^s - e^k) dk \right) ds \\ &= e^{-rT} \int_{-\infty}^{\infty} q_T(s) \left( \int_{-\infty}^s (e^s e^{(\alpha+iv)k} - e^{(1+\alpha+iv)k}) dk \right) ds \\ &= e^{-rT} \int_{-\infty}^{\infty} q_T(s) \left[ \frac{e^{s(1+\alpha+iv)}}{\alpha+iv} - \frac{e^{s(1+\alpha+iv)}}{1+\alpha+iv} \right] ds \\ &= \frac{e^{-rT}}{(\alpha+iv)(1+\alpha+iv)} \int_{-\infty}^{\infty} q_T(s) e^{is(v-i(1+\alpha))} ds \\ &= \frac{e^{-rT}}{(\alpha+iv)(1+\alpha+iv)} \mathbb{E}_{\mathbb{Q}}[\exp i(v-i(1+\alpha)) \log(S_T)] \\ &= \frac{e^{-r(T)} \phi(T, (v-i(\alpha+1)))}{(\alpha+iv)(1+\alpha+iv)} \end{aligned} \quad (4.4.8)$$

$\phi$  represents the Fourier transform of  $q_T$ .

We can determine the vanilla call formula by taking the inverse Fourier transform of the equation (4.4.5):

$$C(k; T) = \frac{\exp(-\alpha k)}{2\pi} \int_{\mathbb{R}} e^{-ivk} \psi(T; v) dv. \quad (4.4.9)$$

Since the vanilla call option  $C(k, T)$  is a real function, the imaginary part of  $\Psi$  is odd and its real part is even. Hence, we consider the symmetry of above integration (4.4.9):

$$C(k; T) = \frac{\exp(-\alpha k)}{\pi} \int_0^{\infty} e^{-ivk} \psi(T; v) dv, \quad (4.4.10)$$

where  $\psi(T; v)$  is given at equation (4.4.8). We observe that the integral (4.4.9) is a direct Fourier transform therefore, we only need the FFT to compute this integral. Peter Carr

and Dilip Madan [24] stated that if  $\alpha = 0$  then the dominator vanishes when  $v = 0$ , inducing a singularity in the integrand. Since the FFT computes the integrand at  $v = 0$ , the use of the factor  $\exp(\alpha k)$  or something similar is required (Peter Carr and Dilip Madan [24]). Peter Carr and Dilip Madan [24] also states that a sufficient condition for the modified call  $c(k, T)$  to be integral in positive log strike direction, and hence for it to be a square integrable as well is given by  $\psi(0, T)$  being finite. From Equation (4.4.8), one observes that the  $\psi(0, T)$  is finite provided  $\psi(-(\alpha + 1)i, T)$  is finite (Peter Carr and Dilip Madan [24]). In appendix, we discuss the method for computing the integral (4.4.9) using the Fast Fourier transform.

Having discussed the calibration problem and the possible methods to address it, we decided to use the calibration method introduced above to estimate the model parameters for the risk-neutral density functions of our model of the S&P500 index data. To perform the calibration procedure we need to obtain the closed-form option pricing formula for pure jump models, that can be obtained using the FFT transform which inverts the generalized Fourier transform of the call price (Peter Carr and Dilip Madan [24]). The FFT method is an efficient and fast method for calculating option prices, particularly for the model prices where the closed-form solution of a European call and put option are unknown as in this case (Jianwei Zhu [78]). The FFT can compute the option prices for a large range of strikes which is useful, since this ability significantly reduces computation times for model calibration (Peter Carr and Dilip Madan [24]).

In chapter 5, we determine the model parameters for all models discussed in this research. This will be done by calibrating our models to the observed market prices, and seeing how our models perform when fitted to the observed data.

## Chapter 5

# Calibration of Model to Market data

In chapter 3 we used Maximum likelihood estimation (MLE) to fit the density distribution of our models to S&P500 time series data in order to estimate "CGMY-world" parameters. In this chapter, we investigate the use of the LSE method to estimate risk-neutral parameters. We use the risk-neutral parameters to price the exotic options. To conduct the calibration procedures we use two kinds of market data.

- We use the S&P500 index data. The S&P500 index data is (cross-sectional) option price data taken from the book of (Wim Schoutens [72]).
- We also use the "CGMY-world" data. The "CGMY-world" data were obtained as follows: For each set of the varying parameters of the CGMY model (the reader can refer to section 5.2 for more detail about the varying parameters of CGMY model), we price the vanilla calls via Fast Fourier transform (FFT) for the CGMY model. To do this, we consider 4 different maturities for the S&P500 index data closing from May 2002, June 2002, September 2002 and December 2002. We consider 12 strikes ranging from 975 to 1135, the risk-free interest rate  $r$  is equal to 19% and the dividend  $q$  is equal to 12% (Wim Schoutens [72]). We refer to the vanilla calls obtained as "CGMY-world" data.

For each kind of market data we estimate the risk-neutral parameters of the VG, NIG, CGMY and BS models. This was achieved by minimizing the root mean-square error (RMSE) between the given models prices and the market data. The calibration procedure works by finding a "best guess" of the model parameters, i.e. those parameters which yield model prices that are close to the observed market prices. We also analyse the model parameters obtained with the calibration procedure. We then compare the prices of vanilla calls computed with those models. We will use the risk-neutral pa-

rameters calibrated to "CGMY-world" data to price exotic options in chapter 6, and to compute the model risks.

We conclude this chapter by computing the model implied volatility surfaces using the risk-neutral parameters calibrated to S&P500 index data, to see if these implied volatility surfaces can capture the smile behaviour of the market's implied volatility surface. If the calibration is accurate, a volatility smile will be observed. In the following section we describe the method of estimating the risk-neutral parameters.

## 5.1 Estimation Parameters for the Pure Jump models

In this section we consider 77 call options on the S&P 500 index data, closing prices from 18 April 2002. The maturities range from the one to twenty months with twenty-seven strikes priced from 975 to 1500. The level of the S&P 500 index data closed at 1124.47, and we used the values of the dividend  $q = 1.2\%$  and interest rate  $r = 1.9\%$ . The S&P 500 index data is taken from the book of Wim Schoutens [72] and can be found in appendix A.

The optimization proceeds as follows: We first calibrate each model to the observed market prices, whilst considering multiple maturities and strikes, to obtain the risk-neutral parameters. The risk-neutral parameters for each model are as follows:  $(\sigma_{VG}, \theta, \nu)$  for the VG,  $(\alpha, \beta, \delta)$  for the NIG,  $(\sigma_{BS})$  for the Black-Scholes and  $(C, G, M, Y)$  for the CGMY. We use the LSE method to estimate these risk-neutral parameters. Secondly, we also fit each model to the observed market prices based on a single maturity of December 2002 and all ranges of strikes. These risk-neutral parameters will be used to price the vanilla calls since these option prices can only be priced at maturity time. The risk-neutral parameters obtained with the calibration for multiple maturities are called "multiple parameters set" and those obtained with the calibration for single maturity are called "single set" parameters. In chapter 6 we will use the "multiple parameters" to price barrier and lookback options, so that we incorporate information covers all maturities.

Finally, we vary the multiple parameters of the CGMY model ( see section (5.2) for more detail about the procedure for varying the multiple parameters set of the CGMY model), and we compute new vanilla calls using the varying parameters set of the CGMY model. These option prices are called "CGMY-world" data as mentioned in introduction of this chapter, and we fit the VG, NIG, CGMY and BS models to "CGMY-world" data, using LSE. Thus, the risk-neutral parameters for the VG, NIG and BS models obtained with the calibration of our models to "CGMY-world" data are called "new parameters set". We use "new parameters" in Chapter 6 to price and compute the model risks

of barrier and lookback options, in order to see if the prices of barrier and lookback options obtained with the VG, NIG, CGMY and BS models resemble those computed with the CGMY model using its varying parameters, since these prices are considered to be our "true" prices. The risk-neutral parameters obtained with the above procedures are referred to as:

- Multiple parameters set
- Single parameters set
- New parameters set
- Varying parameters set

### 5.1.1 Results of Estimation Parameters for the Lévy models

Here we present the calibration results for the four models. Note that the model parameters we considered are the unknown parameters of our models (NIG, VG, CGMY and BS models) which were obtained using the calibration procedure. We estimated the model parameters using the least square error (LSE) method. We express the classical formula of root mean square error RMSE by:

$$RMSE = \sqrt{\frac{\sum_{j=1}^N (C_{obs,j} - C_{mod,j})^2}{N}} \quad (5.1.1)$$

where  $C_{obs}$  is the observed market price and  $C_{mod}$  is the model price at time, which is computed via the FFT. The risk-neutral parameters obtained from the calibration are presented and discussed below.

Table 5.1 shows that there are differences between the multiple parameters and the single parameters of our models. Hence, we consider the VG model results. Table (5.1) shows that the value of  $\theta$  for the VG model is larger, by 0.0232, in the multiple maturities case than in the single maturities. Similarly the value of  $\gamma$  for the CGMY model and  $\sigma_{BS}$  for the Black-Scholes model are larger, by 0.0993 and 0.0071, in multiple maturity case than in the multiple maturity .

However, we observed that the value of  $\alpha$  for the NIG model is larger in the single maturity than in the multiple maturities case by 3.6046. As the parameters for each model are risk-neutral parameter, the difference between the single and multiple parameter for each risk-neutral parameter can affect the values of the vanilla calls.



**Table 5.1:** Table of Calibrated Risk-Neutral parameters from S& P 500 indexed options

Calibration result for optimal neutral parameters					
Model prices	Risk-neutral parameters				RMSE
Multiple parameters					
CGMY model	C	G	M	Y	3.4335
		0.0332	0.4614	15.6995	
VG model	$\sigma_{VG}$		$\theta$	$\nu$	4.0934
		0.1830	-0.1429	0.6804	
NIG model	$\alpha$		$\beta$	$\delta$	3.7716
		7.9877	-5.5124	0.1739	
Black-Scholes model	$\sigma_{BS}$				6.9310
		0.1843			
Single parameters					
CGMY model	C	G	M	Y	0.3737
		0.0476	1.3669	13.0605	
VG model	$\sigma_{VG}$		$\theta$	$\nu$	0.3566
		0.1648	-0.1655	0.4225	
NIG model	$\alpha$		$\beta$	$\delta$	0.1903
		11.5923	-7.1490	0.2346	
Black-Scholes model	$\sigma_{BS}$				5.1223
		0.1772			

Given this, it will be interesting to compare the prices of the vanilla calls computed with both multiple and single parameter sets for all models, and to see if the difference between two sets affects the prices of the vanilla calls.

Table 5.1 shows that the calibration error among models differs. Note that a small value for the RMSE implies a better fit. Table 5.1 also shows that the CGMY model performs better than the VG, NIG and Black-Scholes models. This is reflected by the degrees of freedom; models with more degrees freedom are more likely to fit the data better than models with fewer degrees of freedom, although these are not necessarily better models. The NIG model, which has the same number of risk-neutral parameters as the VG model, performed better than the VG model, while the Black-Scholes model performed worst. In table 5.1 we see that the calibration with single maturity for all four model prices gives a smaller value of the RMSE. This is because fewer maturities lead to fewer option prices. Note that the different risk-neutral parameters of the models may lead to significant differences in the values of the vanilla calls and exotic options.

Given these different scenarios, it will be interesting to price exotic options (barrier and lookback options) with the multiple parameters for all models, which is done in

chapter 6. In the following section we vary the multiple parameters of CGMY model.

## 5.2 Varying the model parameters for the CGMY model

In this section, we consider the multiple parameters ( $C = 0.0332, G = 0.4614, M = 15.6995, Y = 1.2882$ ) of the CGMY model presented in the table 5.1. Then, we vary the corresponding parameters by decreasing and increasing them, and record this effect on the density of the Lévy measure. We chose the corresponding multiple parameters ( $C, G, M, Y$ ) to illustrate the effect of changing parameter values on the risk-neutral density of the Lévy models. The procedure of increasing and decreasing the multiple parameters is given as follows: First we need to compute the delta values of these parameters as follows ( $\Delta = x\%C, x\%G, x\%M, x\%Y$ ), where  $x$  can take any value from the intervals (20, 40, 60, 80, 100). Secondly, we compute the values of ( $\Delta = x\%C, x\%G, x\%M, x\%Y$ ) taking each value of  $x$  from the interval (20, 40, 60, 80, 100). Finally, we increase and decrease each multiple parameter using the following form ( $C \pm \Delta, G \pm \Delta, M \pm \Delta, Y \pm \Delta$ ). After obtaining the sets of the parameters, we plot the Lévy density for the logarithm return of the CGMY model using these parameters. The parameters obtained here shall be called the "varying parameters" set.

Figures 5.1, 5.2, 5.3, 5.4 and 5.5 summarise the effect of varying parameters with ( $x = 20\%, 40\%, 60\%$  and  $80\%$ ) on the density of the Lévy measure.

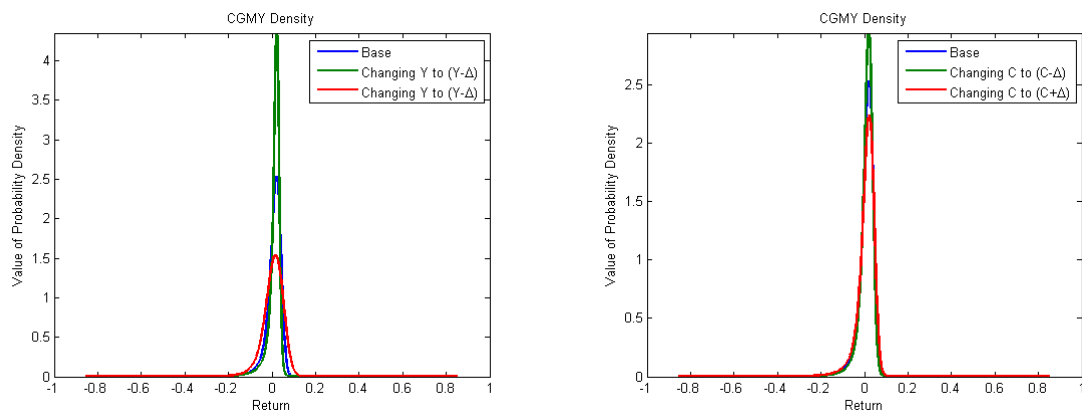


**Figure 5.1:** The Lévy measure of the CGMY model. The figures summarise the effect of varying the model parameters  $C = 0.0332$  and  $Y = 1.2882$  on the Lévy measure. Top left, we consider the varying of  $(C + \Delta, C - \Delta)$  with  $\Delta = 20\%C$  and in the top right  $(Y + \Delta, Y - \Delta)$  with the value of  $\Delta = 20\%Y$

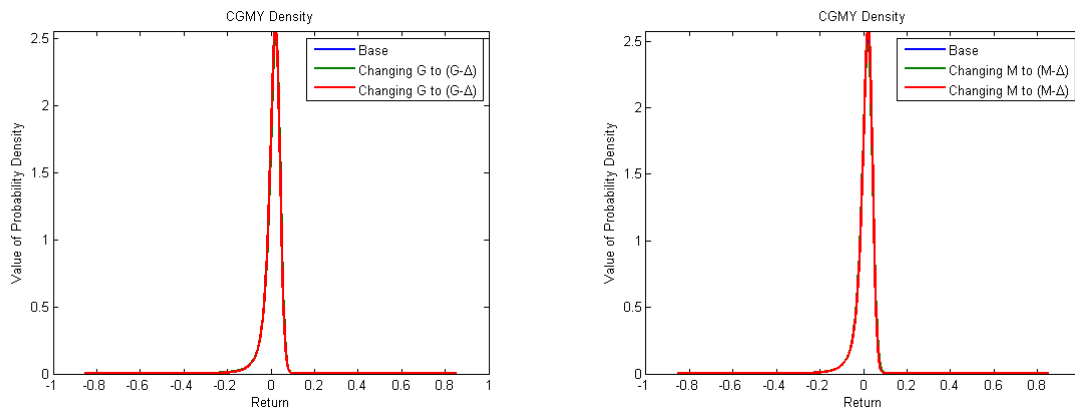


**Figure 5.2:** The Lévy measure of the CGMY model. The figures summarise the effect of varying model parameter  $G = 0.4614$  and  $M = 15.6995$  on the Lévy measure. In the top left, we consider the varying of  $(G + \Delta, G - \Delta)$  with  $\Delta = 20\%G$  and in the top right  $(M + \Delta, M - \Delta)$  with  $\Delta = 20\%M$

Let us start by considering the effect of both parameters  $C$  and  $Y$  when  $x = 20\%$ . Figure 5.1 shows that increasing the values of  $C$  and  $Y$ , leads to a flatter probability density while decreasing their values leads to a more peaked probability density (we can also say that the density exhibits greater leptokurtosis when  $C$  and  $Y$  decrease). The fact that  $C$  increases and  $Y$  decreases, should make it easier to find optimal values for  $C$  and  $Y$  (or there are multiple optimal values for  $C$  and  $Y$ ). When we increase and decrease parameters  $G$  and  $M$  (see figure 5.2) when  $x = 20\%$ , the changing parameter values of  $G$  and  $M$  do not lead to either a flatter or a peaked probability density. However, when  $x = 40\%$ ,  $x = 60\%$  and  $x = 80\%$  (see figures 5.3, 5.4 and 5.5), we observe that increasing the values of both parameters  $G$  and  $M$  leads to a peaked probability density while decreasing their values leads to a flatter probability density. However, if the changes in  $G$  and  $M$  are slight, they do not lead to a flatter or a peaked probability density. We can see that the Lévy density is insensitive to  $G$  and  $M$ , but does that mean that it will be hard to find optimal values for  $G$  and  $M$ ? Given this scenario, it will be interesting to compare the values of the vanilla calls and exotic options computed with the CGMY model using the varying parameters sets.

Thus, to vary our model parameters, we use  $x = 20\%$ . Thus, by only slightly increasing and decreasing the parameters  $C$  and  $Y$ , changing parameter values of  $G$  and  $M$  does not lead to a flatter or a peaked probability density. Hence, we can use the above procedure to determine the sets of the varying parameters. In doing so, we obtained 9 different sets of the varying parameters.

For each set of the varying parameters we price the vanilla call options using the

**Table 5.2:** Here we present the results of 9 sets of the varying parameters of CGMY model obtained by increasing and decreasing the multiple parameters which is given under this form  $(C \pm \Delta, G, M, Y \pm \Delta)$  with  $(\Delta = 20\%C, 20\%Y)$ .

The values of 9 sets of the varying parameters of CGMY model obtained by varying the multiple parameters of CGMY model				
Multiple parameters (C, G, M, Y)	C	G	M	Y
		0.0332	0.4614	15.6995
Varying parameter (C-20%C = C <sup>-</sup> , G, M, Y)	C <sup>-</sup>	G	M	Y
	0.0266	0.4614	15.6995	1.2882
Varying parameter (C+20%C = C <sup>+</sup> , G, M, Y)	C <sup>+</sup>	G	M	Y
	0.0398	0.4614	15.6995	1.2882
Varying parameter (C <sup>-</sup> , G, M, Y-20%Y = Y <sup>-</sup> )	C <sup>-</sup>	G	M	Y <sup>-</sup>
	0.0266	0.4614	15.6995	1.0306
Varying parameter (C <sup>-</sup> , G, M, Y+20%Y = Y <sup>+</sup> )	C <sup>-</sup>	G	M	Y <sup>+</sup>
	0.0266	0.4614	15.6995	1.2948
Varying parameter (C <sup>+</sup> , G, M, Y <sup>-</sup> )	C <sup>+</sup>	G	M	Y <sup>-</sup>
	0.0398	0.4614	15.6995	1.0306
Varying parameter (C <sup>+</sup> , G, M, Y <sup>+</sup> )	C <sup>+</sup>	G	M	Y <sup>+</sup>
	0.0398	0.4614	15.6995	1.2948
Varying parameter (C, G, M, Y <sup>-</sup> )	C	G	M	Y <sup>-</sup>
	0.0332	0.4614	15.6995	1.0306
Varying parameter (C, G, M, Y <sup>+</sup> )	C	G	M	Y <sup>+</sup>
	0.0332	0.4614	15.6995	1.2948

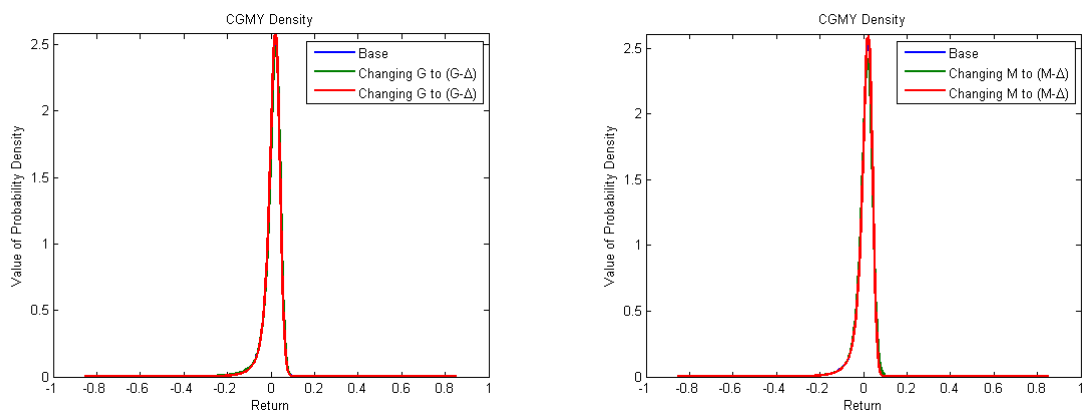


**Figure 5.3:** The Lévy measure of the CGMY model. Here we summarize the effect of varying the model parameters of G and M on the Lévy measure. In the top left we consider the varying of  $(G + \Delta, G - \Delta)$  with the  $\Delta = 40\%G$  and in the top right  $(M + \Delta, M - \Delta)$  with the  $\Delta = 40\%M$

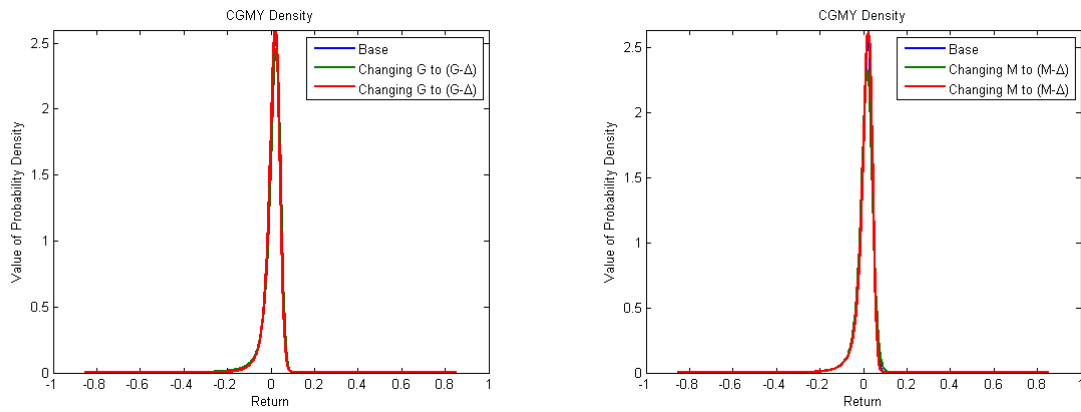


**Figure 5.4:** The Lévy measure of the CGMY model. Here we summarize the effect on the Lévy measure of varying the model parameters of  $G$  and  $M$ . In the top left we consider the vary of  $(G + \Delta, G - \Delta)$  with the  $\Delta = 60\%G$  and in the top right  $(M + \Delta, M - \Delta)$  with the  $\Delta = 60\%M$

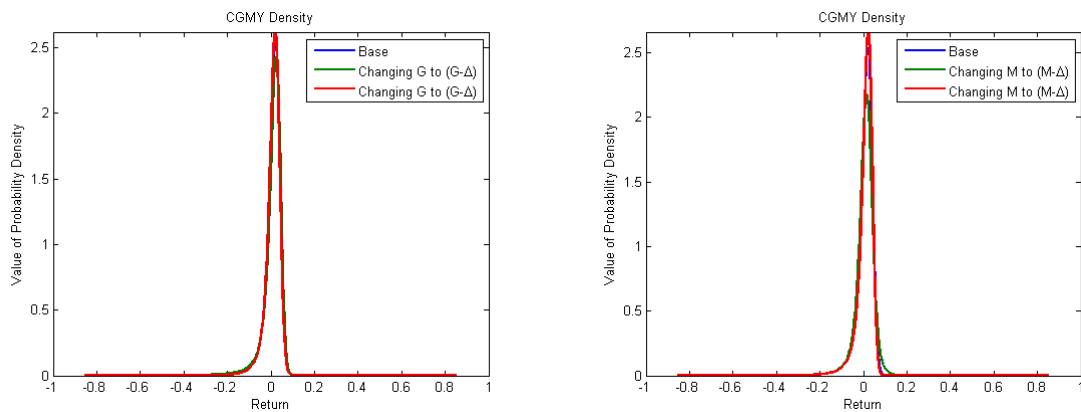


**Figure 5.5:** The Lévy measure of the CGMY model. Here we summarize the effect on the Lévy measure of varying the model parameters of  $G$  and  $M$ . In the top left we consider the vary of  $(G + \Delta, G - \Delta)$  with the  $\Delta = 80\%G$  and in the top right  $(M + \Delta, M - \Delta)$  with the  $\Delta = 80\%M$

FFT model. The different data of the vanilla call prices obtained via the 9 sets of the varying parameters will be called "CGMY-world" data as mentioned in the introduction of this chapter. We call them "CGMY-world" data because these vanilla call prices do not contain noise or bias and they are not mispriced. In the next section we proceed to fit each model (NIG, VG and Black-Scholes models) to the obtained "CGMY-world" data.

### 5.2.1 Calibration for the CGMY, NIG, VG and Black-Scholes models to the "CGMY-world" data

In this section we USE the "CGMY-world" data to perform our calibration. The "CGMY-world" data are obtained as follows: For each set of the varying parameters of the CGMY model (the reader can refer to section 5.2 for more detail about the varying parameters of CGMY model), we price the vanilla calls via Fast Fourier transform (FFT) for the CGMY model. To do this, we consider 4 different ranges of maturities for the S&P 500 index data closing from May 2002, June 2002, September 2002 and December 2002. We consider 12 strikes ranging from 975 to 1135, the risk-free interest rate  $r$  is equal to 19% and the dividend  $q$  is equal to 12% obtained from the book (Schoutens [72]). These vanilla call prices obtained via the 9 sets of the varying parameters will be consider as "GMY-world" data. We then fit the NIG, VG, CGMY and Black-Scholes models to each set of the "CGMY-world" data with the same range of strike and maturities, the risk-free interest rate  $r = 19\%$  and the dividend  $q = 19\%$ . We estimate the model parameters of NIG, VG and Black-Scholes models using least square error (LSE), and we compare the performance of our models to the "CGMY-world" data using root mean square error. The model parameters obtained with this procedure will be referred to as "new parameters", and we will use them when we price exotic options and compute model risk. In tables 5.3, 5.4, 5.5 we report the values of models estimated for all cases.

**Table 5.3:** Results of the new parameters for the CGMY, NIG, VG and Black-Scholes models obtained by fitting these models to the different sets of "CGMY-world" data.

Results of the new parameters calibrated to the different sets of the "CGMY-world" data					
Model prices	The new parameters obtained by fitting CGMY, NIG, VG and Black-Scholes model to "CGMY-world" data computed with the varying parameters ( $C, G, M, Y$ )				RMSE
CGMY model	C	G	M	Y	0.1174
	0.0324	0.4026	15.6990	1.2888	
VG model	$\sigma$		$\theta$	$\nu$	1.0615
	0.1593		-0.1906	0.5071	
NIG model	$\alpha$		$\beta$	$\delta$	0.4837
	8.2147		-5.1016	0.2027	
Black-Scholes model	$\sigma$				4.7329
	0.1895				
The new parameters obtained by fitting CGMY, NIG, VG and Black-Scholes model to "CGMY-world" data computed with the varying parameters ( $C^-, G, M, Y$ )					
CGMY model	C	G	M	Y	0.0887
	0.0258	0.4018	15.600	1.2916	
VG model	$\sigma$		$\theta$	$\nu$	0.5113
	0.1340		-0.1682	0.5619	
NIG model	$\alpha$		$\beta$	$\delta$	0.4870
	9.544		-6.0933	0.1711	
Black-Scholes model	$\sigma$				4.5240
	0.1667				
The new parameters obtained by fitting CGMY, NIG, VG and Black-Scholes model to "CGMY-world" data computed with the varying parameters ( $C^+, G, M, Y$ )					
CGMY model	C	G	M	Y	0.1603
	0.0373	0.3504	15.6900	1.2992	
VG model	$\sigma$		$\theta$	$\nu$	1.0629
	0.1840		-0.2084	0.4684	
NIG model	$\alpha$		$\beta$	$\delta$	0.5113
	9.5689		-6.3841	0.2417	
Black-Scholes model	$\sigma$				4.8826
	0.2101				

**Table 5.4:** Results of the new parameters for the CGMY, NIG, VG and Black-Scholes models obtained by fitting these models to the different sets of "CGMY-world" data.

Results of the new parameters calibrated to the different sets of the "CGMY-world" data					
Model prices	New parameters obtained by fitting CGMY, NIG, VG and Black-Scholes model to "CGMY-world" data computed with the varying parameters ( $C^-$ , $G$ , $M$ , $Y^+$ )			RMSE	
CGMY model	C	G	M	Y	0.0866
	0.0239	0.3614	15.6902	1.3278	
VG model	$\sigma$		$\theta$	$\nu$	1.0734
	0.1473		-0.1527	0.5503	
NIG model	$\alpha$		$\beta$	$\delta$	0.4918
	9.7062		-6.1889	0.1755	
Black-Scholes model	$\sigma$				4.4863
	0.1681				
New parameters obtained by fitting CGMY, NIG, VG and Black-Scholes model to "CGMY-world" data computed with the varying parameters ( $C^+$ , $G$ , $M$ , $Y^-$ )					
CGMY model	C	G	M	Y	0.0416
	0.0365	0.3737	15.6910	1.0586	
VG model	$\sigma$		$\theta$	$\nu$	0.9954
	0.1507		-0.1155	1.41136	
NIG model	$\alpha$		$\beta$	$\delta$	0.2608
	8.0037		-6.3638	0.1003	
Black-Scholes model	$\sigma$				6.4368
	0.1627				
New parameters obtained by fitting CGMY, NIG, VG and Black-Scholes model to "CGMY-world" data computed with the varying parameters ( $C^-$ , $G$ , $M$ , $Y^-$ )					
CGMY model	C	G	M	Y	0.0640
	0.0285	0.5518	15.6911	1.0117	
VG model	$\sigma$		$\theta$	$\nu$	0.8855
	0.1581		-0.0478	2.2758	
NIG model	$\alpha$		$\beta$	$\delta$	0.2080
	7.0215		-5.4453	0.0675	
Black-Scholes model	$\sigma$				5.6980
	0.1256				

Tables 5.3, 5.4 and 5.5 show that the RMSE value for the CGMY model is smaller than the RMSE value obtained with NIG, VG and BS models with different calibrations. The smaller value of RMSE implies a better fit of the model to the observed market price as we mentioned in the above section, which is evident since the CGMY model is cal-



**Table 5.5:** Results of the new parameters for the CGMY, NIG, VG and Black-Scholes models obtained by fitting these models to the different sets of "CGMY-world" data.

Results of the new model parameters calibrated to the different sets of the real world data					
Model prices	New parameters obtained by fitting CGMY, NIG, VG and Black-Scholes model to "CGMY-world" data computed with the varying parameters ( $C^+, G, M, Y^+$ )				RMSE
CGMY model	C	G	M	Y	0.1065
	0.0374	0.3650	15.6902	1.3080	
VG model	$\sigma$		$\theta$	$\nu$	1.0647
	0.1784		-0.2242	0.4535	
NIG model	$\alpha$		$\beta$	$\delta$	0.4950
	8.2482		-5.1694	0.2449	
Black-Scholes model	$\sigma$				4.8361
	0.2117				
New parameters obtained by fitting CGMY, NIG, VG and Black-Scholes model to "CGMY-world" data computed with the varying parameters( $C, G, M, Y^+$ )					
First new single parameter					
CGMY model	C	G	M	Y	0.0854
	0.0381	0.4252	15.6894	1.3081	
VG model	$\sigma$		$\theta$	$\nu$	1.0601
	0.1600		-0.1952	0.4890	
NIG model	$\alpha$		$\beta$	$\delta$	0.4877
	8.2363		-5.0792	0.2076	
Black-Scholes model	$\sigma$				4.6901
	0.1910				
New parameters obtained by fitting CGMY, NIG, VG and Black-Scholes model to "CGMY-world" data computed with the varying parameters ( $C, G, M, Y^-$ )					
CGMY model	C	G	M	Y	0.0462
	0.0305	0.3687	15.6909	1.0567	
VG model	$\sigma$		$\theta$	$\nu$	0.9568
	0.1299		-0.1025	1.550	
NIG model	$\alpha$		$\beta$	$\delta$	0.2244
	7.0300		-5.4360	0.0849	
Black-Scholes model	$\sigma$				6.1203
	0.1447				

ibrated to "CGMY-world" data. We observed that on calibrating the CGMY model to "CGMY-world" data, the risk-neutral parameters calibrated differ slightly to the "varying parameters", despite the fact that the "CGMY-world" data are obtained with the varying parameters. Thus the calibration of the CGMY model to "CGMY-world" data does not replicate the same risk-neutral parameters, and we can say that there is not unique the unique risk-neutral parameters. Hence, there is calibration risk. We also observed that the RMSE value for the NIG model is smaller than the RMSE value obtained from the VG and Black-Scholes models with different calibrations. Once again, we see that the NIG model fits "CGMY-world" data better than the VG and Black-Scholes models in terms of RMSE, despite both the NIG and VG models having the same number of model parameters, and also that the VG model is a particular case of the CGMY model. Given these results, we then priced the vanilla call and exotic options with the VG, NIG and BS models using their calibrated new parameters, and compared their prices with those obtained with the varying parameters of the CGMY model. In next section we compare the values of European vanilla prices obtained with the new parameters set.

### 5.3 Pricing Call Options

In this section, we present the graphs of the results from the calibration procedure. We also compare the values of vanilla calls computed with each model using multiple and single parameters. Finally we compare the values of the vanilla calls obtained with the new parameter sets of the VG, NIG and BS models to those computed with the varying parameters set of the CGMY model.

Figures 5.8, 5.9, 5.6 and 5.7 display the graphs for the calibration of our models to the S&P 500 index data with single parameters and multiple parameters. Figures 5.8 and 5.9 show that, the calibration of the NIG, VG and CGMY models to S&P 500 index data with a single maturity are better than those calibrated with the multiple parameters. Thus, the calibration of models to market data with a significant number of options for various maturities and strikes is difficult.

From Table 5.6 and Figure 5.10, we see that the values of the call prices computed via Fast Fourier transform (FFT) for NIG, VG and CGMY models using their single parameters are very close to the prices of S&P 500 index call options for one maturity from December 2002, while the call prices obtained from Black-Scholes model are largely different. This means that the NIG, VG and CGMY models are suitable for pricing European vanilla prices while the Black-Scholes model is not.

In Figure 5.13, we show the comparison between the values of the vanilla calls com-

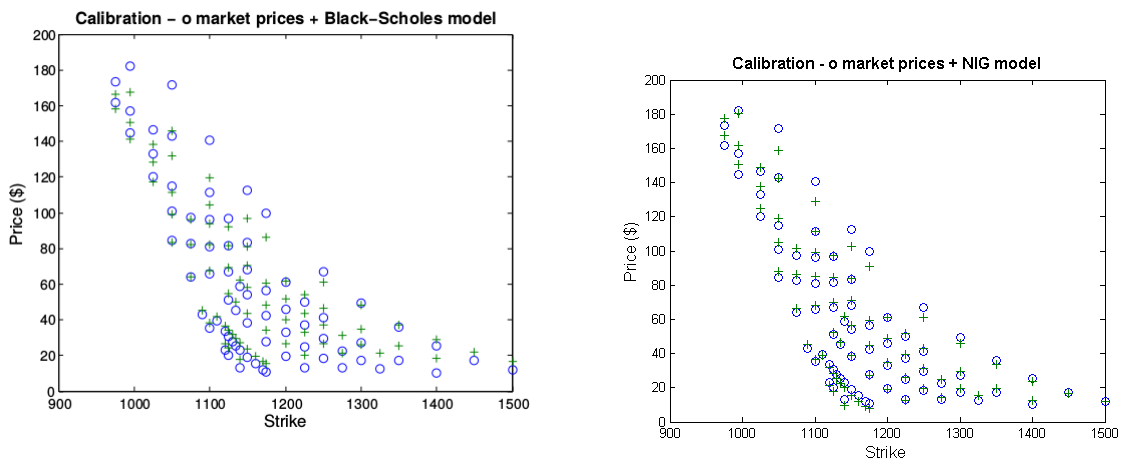


**Figure 5.6:** Calibration for multiple parameters of Black-Scholes and NIG models to S&P 500 index call options

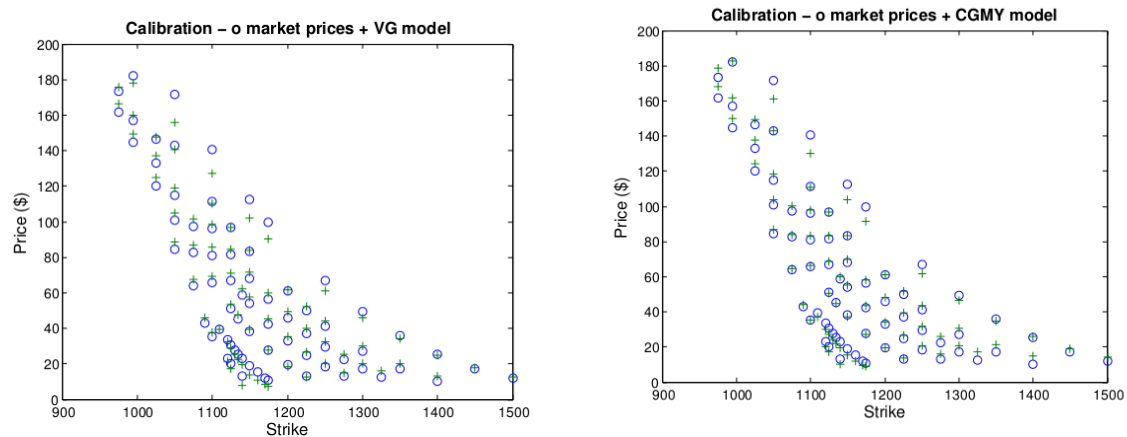


**Figure 5.7:** Calibration for multiple parameters of VG and CGMY models to S&P 500 index call options

puted via FFT for all model (CGMY, VG, NIG and BS) using multiple and single parameters. In pricing these vanilla calls we used the single maturity from December 2002 (i.e.  $T = 0.67123$ ). We see that the values of the vanilla calls computed with the CGMY model using multiple parameters are close to those obtained with single parameters, especially at a strike equal to 975. The scenario was similar with the VG and BS models. However, the values of the vanilla calls computed with NIG model using the multiple parameter are larger than they are in the single parameter, especially when the strike

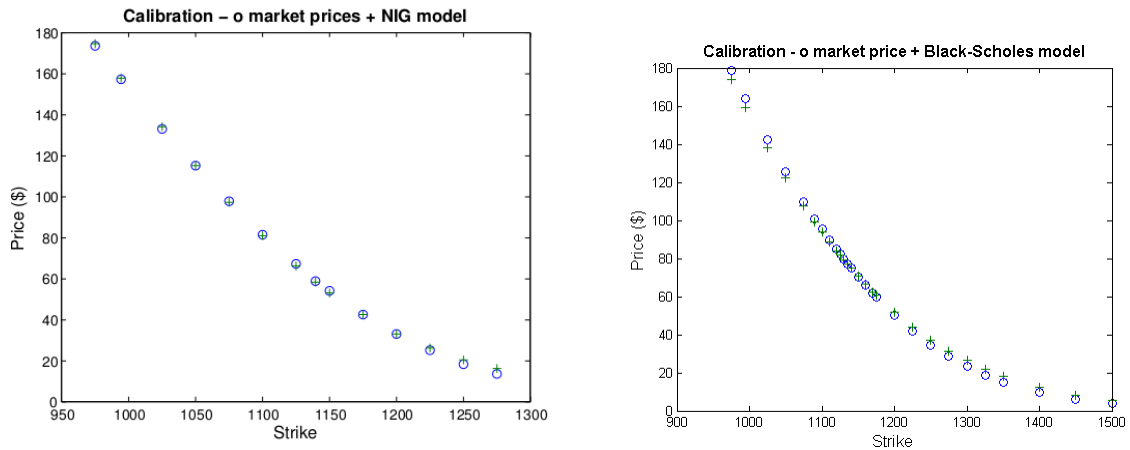


**Figure 5.8:** Calibration of single parameter of NIG and BS models to S&P 500 index call options

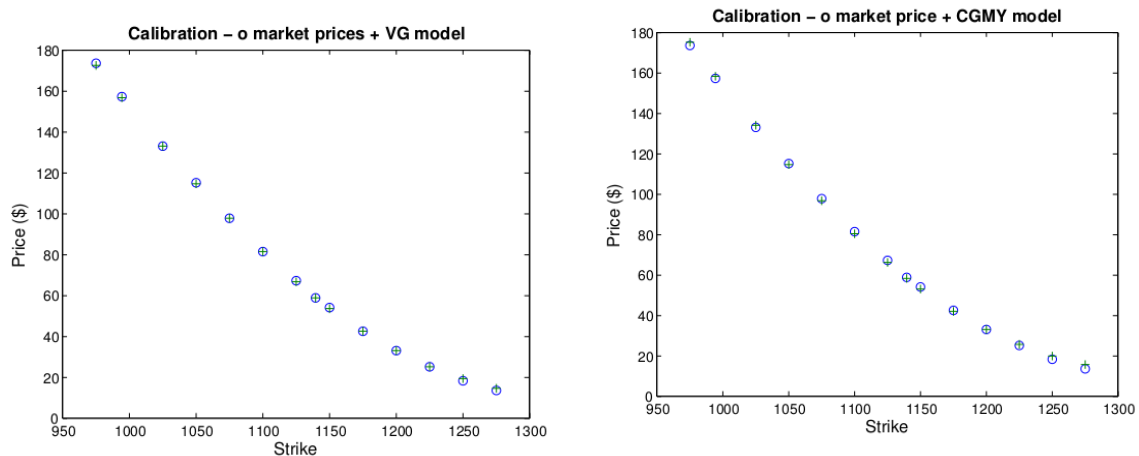


**Figure 5.9:** Calibration of single parameters of VG and CGMY models to S&P 500 index call options

equals 975. Once again, we noticed the opposite scenario with the NIG model, which may be because the values of the single parameter for the NIG model were larger than the values of the multiple parameters (as shown section 5.1.1). We also needed to compare the vanilla call prices computed with the NIG, VG and Black-Scholes models using their new parameters against the original vanilla call values obtained with the varying parameters of CGMY model. In order to compute the vanilla call with the new parameters of NIG, VG and Black-Scholes models obtained by fitting those models to the "CGMY-world" data (see section 5.2.1). We considered the single maturity on the S&P

**Table 5.6:** The values of the vanilla call prices computed via FFT technique for all models using their single parameters, and with one maturity from December 2002 (i.e  $T = 0.67123$ ) taken from the S&P 500 index call options

Strike	Original price from 12/2002	BS prices	VG prices	NIG prices	CGMY prices
975	173.30	164.9684	172.4836	173.2389	173.8473
995	157.00	149.0089	156.3305	156.9431	157.3344
1025	133.10	126.5714	133.1243	133.4978	133.5680
1050	114.80	109.3841	114.8524	115.0235	114.8607
1075	97.60	93.6650	97.6820	97.6719	97.3392
1090	0.000	84.9604	87.9611	87.8634	87.4701
1100	81.00	79.4636	81.7401	81.5960	81.1824
1110	0.000	74.2118	75.7362	75.5572	75.1399
1120	0.000	69.2040	69.9572	69.7558	69.3518
1125	66.90	66.7911	67.1546	66.9469	66.5558
1130	0.000	64.4384	64.4112	64.2008	63.8266
1135	0.000	62.1456	61.7281	61.5182	61.1649
1140	58.90	59.9123	59.1060	58.9001	58.5715
1150	53.90	55.6218	54.0484	53.8605	53.5914
1160	0.000	51.5628	49.2454	49.0879	48.8906
1170	0.000	47.7303	44.7035	44.5870	44.4711
1175	42.50	45.8971	42.5320	42.4392	42.3668
1200	33.00	37.5314	32.6927	32.7332	32.8901
1225	24.90	30.4190	24.5781	24.7230	25.0951
1250	18.30	24.4410	18.1679	18.3119	18.8473
1275	13.20	19.473	13.3123	13.3342	13.9621
1300	0.000	15.3865	9.7187	9.5764	10.2277
1325	0.000	12.0613	7.0876	6.8073	7.4286
1350	0.000	9.3820	5.1714	4.8061	5.3648
1400	0.000	5.5528	2.7676	2.3754	2.7787
1450	0.000	3.1968	1.4968	1.1775	1.4464
1500	0.000	1.7941	0.8198	0.5915	0.7656

500 index call option closing from December 2002 (i.e.  $T = 0.67123$ ), 12 strikes ranging from 975 to 1135, the risk-free interest rate  $r = 19\%$ , dividend  $q = 12\%$  and spot price  $S_0 = 1124.47$  obtained in the book (Schoutens [72]). Figures 5.11, 5.12, 5.14 and 5.16 show that the errors between the true vanilla call prices (vanilla call computed with the varying parameters of CGMY model) and the vanilla call obtained with the NIG and VG models are very small close to zero.

The large error between the true vanilla call prices and vanilla calls obtained with the Black-Scholes model, implies that the Black-Scholes model misprices the vanilla calls

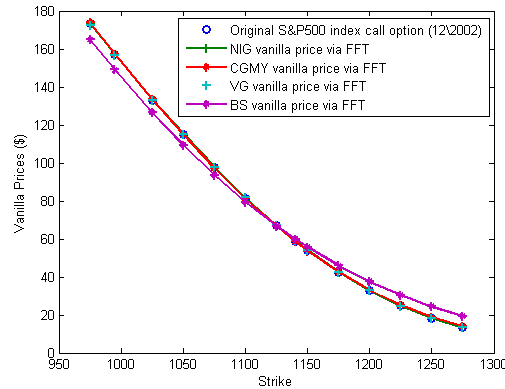


**Figure 5.10:** Comparing the vanilla call prices computed via Fast Fourier transform (FFT) for NIG, VG and CGMY models using their single parameters between those from the S&P 500 index call options for a single maturity from December 2002 (i.e  $T = 0.67123$ )

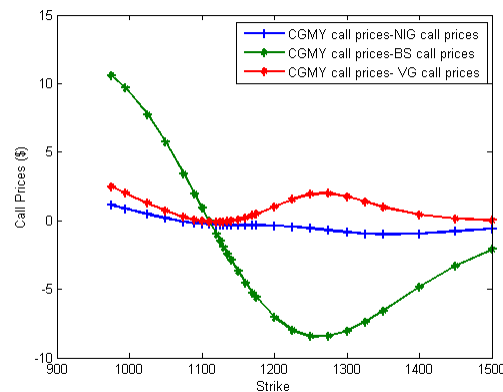


**Figure 5.11:** Comparing the vanilla call prices NIG, VG and BS models against the true vanilla call prices computed via the CGMY model with the new parameters  $(C, G, M, Y)$  and  $(C^-, G, M, Y)$ . We consider the single maturity from December 2002 (i.e  $T = 0.67123$ )

while models driven by a Lévy dynamics (NIG, VG or CGMY model) gave more accurate values. Therefore, the models driven by Lévy dynamics are more suitable for the pricing of vanilla options. Bearing this in mind, it would be interesting to compare the prices of the exotic option computed with all four models.

### 5.3.1 Models Implied Volatility Surfaces

We know that the market prices of options are largely cited in terms of implied volatilities. This does not signify that the market participants regard the Black-Scholes model as

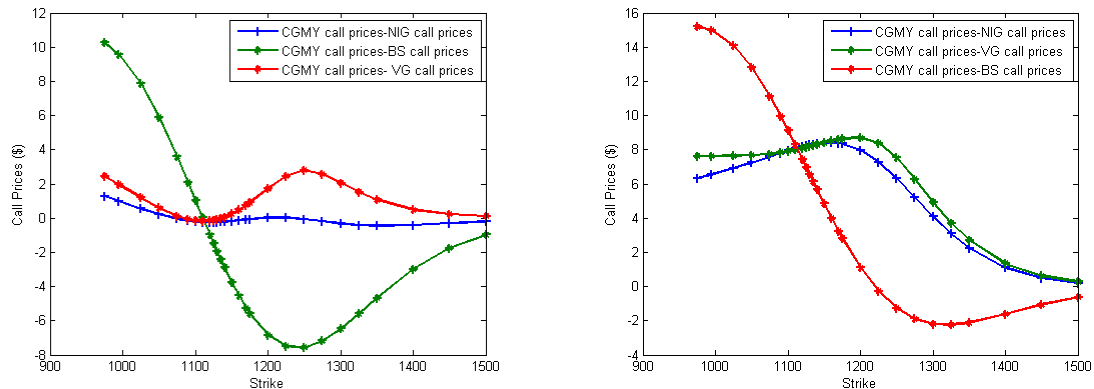


**Figure 5.12:** Comparing the vanilla call prices obtained with NIG, VG and BS models against the true vanilla call prices computed via the CGMY model with the new model parameters  $(C^-, G, M, Y)$  and  $(C^+, G, M, Y)$ . We consider the single maturity from December 2002 (i.e.  $T = 0.67123$ )

more efficient than others models (like CGMY, NIG and VG models). However, Black-Scholes model is only considered as a tool for translating the observed market prices (Cont and Tankov [29], pg.23). The implied volatility surfaces at any given time  $t$  with respect to the strike  $K$  is expressed as follows (Cont and Tankov [29], pg : 23) :

$$\Sigma : (T, K) \rightarrow \Sigma(T, K)$$

where  $\Sigma$  is the implied volatility surface. In figures 5.17 and 5.18 we see that our model prices (NIG, VG and CGMY models) effectively captured the implied volatility surface of the S&P 500 index option data. However, although the model prices performed well using S&P 500 index option data, this does not imply that the exponential Lévy model will perform well for all data sets especially when using market data with short maturities. We also noted that the implied volatility surface is a function of the strikes and maturities, i.e. it is not constant (Cont and Jose da Fonseca [27], Cont et al [31], and Riccardo [66]). This illustrated in figure 5.17 for S&P 500 index data.

There is usually a strong dependence between the implied volatility surface and the strike price as illustrated by a U-shaped "smile" or "Skew" (Cont and Tankov [29], pg : 24). This dependence relative to a strike price  $K$  may decrease with maturity; and when the maturity increases, the skew and smile flatten out. The patterns of implied volatility surfaces vary less in time  $t$  than in strike  $K$ , especially when it is represented as a function of the moneyness ( $m = K/S$ ) (Rama Cont and Peter Tankov [29], pg : 24).

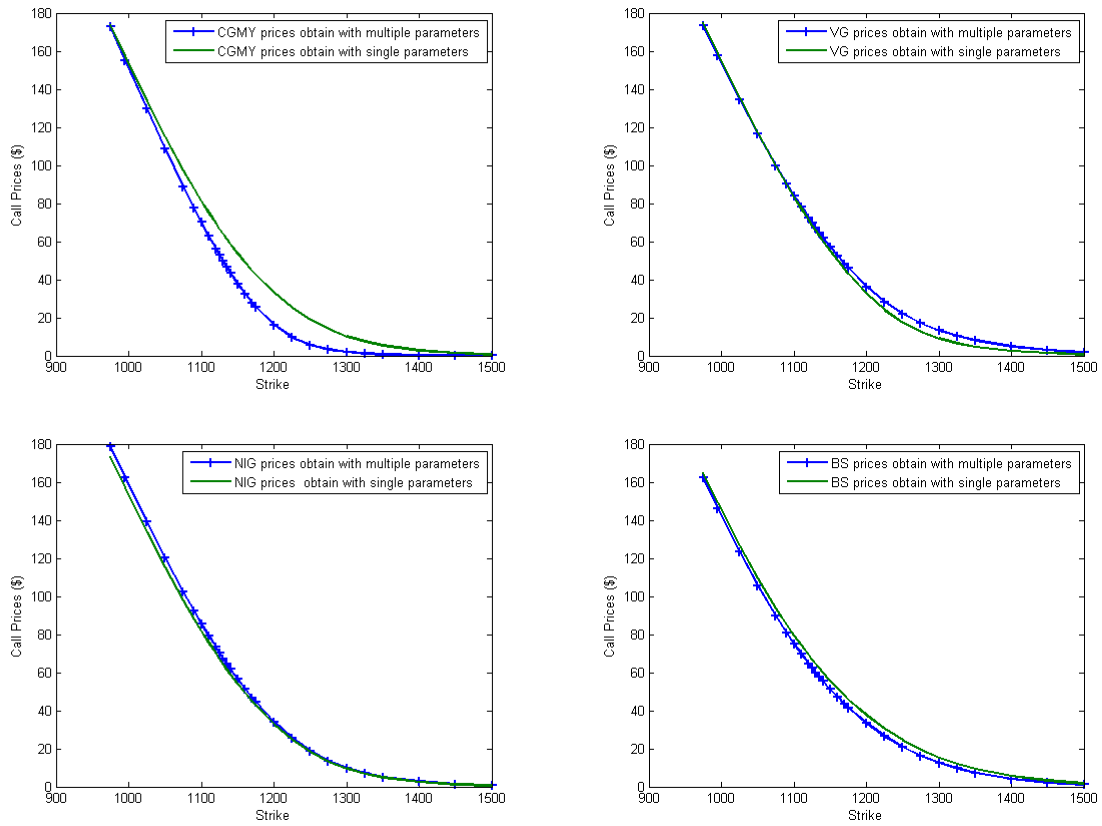


**Figure 5.13:** Comparison between the values of the vanilla calls computed via FFT for CGMY, VG, NIG and BS models using their multiple and single parameters. In pricing these vanilla calls we consider the single maturity from December 2002 (i.e  $T = 0.67123$ )

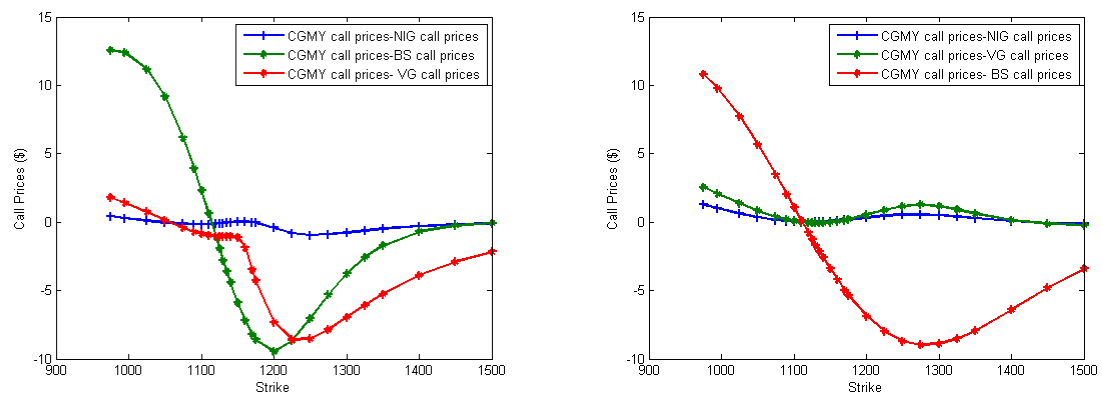


**Figure 5.14:** Comparison between the call prices for all model prices obtained with the model parameters for CGMY model ( $C^-, G, M, Y^-$ ) and ( $C^-, G, M, Y^+$ ). We consider the single maturity from December 2002 (i.e  $T = 0.67123$ )



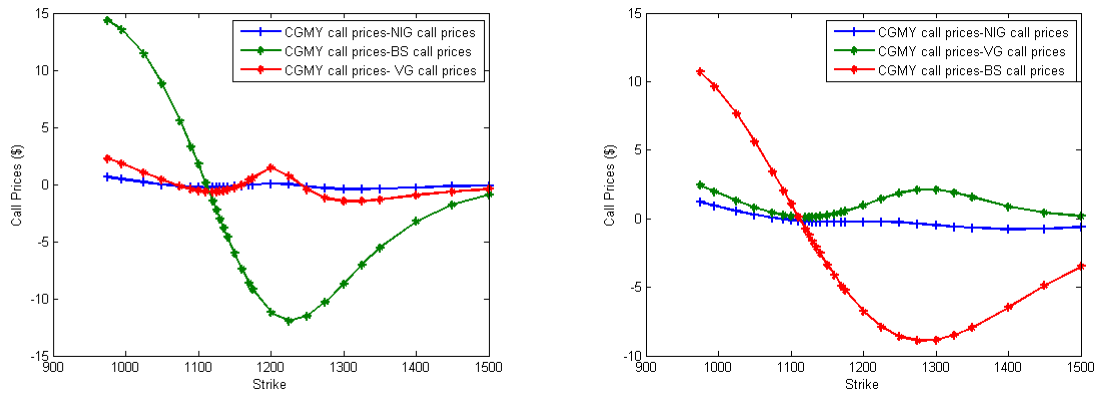


**Figure 5.15:** Comparing the vanilla call prices obtained with NIG, VG and BS models against the true vanilla call prices computed via the CGMY model with the new model parameters  $(C^+, G, M, Y^-)$  and  $(C^+, G, M, Y^+)$ . We consider the single maturity from December 2002 (i.e  $T = 0.67123$ )

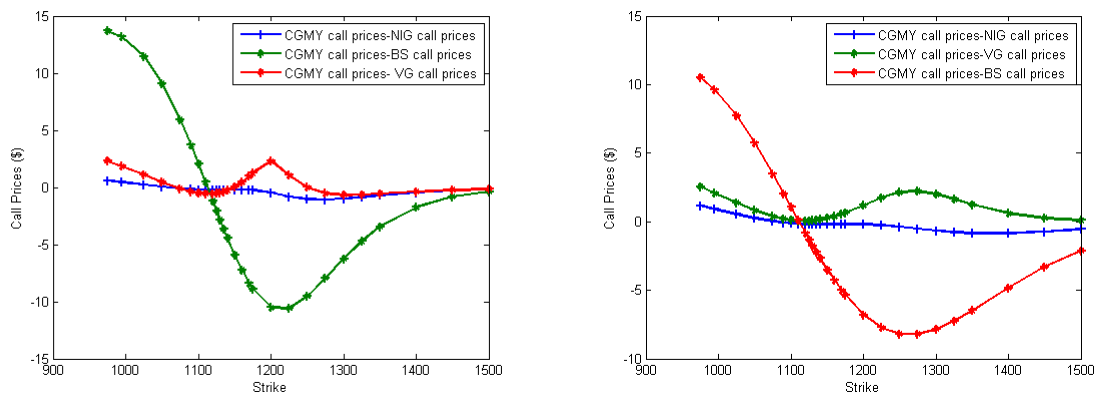


**Figure 5.16:** Comparing the vanilla call prices obtained with NIG, VG and BS models against the true vanilla call prices computed via the CGMY model with the new model parameters  $(C, G, M, Y^-)$  and  $(C, G, M, Y^+)$ . We consider the single maturity from December 2002 (i.e  $T = 0.67123$ )

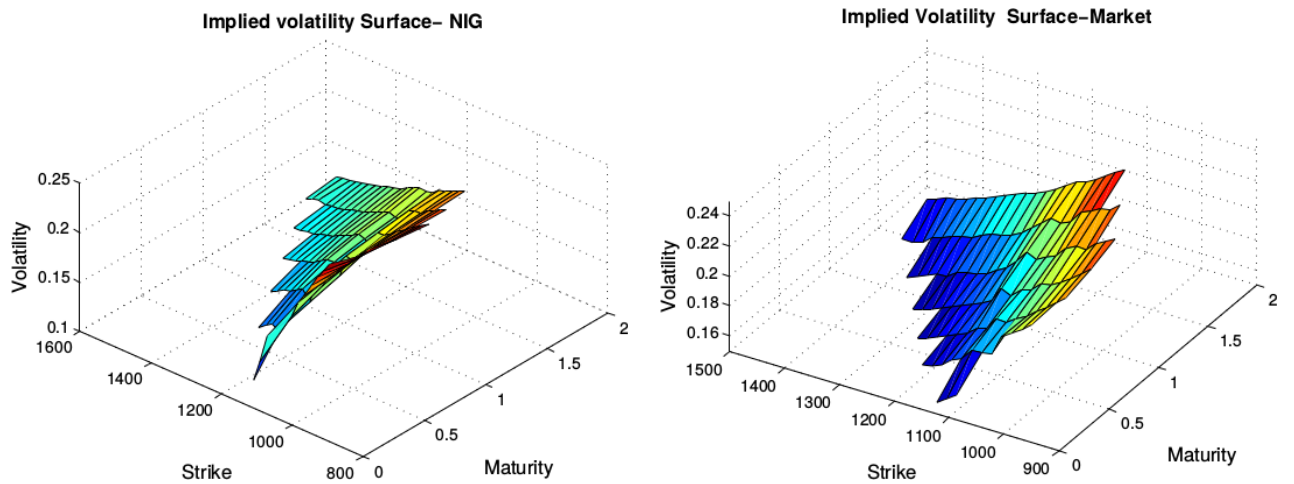


Figure 5.17: Implied Volatility Surface for NIG model and S& P500 indexed options

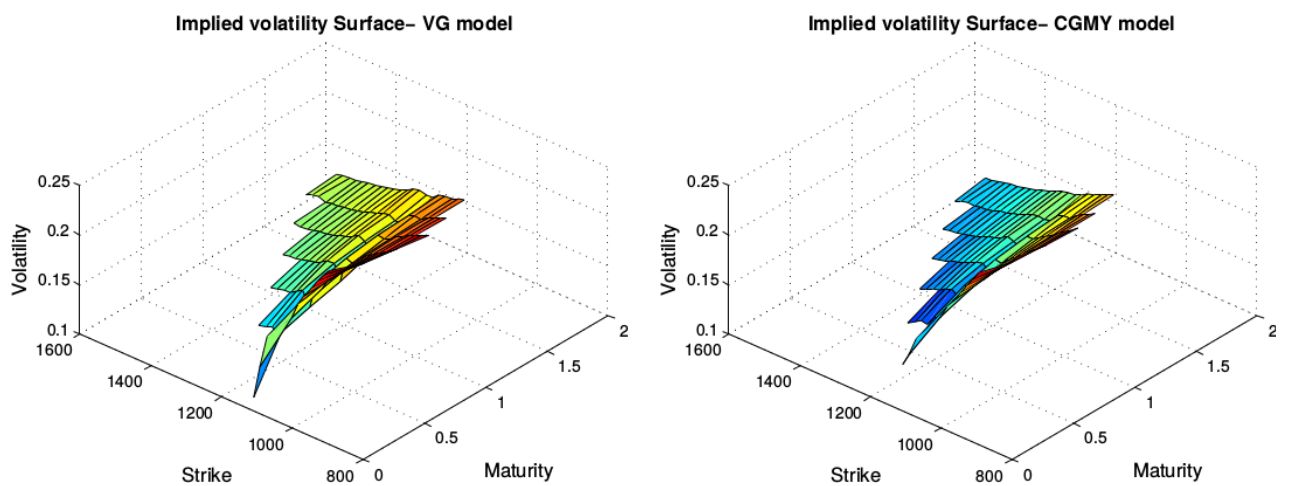


Figure 5.18: Implied Volatility Surface for VG model and CGMY model

## Chapter 6

# Pricing Exotic Options and Model Risk

This chapter focuses on exotic options, and model risk. Model risk arises when the "wrong" financial models are applied to price financial derivatives. The statistician GEP Box wrote "All models are wrong, but some are useful" (George EP Box and Norman R Draper, [16], pg. 424). In finance the models can be "wrong" when the numerical methods are not stable, or when the calibration methods are incorrect. The model risk may occur when the model prices used to compute the financial derivatives are inappropriate, and may also be because of an inexact (or a reasonable) method for the hedging of the derivative. Even if there is a method, we may choose the wrong one. In this chapter, we focus on the risks involved when we price exotic options. We will pay limited attention to the risks that arise from calibration to market prices, because we have already considered the risk-neutral parameters obtained with the calibration of "CGMY-world" data (see chapter 4 for more details). Here, we compute a measure of model risk of call options and exotic options using the new parameters.

This chapter is organised as follows: First, we discuss the procedure of pricing exotic options and the results. We then discuss the Monte Carlo method. Finally, we compute a measure of model risk of exotic options using an improvement of the model risk formula introduced by Rama Cont [26].

### 6.1 Pricing Exotic options

Exotic options have prices that are not quoted on the open market. Therefore, risk-neutral parameters calibrated to the observed market prices are needed in order to com-

pute exotic option prices. Exotic options may be path-dependent options, which means that their terminal values (at expiration or exercise) depends on the values of the underlying, not only at that exact time, but also at prior points to that [5]. We note that the application of different models calibrated to market prices can lead to different values, which happens regularly in exotic options such as lookback and barrier options.

### 6.1.1 Pricing Barrier Option

The barrier option is one of the simplest types of path-dependent option where the holder has the right to buy or sell the underlying asset at any specific price when the contract expires. The important feature about a barrier option is that its payoff does not only depend on the last (final) price of underlying asset but also on whether or not the underlying asset may reach some level of  $H$  (the barrier level) during the lifetime of the option (Andreas Kyprianou, Wim Schoutens, and Paul Wilmott [53]). The barrier may consist of more than two barriers, but here we focus on those with one barrier with an option payoff, up-and-in, or up-and-out calls, which we discuss in the next section.

#### 6.1.1.1 Up-and-in call

Let  $K$  be a strike price and  $H$  a barrier level. The payoff of an up-and-in call with  $K$  and  $H$  is equal to the payoff of a standard European call, provided that if the maximum of the underlying asset reaches (or crosses) (between the time  $t \in [0, T]$ ) the barrier  $H$  at time  $t$ , while otherwise it is zero. We define the price of an up-and-in call as an expectation under the risk neutral measure  $Q$  of the discounted payoff:

$$C^{UI} = \mathbb{E}_Q[e^{-rT}(S_T - K)^+ 1_{M_T \geq H}] \quad (6.1.1)$$

where  $M_T$  represents the maximum of the underlying asset  $(S_t)_{t \in [0, T]}$ . i.e.

$$M_t = \sup\{S_u; 0 \leq u \leq t\},$$

and  $r$  is an interest rate. We note that the value of the standard European call and the up-and-in call can be the same, if the barrier level  $H$  is lower than the strike price  $K$  (i.e.  $H \leq K$ ). If  $S_T - K > 0$ , this means that the barrier  $H \leq K$  has been crossed before the expiry time  $T$ .

#### 6.1.1.2 Up-and-out call

Like the price of an up-and-in call, the price of an up-and-out call is equal to the standard European call price with strike  $K$ , if the maximum of the underlying asset at time  $t \in$

$[0, T]$  stays below the barrier level  $H$ , while otherwise it is zero. One can define the value of an up-and-out call:

$$C^{UO} = \mathbb{E}_{\mathbb{Q}}[e^{-rT}(S_T - K)^+ \mathbf{1}_{M_T < H}]. \quad (6.1.2)$$

As mentioned previously, when we sum both barriers up-and-in call, and up-and-out call which is called in-out parity with the same maturity  $T$  and strike  $K$  for any given asset price, we obtain

$$\begin{aligned} C^{UO} + C^{UI} &= \mathbb{E}_{\mathbb{Q}}[e^{-rT}(S_T - K)^+ \mathbf{1}_{M_T < H}] + \mathbb{E}_{\mathbb{Q}}[e^{-rT}(S_T - K)^+ \mathbf{1}_{M_T \geq H}] \\ &= e^{-rT} \mathbb{E}_{\mathbb{Q}}[(S_T - K)^+ \mathbf{1}_{M_T \geq H} + (S_T - K)^+ \mathbf{1}_{M_T < H}] \\ &= e^{-rT} \mathbb{E}_{\mathbb{Q}}[(S_T - K)^+]. \end{aligned} \quad (6.1.3)$$

Hence, this sum is equal to the standard European call option with the strike price  $K$  and maturity  $T$ . In the next section we discuss the pricing of the lookback fixed option.

## 6.1.2 Pricing the Lookback Fixed Option

A lookback option is a path-dependent option where the payoff depends on the minimum or maximum price of the underlying asset during the life of an option. The holder of the lookback option may "look back" over the period to determine the payoff. More detail about lookback option can be found in the literature of Andreas Kyprianou, Wim Schoutens, and Paul Wilmott [53], Laurent Nguyen-Ngoc [61] and Steven E Shreve [76]. There are two types of lookback option, the floating strike lookback option and the fixed strike lookback options, but here we focus on the lookback fixed option only.

### 6.1.2.1 Lookback fixed option

The payoff of a lookback fixed option is only dependent on the maximum of underlying asset and the strike price (or the difference between the maximum of underlying asset and the strike price during the lifetime of the option). The lookback fixed option is a type of path-dependent option that is only settled in cash, with the strike only being predetermined at inception [1]. The lookback price formula is given by:

$$C_{fixed}(S_T, K, T) = e^{-rT} \mathbb{E}_{\mathbb{Q}}[(\max_{0 \leq t \leq T} S_t - K, 0)] \quad (6.1.4)$$

where  $(S_t)_{t \in [0, T]}$  is an underlying asset,  $r$  an interest rate and  $K$  the strike. The lookback option is more expensive than the similar plain vanilla option.

Having discussed lookback fixed options, we need to find the distribution of the maximum of the underlying asset process for them. The explicit form for the distribution of maximum of a general exponential Lévy model is often unknown. Thus, a numerical technique is needed, such as Monte Carlo simulation, to compute the value of an exotic option (Andreas Kyprianou, Wim Schoutens, and Paul Wilmott [53]), and we discuss this in the next section.

### 6.1.3 Monte Carlo Method

Wim Schoutens [72] highlighted that the value of the standard error obtained by simulating a large number of paths without using the variance reduction method may be similar to those obtained via the simulation of the paths of the underlying asset based on the variance reduction method for an exotic option. To check the accuracy of the Monte Carlo simulation we price the European calls using 50 000 paths of the underlying asset for each model based on single parameters calibrated to S&P500 index option call. Figure 6.1 shows that pricing the European call option using the CGMY, NIG, BS and VG models gives very satisfactory results. With respect to their analytic calibration values, prices values differed less than 0.2% among the pure jump models and 30% using the Black-Scholes model. Thus, we computed the above lookback fixed option and barrier option using 50 000 paths of the underlying asset for each model. We outline how to compute the Monte Carlo method for an exponential Lévy model as follows (Paul Glasserman [41] and John Hull [46]):

- 1 Estimate the risk-neutral parameters using an optimization procedure (minimizing error between the observed plain vanilla S&P500 index data with model price ). This was done in chapter 4.
- 2 Use the risk-neutral parameters obtained via procedure (1) to simulate the  $N$  paths (trajectories) of the underlying asset for each model price. This procedure is carried out in section A.3.
- 3 Compute the value of payoff  $(P_j)_{1 \leq j \leq N}$  for each of the trajectories of the underlying asset.
- 4 Estimate the expected payoff of  $P$  by taking the mean of the payoff  $P_j$ , denoted:

$$P = \frac{1}{N} \sum_{j=1}^N P_j$$

5 We discount:

$$D = e^{-rT}P.$$

In Appendix we present methods for the simulation of the trajectories of the pure jump Lévy model using Monte Carlo method.

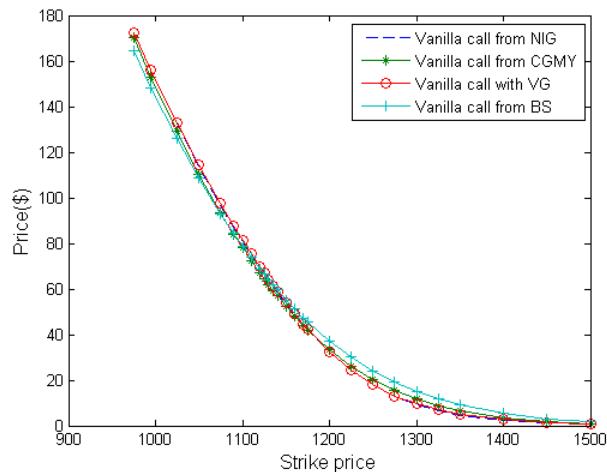


**Figure 6.1:** The vanilla call prices computed with CGMY, NIG and VG models using the Monte Carlo method with the strike price  $K = 1130$ , maturity  $T = 0.67123$  and the stock price  $S_0 = 1124.47$ .

## 6.2 Results and Discussion

In this section, we compare the prices of the barrier and lookback options computed with all models (Black-Scholes model, NIG, VG and CGMY models) and discussed it. We consider the multiple parameters calibrated to the S&P500 index data (see Chapter 5, Table 5.1) to value the exotic options. We compute the exotic option prices using the Monte Carlo method discussed above. We use the maturity from December 2002 ( $T = 0.6543$ ). The barrier level is a function of the stock price (ranging from  $0.5(S_0)$  to  $1.5(S_0)$ ). We simulate 50 000 underlying assets for each model. In Table 6.1 we present the results of the barrier and lookback fixed options computed with CGMY, NIG, VG and Black-Scholes models. We observe that the sum of the values of the up-and-in call and up-and-out call options substantiate the identity of the *(Up-and-In)+ (Up-and-Out)= plain vanilla*.

**Table 6.1:** Results of the barrier and lookback fixed options for each model price. The barrier level ranges from  $(0.5S_0$  to  $1.5S_0)$  and the strike price  $K = 1130$ , maturity  $T = 0.67123$  and the stock price  $S_0 = 1124.47$ .

Exotic options	CGMY model	NIG model	VG model	BS
Lookback fixed	115.5749	100.0157	96.1811	129.5181
Barrier level	Up-In & Up-out	Up-In & Up-out	Up-In & Up-out	Up-In & Up-out
Up-out+Up-In	61.8570	64.1673	64.0775	68.4472
562.2	61.8570 & 0.000	64.1673 & 0.000	64.0775 & 0.000	68.4472 & 0.000
618.5	61.8570 & 0.000	64.1673 & 0.000	64.0775 & 0.000	68.4472 & 0.000
674.7	61.8570 & 0.000	64.1673 & 0.000	64.0775 & 0.000	68.4472 & 0.000
730.9	61.8570 & 0.000	64.1673 & 0.000	64.0775 & 0.000	68.4472 & 0.000
787.1	61.8570 & 0.000	64.1673 & 0.000	64.0775 & 0.000	68.4472 & 0.000
843.4	61.8570 & 0.000	64.1673 & 0.000	64.0775 & 0.000	68.4472 & 0.000
899.6	61.8570 & 0.000	64.1673 & 0.000	64.0775 & 0.000	68.4472 & 0.000
955.8	61.8570 & 0.000	64.1673 & 0.000	64.0775 & 0.000	68.4472 & 0.000
1012.0	61.8570 & 0.000	64.1673 & 0.000	64.0775 & 0.000	68.4472 & 0.000
1068.2	61.8570 & 0.000	64.1673 & 0.000	64.0775 & 0.000	68.4472 & 0.000
1124.5	61.8570 & 0.000	64.1673 & 0.000	64.0775 & 0.000	68.4472 & 0.000
1180.7	61.4715 & 0.3855	62.6379 & 1.5294	60.6112 & 3.4663	68.1589 & 0.2883
1236.9	57.3557 & 4.5013	53.4172 & 10.7501	48.5999 & 15.4776	65.1845 & 3.2627
1293.1	47.7503 & 14.1066	37.0613 & 27.1060	32.2969 & 31.7806	57.4158 & 11.0315
1349.4	34.9839 & 26.8731	22.4209 & 41.7464	19.2353 & 44.8423	46.0650 & 22.3822
1405.6	22.8381 & 39.0189	12.3669 & 51.8004	11.3951 & 52.6825	33.2846 & 35.1626
1461.8	13.7196 & 48.1374	6.5848 & 57.5825	6.6119 & 57.4656	22.2415 & 46.2058
1518.0	7.4452 & 54.4117	3.6124 & 60.5549	3.8153 & 60.2622	14.1877 & 54.2595
1574.3	3.7853 & 58.0716	1.7984 & 62.3689	2.1468 & 61.9307	8.3660 & 60.0812
1630.5	1.8640 & 59.9930	0.9429 & 63.2244	1.2145 & 62.8630	4.7021 & 63.7451
1686.5	0.9189 & 60.9380	0.4400 & 63.7273	0.8094 & 63.2681	2.5324 & 65.9148

Table 6.1, as well as Figure 6.2 show that the values of the up-and-in and up-and-out call obtained with the NIG, and VG models are very similar but they differ from the values obtained from the CGMY and Black-Scholes models. The up-and-in and up-and-out call computed using the Black-Scholes model are larger than those obtained using the NIG, VG and CGMY models. Since the "true" or "real" prices of the exotic options are unknown, it is difficult to judge which model gives the best price for the barrier option.

Similarly, the prices of the lookback fixed option computed with the VG, NIG, CGMY and Black-Scholes models are different to each other. Once again the price of a lookback option computed with the Black-Scholes model is larger than the prices of lookback



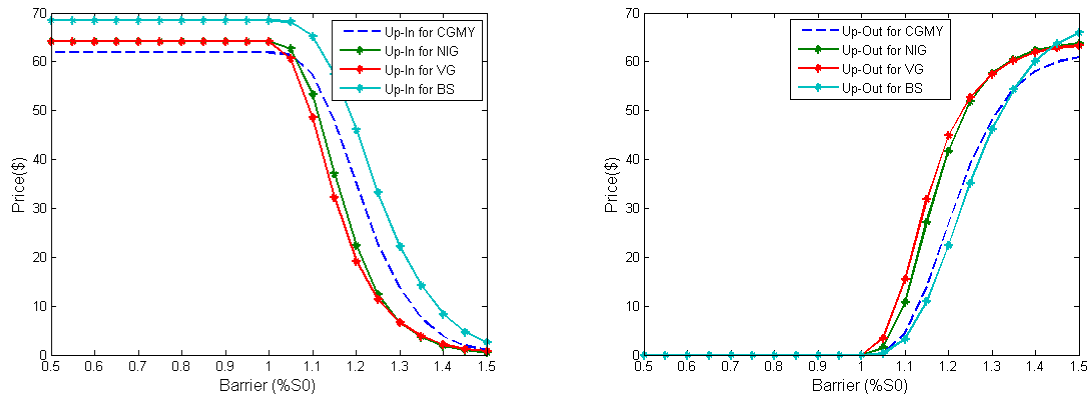


**Figure 6.2:** The figures of up-and-in and up-and-out calls for NIG, VG, CGMY and Black-Scholes models, with the strike price  $K = 1130$ , maturity  $T = 0.67123$  and the stock price  $S_0 = 1124.47$ . The barrier level is range from  $(0.5S_0$  to  $1.5S_0$ )

option computed using the NIG, VG and CGMY models. In addition, the prices of the lookback option computed with the NIG and VG models differ slightly, while the price obtained with the CGMY model differs from those of the NIG, VG and Black-Scholes models. Hence, the situation is comparable to that of the up-and-in and up-and-out calls, as it is difficult to tell which model prices the exotic option best as the "true" prices of the exotic options are unknown. Therefore, in next the section, we use the exotic prices computed with the CGMY model (using the varying parameters of CGMY model see Chapter 5, Section 5.2) as our "true" prices and compare the prices of the exotic options obtained from the VG, NIG and Black-Scholes models against these prices.

### 6.3 Model risk

In the previous section we found it difficult to justify which of four models produced the best price for an exotic options, since the "true" prices were unknown. Here, we price both of exotic options (barrier and lookback options) with the CGMY model using its varying parameters (the parameters obtained by increasing and decreasing the multiple parameters of CGMY model as described in Section 5.2), and we consider those prices as our "true" exotic prices. The aim here is to check which of the four models can price the exotic options best when we compare their prices to the "true" prices obtained with the CGMY model. To price the exotic options with NIG, VG and Black-Scholes models, we consider their risk-neutral parameters calibrated to "CGMY-world" data (i.e. the market prices computed with the CGMY model using its varying parameters). We use

the Monte Carlo method to compute the price of the up-and-in, up-and-out calls and the lookback options. We simulate 50 000 paths of the underlying assets for each model. We consider the strike price when the option is out-of-the-money and in-the-money  $K = 110$  and 95 respectively, the spot price 100, the interest rate at  $r = 0.019$ , the dividend yield at  $q = 0.012$  and one year of maturity  $T = 1$ . We assume that a year consists of 250 trading days. The barrier level is a function of the initial stock price (ranging from 150 to 1.550). Below we compare the prices of the barrier and lookback options both when the option prices are in-the-money and out-the-money and computed with all models. We start by comparing the prices of the barrier and lookback option when the option is out-of-the-money, (i.e.  $K = 110 > S_0 = 100$ ).

Figures 6.3, 6.4, 6.5, 6.6 and 6.7 show the results of the comparison for the barrier prices of the up-and-in call computed with the various sets of the new parameters of the CGMY, NIG, VG and BS models between the "true" prices of the up-and-in call (i.e. prices computed with CGMY model using its varying parameters sets) when the option is out-the-money.

The aforementioned figures also show that the prices of barrier options computed with the various sets of the new parameters differ from each other. This is to be expected since different sets of the parameters may lead to the different exotic options prices. If the barrier level is equal to the spot price (i.e. the value of the up-and-in calls = vanilla calls), we see in the Figure 6.3 that the prices of the up-and-in calls computed with the BS model are larger than our current "true" prices while the prices of the up-and-in calls obtained with the NIG and VG models are smaller than current "true" prices. In the paper of Schoutens [74], he shows that the difference between barrier option prices computed across models may be as much as 200%. Similarly, here we notice that the percentage error between the values of the up-and-in calls obtained between the BS prices and "true" prices with new parameters calibrated to "CGMY-world" data obtained from the following varying sets  $((C^+, G, M, Y^-), (C, G, M, Y^-), (C^+, G, M, Y^+))$  are 40%, 79%, 12% and the ones obtained with NIG and VG models are 57%, 8%, 31% and 58%, 30%, 54%. This suggests evidence of the model risk. For example, the BS model overprices the prices of the up-and-in call, as is illustrated by the percentage error between the BS and the "true" price of the up-and-in calls of 79%, while the percentage error between the prices of up-and-in call obtained with VG and NIG models is up to 30% and 8%. Here it is clear that BS model is an inappropriate model because of its poor calibration. In addition, the percentage error between the prices of the up-and-in calls computed with CGMY model with all set of the new parameters and our current "true" prices are

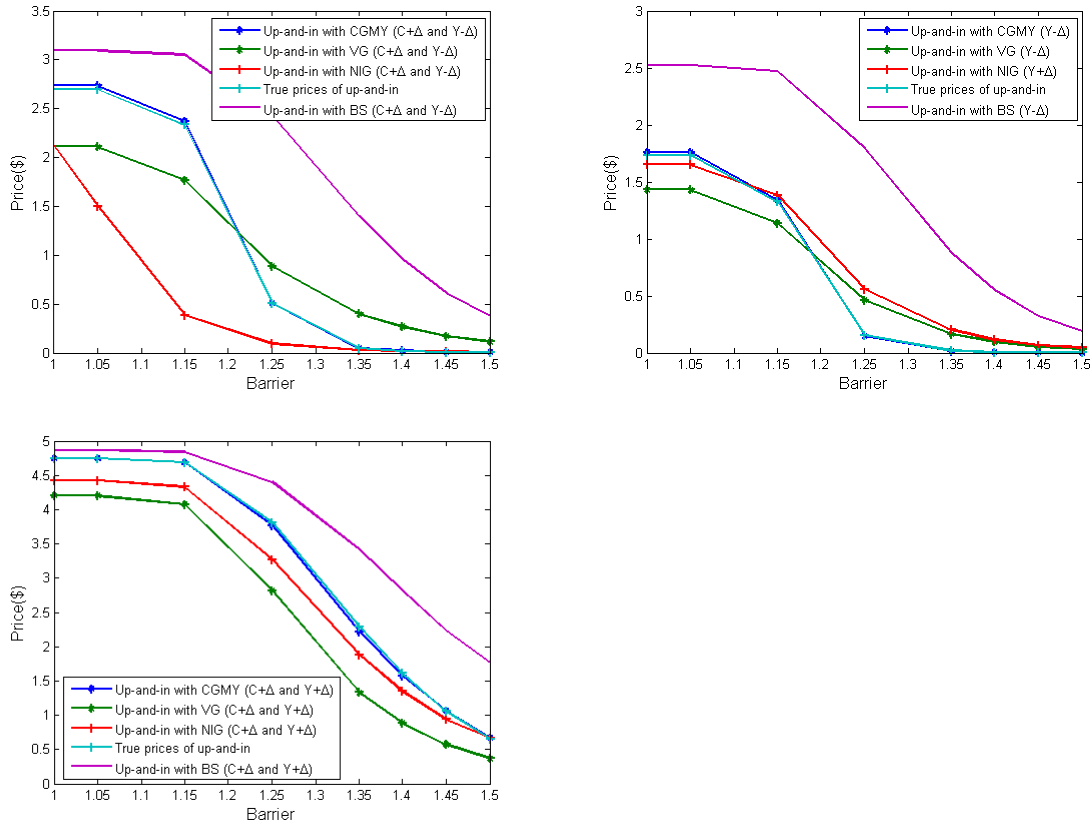


**Figure 6.3:** We computed the prices of the up-and-in and up-and-out options for the NIG, VG, CGMY and BS models obtained with the model parameters calibrated from the vanilla call computed with the model parameters  $(C^+, G, M, Y^-)$ ,  $(C, G, M, Y^-)$  and  $(C^+, G, M, Y^+)$ . The barrier level ranges from  $1(S_0)$  to  $1.5(S_0)$ , the strike price is  $K = 110$ , the spot price is equal  $S_0 = 100$ , the risk-interest rate  $r = 19\%$ , dividend yield at  $q = 12\%$  and maturity  $T = 1$

$(-2.81\%, 1.28\%, 5.7\%, -0.04\%, -2.62\%, -3.75\%, -0.02\%, -2.45\%, -26.44\%)$  which differs from zero, despite the fact that these new parameters are calibrated to "CGMY-world" data. We expected this since we observed a slight difference between the new parameters of CGMY model and its varying parameters (see Section 5.2.1).

That means the prices of the up-and-in calls are very sensitive to calibration risk, and also that calibration risk can be seen as a cause of model risk.

In Figures 6.6, 6.7 and 6.4, we show that the prices of the up-and-in call computed with BS model with the new parameters calibrated to "CGMY-world" data obtained with varying parameters set  $((C^-, G, M, Y), (C^-, G, M, Y^+), (C^+, G, M, Y^-), (C, G, M, Y^+)$  and  $(C, G, M, Y))$  are similar to "true" prices while the ones obtained with the NIG and VG model are different to current "true" prices. Thus by pricing up-and-in calls with NIG

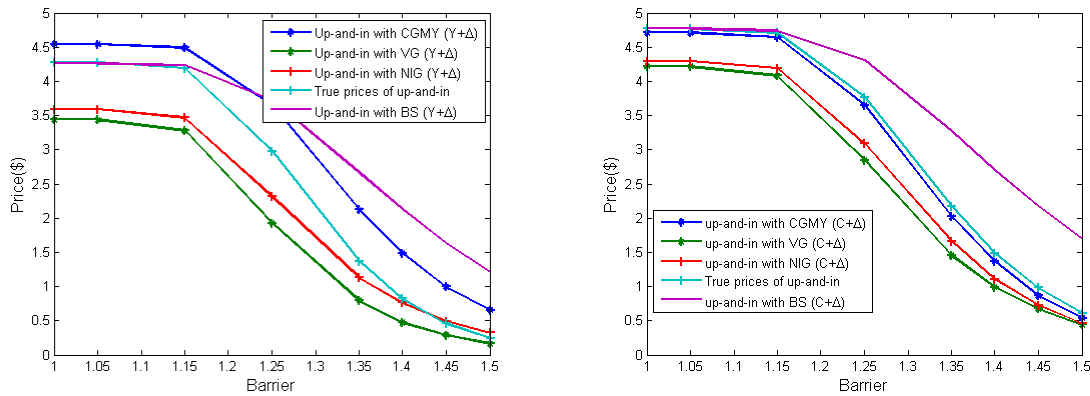


**Figure 6.4:** We computed the prices of the up-and-in and up-and-out options for NIG, VG, CGMY and BS models obtained with the model parameters calibrated from the vanilla call computed with the model parameters  $(C, G, M, Y^+)$  and  $(C^+, G, M, Y)$ . The barrier level ranges from 150 to 1.550, the strike price is  $K = 110$ , the spot price is equal  $S_0 = 100$ , the riskless  $r = 19\%$ , dividend yield  $q = 12\%$  and maturity  $T = 1$

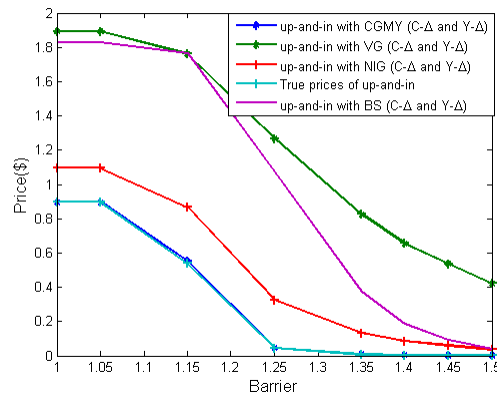


**Figure 6.5:** We computed the prices of the up-and-in and up-and-out options for the NIG, VG, CGMY and BS models obtained with the model parameters calibrated from the vanilla call computed with the model parameters.  $(C^-, G, M, Y^-)$ . The barrier level ranges from 150 to 1.550, the strike price is  $K = 110$ , the spot price is equal  $S_0 = 100$ , the risk-interest rate  $r = 19\%$ , dividend yield  $q = 12\%$  and maturity  $T = 1$

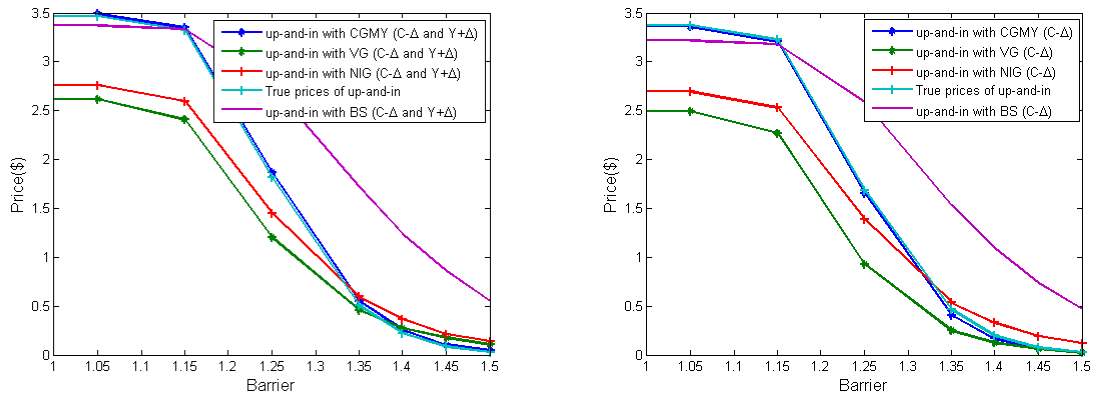


**Figure 6.6:** We computed the prices of the up-and-in and up-and-out options for the NIG, VG, CGMY and BS models obtained with the model parameters calibrated from the vanilla call computed with the model parameters  $(C^-, G, M, Y^+)$  and  $(C^-, G, M, Y)$ . The barrier level ranges from  $1.5S_0$  to  $1.5S_0$ , the strike price is  $K = 110$ , the spot price is equal  $S_0 = 100$ , the risk-interest rate  $r = 19\%$ , dividend  $q = 12\%$  and maturity  $T = 1$

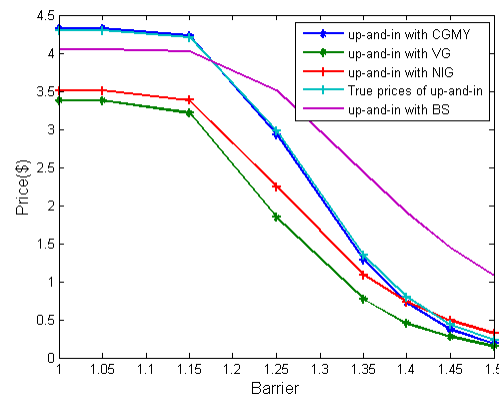


**Figure 6.7:** We computed the prices of the up-and-in and up-and-out options for the NIG, VG, CGMY and BS models obtained with the model parameters calibrated from vanilla calls computed with the model parameters  $(C, G, M, Y)$ . The barrier level ranges from  $1.5S_0$  to  $1.5S_0$ , the strike price is  $K = 110$ , the spot price is equal  $S_0 = 100$ , the riskless  $r = 19\%$ , dividend yield  $q = 12\%$  and maturity  $T = 1$

and VG models, we are exposed to model risk as there are huge differences between the "true" price of the up-and-in call and the ones obtained with NIG and VG models (48%, 69%, 70%, 68%, 78% and 55%, 84%, 85%, 88%, 92% respectively), despite the fact that NIG and VG models fit the "CGMY-world" data better than BS model. In contrast, the percentage error between the "true" price of the up-and-in call and the ones obtained with BS model are only 0.35%, 2%, 9%, 15%, 25%. Once again, we agree with Schoutens [74] that the difference of the barrier between model may be up to (200%).

Finally, in Figure 6.5, we show that the price of up-and-in call computed with the NIG model using the new parameters calibrated to "CGMY-world" data obtained with the varying parameters set  $(C^-, G, M, Y^-)$  are close to "true" prices while the ones obtained with the VG and BS models differ to current "true" prices, despite the fact that VG and NIG model have a same number of risk-neutral parameters and also fit the "CGMY-world" data better than BS model. The difference between the up-and-in call obtained with NIG model and "true" prices is up (20%) while the ones between the VG and BS models and "true" prices are 100% and 94%.

Furthermore, we note that when the option is out-the-money, it is difficult to avoid model risk when we price the barrier (especially the up-and-in call) since any model carries model risk. We observed that the percentage error between the up-and-in calls obtained with NIG, VG and BS models and our current "true" price may be as much as 100%.

Tables 6.2 and 6.3 display the results of the lookback option and the percentage relative error between the "true" prices of the lookback options (the prices of the lookback options computed with the CGMY model using the varying parameters) and the lookback prices compute with CGMY, NIG, VG and BS models using their new parameters sets. In table 6.2, we observe that the values of the lookback prices computed with the NIG and VG models for all new parameters set are small and close to "true" prices while those obtained with BS model are larger than the values of our "true" prices. Tables 6.2 and 6.3 show the percentage relative error between the prices of the lookback options obtained with CGMY, NIG, BS and VG models computed with all new parameters sets and "true" prices. The positive values for the percentage relative error indicate that the prices of the lookback options are small compare to "true" prices while negative values indicates large prices compared to "true" prices. Here, the BS model overprices the lookback options since their values are large than our "true" prices of lookback options. The prices of lookback options computed with NIG and VG model are similar in each case. As well as differences between the prices of lookback option computed with NIG, VG and BS models and "true" prices, it is important to note difference in magni-

**Table 6.2:** The price values of the lookback options computed with all different model parameters. Strike price  $K = 110$ , spot price  $S_0 = 100$ , interest rate  $r = 19\%$ , dividend yield  $q = 12\%$  and  $T = 1$

CGMY, NIG, VG and BS parameters calibrated to "CGMY-world" data obtained with the following set of varying parameters	"True" prices	CGMY prices	NIG prices	VG prices	BS prices
$(C, G, M, Y)$	6.5663	6.5332	5.2227	4.9078	7.8403
$(C^-, G, M, Y)$	4.9122	4.8593	3.9355	3.5030	6.2116
$(C^+, G, M, Y)$	7.7543	7.6380	6.5446	6.2431	9.4155
$(C^-, G, M, Y^-)$	1.2443	1.2608	1.3921	2.2502	3.4343
$(C^-, G, M, Y^+)$	5.0595	5.0886	4.0304	3.7204	6.3973
$(C^+, G, M, Y^-)$	3.5190	3.5420	2.8348	2.6430	6.2116
$(C^+, G, M, Y^+)$	7.8084	7.7701	6.7779	6.2489	9.5461
$(C, G, M, Y^-)$	2.3022	2.3090	2.1477	1.7673	4.7501
$(C, G, M, Y^+)$	6.6417	7.5967	5.3596	5.0049	8.2665

tude (Schoutens [74]). We also note that the percentage relative error between the "true" prices of the lookback options and those computed with CGMY model for all new parameters sets are very small, and different to zero, i.e. differences are slight despite the new parameters of CGMY model being calibrated to "CGMY-world" data. We expected this because of the slight difference between the new parameters of CGMY model and its varying parameters (see Section 5.2.1). Thus, the set of the risk-neutral parameters is not unique and the price of the exotic options may not be unique either. Moreover, the prices of the exotic options are difficult to price because of the presence of model risk. Wim Schoutens [74] showed that the difference in prices of lookback options amongst models may vary over 15% and this is comparable to this study when pricing lookback options using NIG, VG, CGMY and BS models where "true" prices may vary by 15%, particularly when the option is out-of-the-money.

In this study we also wish to compare "true" prices of barrier and lookback options with those computed with NIG, VG, CGMY and BS models when the option prices are in-the-money (i.e. strike  $K = 95 < S_0 = 100$ ), and this is discussed below.

Figures 6.8, 6.9, 6.10, and 6.11, show that the prices of the up-and-in and up-and-out

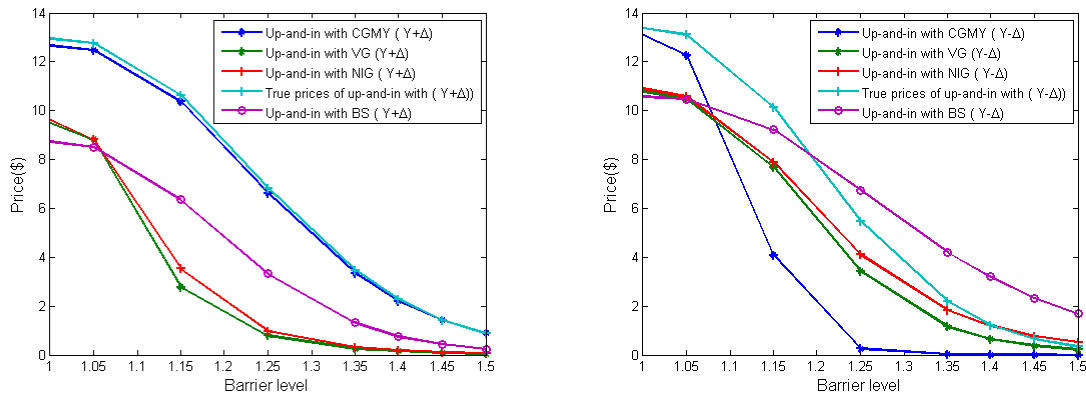


**Figure 6.8:** We computed the prices of the Up-In and Up-Out for NIG, VG, CGMY and BS models obtain with the model parameters calibrated from the vanilla call computed with the model parameters  $(C, G, M, Y^+)$  and  $(C, G, M, Y^-)$ . The barrier level is ranging from 1.50 to 1.550, the strike price is  $K = 95$ , the spot price is equal  $S_0 = 100$ , the risk-interest rate  $r = 19\%$ , dividend yield  $q = 12\%$  and maturity  $T = 1$

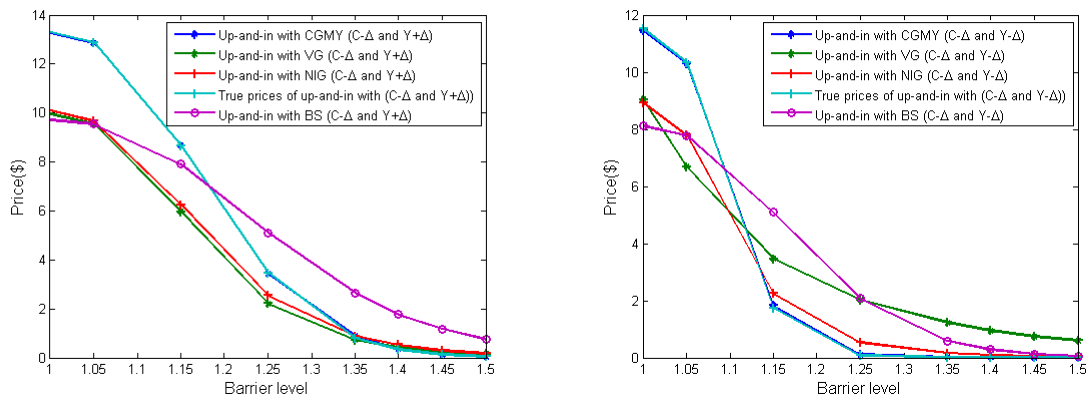


**Figure 6.9:** We computed the prices of the up-and-in and up-and-out calls for NIG, VG, CGMY and BS models obtained with the model parameters calibrated from the vanilla call computed with the model parameters  $(C^-, G, M, Y^+)$  and  $(C^-, G, M, Y^-)$ . The barrier level ranges from 1.50 to 1.550, the strike price is  $K = 95$ , the spot price is equal  $S_0 = 100$ , the risk-interest rate  $r = 19\%$ , dividend  $q = 12\%$  and maturity  $T = 1$



**Table 6.3:** Percentage relative error between the "true" prices of the lookback fixed and the prices obtained with CGMY, NIG, VG and BS models. The strike price  $K = 110$ , spot price  $S_0 = 100$ , interest rate  $r = 19\%$  and dividend  $q = 12\%$  and maturity of one year  $T = 1$

CGMY, NIG, VG and BS parameters calibrated to "CGMY-world" data obtained with the following set of varying parameters	$\frac{\text{True-CGMY}}{\text{True}} * 100$	$\frac{\text{True-NIG}}{\text{True}} * 100$	$\frac{\text{True-VG}}{\text{True}} * 100$	$\frac{\text{True-BS}}{\text{True}} * 100$
(C, G, M, Y)	0.5%	20.46%	25.25%	-19.40%
(C <sup>-</sup> , G, M, Y)	1.076%	19.88%	28.68%	-26.45%
(C <sup>+</sup> , G, M, Y)	1.49%	15.6%	19.48%	-21.42%
(C <sup>-</sup> , G, M, Y <sup>-</sup> )	-1.285%	-11.87%	-80.84%	-176%
(C <sup>-</sup> , G, M, Y <sup>+</sup> )	-0.57%	20.33%	26.46%	-26.44%
(C <sup>+</sup> , G, M, Y <sup>-</sup> )	-0.653%	19.44%	24.89%	-76.51%
(C <sup>+</sup> , G, M, Y <sup>+</sup> )	0.49%	13.19%	19.97%	-22.25%
(C, G, M, Y <sup>-</sup> )	6.691%	6.71%	23.23%	-106.32%
(C, G, M, Y <sup>+</sup> )	-14.378%	19.3%	24.64%	-24.46%

calls computed with the NIG and VG models at barrier level equals the spot price (i.e. the value of up-and-in call = vanilla option), and are close to the "true" prices while those computed with the BS model are very small. Hence, while the the BS model prices up-and-in call prices poorly, the VG and NIG models give a more accurate value of these prices especially when the options are in the money.

In addition, Tables 6.4 and 6.5 show the results of the error between the "true" prices of the lookback option and the lookback prices computed with the NIG, VG and BS models.

Table 6.5 shows that for all new parameters sets, the error between "true" prices of the lookback options and the lookback prices computed are positive with the NIG and VG models but are negative when computed the BS models. Thus, BS model overprices the lookback options as their prices are larger than the "true" prices. As it was for the out-of-the-money options, the BS model performs poorly and the NIG and VG model

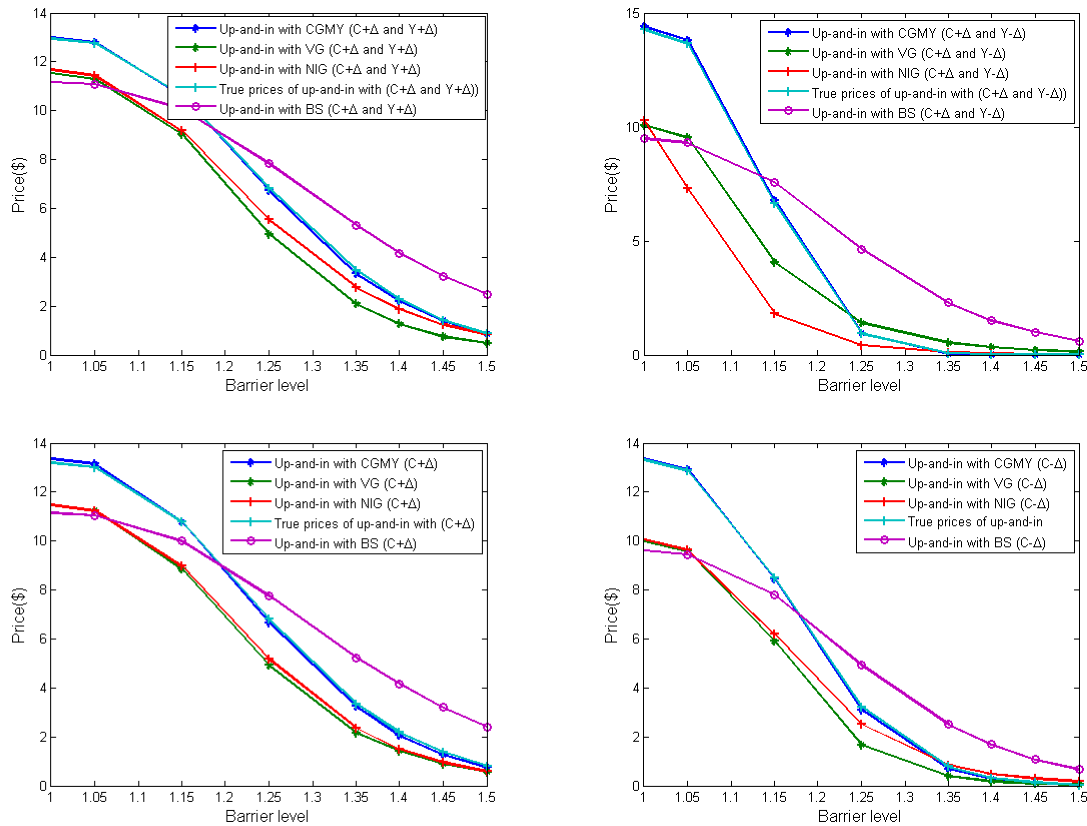


**Figure 6.10:** We computed the prices of the up-and-in and up-and-out calls for NIG, VG, CGMY and BS models obtained with the model parameters calibrated from the vanilla call computed with the model parameters  $(C^+, G, M, Y^+)$  and  $(C^+, G, M, Y^-)$ ,  $(C^+, G, M, Y)$  and  $(C^-, G, M, Y)$ . The barrier level is ranging from 1.50 to 1.550, the strike price is  $K = 95$ , the spot price is equal  $S_0 = 100$ , the risk-interest rate  $r = 19\%$ , dividend  $q = 12\%$  and maturity  $T = 1$

perform well when the options are in-the-money.

Further to the above, we noted that the barrier options (Up-and-In calls) are more sensitive to the model risk than lookback options especially when the options are out-of-the-money. We also observed that models driven by the Lévy dynamics (CGMY, NIG and VG models) are more suitable for the pricing of barrier and lookback option than Black-Scholes models are, especially when the options are in-the-money.

This study shows that the prices of exotic options are model sensitive to the model risk. In the next section we discuss quantifying model risk.

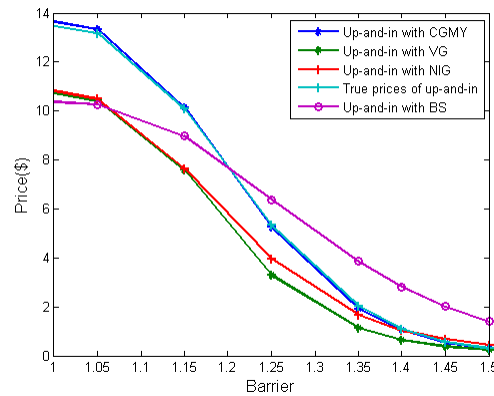


**Figure 6.11:** We computed the prices of the up-and-in and up-and-out calls for NIG, VG, CGMY and BS models obtained with the model parameters calibrated from the vanilla call computed with the model parameters (C,G,M,Y). The barrier level ranges from 1S<sub>0</sub> to 1.5S<sub>0</sub>, the strike price is K = 95, the spot price is equal S<sub>0</sub> = 100, the risk-interest rate r = 19%, dividend q = 12% and maturity T = 1

**Table 6.4:** The price values of the lookback options computed with all different model parameters. Strike price K = 95, spot price S<sub>0</sub> = 100, interest rate r = 19%, dividend yield q = 12% and T = 1

CGMY, NIG, VG and BS parameters calibrated to "CGMY-world" data obtained with the following set of varying parameters	"True" prices	CGMY prices	NIG prices	VG prices	BS prices
(C, G, M, Y)	19.3186	19.2833	17.2853	15.5371	20.2785
(C <sup>-</sup> , G, M, Y)	17.7087	17.6267	15.7756	3.5030	18.4481
(C <sup>+</sup> , G, M, Y)	20.5368	20.4713	18.7955	18.5782	21.9712
(C <sup>-</sup> , G, M, Y <sup>-</sup> )	13.3410	13.3975	12.3247	12.0539	15.0100
(C <sup>-</sup> , G, M, Y <sup>+</sup> )	17.8323	17.8385	15.8989	15.6499	18.5737
(C <sup>+</sup> , G, M, Y <sup>-</sup> )	16.5764	16.6595	14.7683	14.4092	18.4481
(C <sup>+</sup> , G, M, Y <sup>+</sup> )	20.5391	20.4113	19.0091	18.7191	22.1502
(C, G, M, Y <sup>-</sup> )	14.9739	15.0316	13.6113	13.3162	16.5350
(C, G, M, Y <sup>+</sup> )	19.4104	20.2889	17.4585	17.2769	20.6723

**Table 6.5:** Percentage relative error between the "true" prices of the lookback fixed and the prices obtained with CGMY, NIG, VG and BS models. The strike price  $K = 110$ , spot price  $S_0 = 100$ , interest rate  $r = 19\%$  and dividend  $q = 12\%$  and maturity of one year  $T = 1$

CGMY, NIG, VG and BS parameters calibrated to "CGMY-world" data obtained with the following set of varying parameters	$\frac{\text{True-CGMY}}{\text{True}} * 100$	$\frac{\text{True-NIG}}{\text{True}} * 100$	$\frac{\text{True-VG}}{\text{True}} * 100$	$\frac{\text{True-BS}}{\text{True}} * 100$
(C, G, M, Y)	0.182%	10.52%	11.24%	-4.96%
(C <sup>-</sup> , G, M, Y)	0.46%	10.91%	12.26%	-4.17%
(C <sup>+</sup> , G, M, Y)	0.318%	8.47%	9.53%	-6.98%
(C <sup>-</sup> , G, M, Y <sup>-</sup> )	-0.423%	7.61%	9.64%	-12.51%
(C <sup>-</sup> , G, M, Y <sup>+</sup> )	-0.0347%	10.84%	12.23%	-4.15%
(C <sup>+</sup> , G, M, Y <sup>-</sup> )	-0.501%	10.90%	13.07%	-11.29%
(C <sup>+</sup> , G, M, Y <sup>+</sup> )	0.622%	7.44%	8.86%	-7.84%
(C, G, M, Y <sup>-</sup> )	-0.385%	9.09%	11.07%	-10.42%
(C, G, M, Y <sup>+</sup> )	-4, 525%	10.05%	10.99%	-6.5%

## 6.4 Quantifying Model Risk

Having discussed how the model risk can arise when we price exotic options, we now attempt to quantify this model risk. We limit our discussion of details of concerning quantifying model uncertainty measures, which are discussed in detail by Rama Cont [26] and Alok Gupta, Christoph Reisinger, and Alan Whitley [42]. However, quantification of model risk does requires a review of how the model uncertainty measure is quantified.

### 6.4.1 Quantifying Model Uncertainty Measure (Cont [26])

In this section, we review quantifying model uncertainty measure as introduced by Rama Cont [26]. Uncertainty can be considered radically distinct from the familiar concept of risk, although they have never been properly separated (Rama Cont [26]).

Whereas "risk" can be taken in some cases as a quantity susceptible to measurement, at other times it is not (Frank Knight [50]). Let  $(\Omega, F)$  be a set of the market scenario and we also assume that there is no reference probability measure on the set  $\Omega$ . Consider the trajectories of the prices in the market scenario  $(S(\omega), \omega \in \Omega)$  and denote by:  $S : \Omega \mapsto D([0, T])$  where  $D([0, T])$  represents the space which allows the jumps in the prices (or the space of right continuous functions with left limit) (Rama Cont [26]). Let  $H$  be a contingent claim identifies at terminal value at  $T$  of its payoff. We also assume that all asset values and payoffs are of discounted value. Rama Cont [26] states that in order to describe the method for quantifying the model uncertainty he needs the following ingredients:

- The options prices must be observed on the markets (Benchmark instruments). The observed market prices are denoted by  $(C_j^*)_{j \in J}$  and payoffs by  $(H_j)_{j \in J}$ . The range of the observed prices are given by  $C_j^* \in [C_j^{bid}, C_j^{ask}]$  since there is not a unique prices.
- The discount asset prices  $(S_t)_{t \in [0, T]}$  must be a martingale under each  $\mathbb{Q} \in \mathcal{Q}$  with respect to the filtration  $F_t$ : a set of arbitrage-free pricing measure  $\mathcal{Q}$  must consist with the market prices of the benchmark instruments and

$$\mathbb{E}_{\mathbb{Q}}[|H_j|] < \infty \quad \mathbb{E}_{\mathbb{Q}}[H_j] = C_j^* \quad \forall \mathbb{Q} \in \mathcal{Q}, \quad \forall j \in J. \quad (6.4.1)$$

Cont [26] highlights that market prices  $C_j^*$  is only defined up to the bid-ask spread so one needs to modify the above condition 6.4.1 to:

$$\mathbb{E}_{\mathbb{Q}}[|H_j|] < \infty \quad \mathbb{E}_{\mathbb{Q}}[H_j] \in [C_j^{bid}, C_j^{ask}] \quad \forall \mathbb{Q} \in \mathcal{Q}, \quad \forall j \in J. \quad (6.4.2)$$

#### 6.4.1.1 Remark

Kerkhof, Melenberg, and Schumacher [48] highlight the distinction between the "model uncertainty" and "parameters uncertainty". However, Cont [26] said this distinction was irrelevant, on the basis that the family of the parameters of the pricing model  $(\mathbb{Q}_{\theta})_{\theta \in E}$ , and different value  $(\theta_j)_{j \in A}$  of the parameter will define probability measures  $\mathbb{Q}_{\theta_j}$ , which is the only component (ingredient) needed to construct the methodology for quantifying model uncertainty. He also states that the parametric family being integrated into a "one" (or "single") parametric family is purely conventional and that it depends on the arbitrary definition of a "parametric family". In fact by integrating all models in a set  $\mathcal{Q}$  into a single super-model, the model uncertainty can always be represented as "parameter uncertainty" (Cont [26]).

Let  $\mathcal{C}$  be set of the contingent claim with a well-defined price in all Lévy models, and denotes by:

$$\mathcal{C} = \left\{ H \in F_T, \sup_{\mathbb{Q} \in \mathcal{Q}} \mathbb{E}_{\mathbb{Q}}[|H|] < \infty \right\}. \quad (6.4.3)$$

We can now consider a mapping  $\mu : \mathcal{C} \mapsto [0, \infty$  as the model uncertainty on the value of the contingent claim  $X$ . Cont [26] enumerated the following properties:

- a) The model uncertainty of the benchmark instruments can be reduced to the uncertainty on market value:

$$\mu(H_j) \leq |C_j^{ask} - C_j^{bid}| \quad \forall j \in J \quad (6.4.4)$$

- b) Effect of hedging with the underlying asset:

$$\mu\left(X + \int_0^T \phi_t \cdot dS_t\right) = \mu(X) \quad \forall \phi \in S \quad (6.4.5)$$

Particularly, the value of the contingent claim that may be replicated in a model free way by trading in the underlying has no model uncertainty:

$$\left[ \exists x_0 \in \mathbb{R}, \exists \phi \in S, \forall \mathbb{Q} \in \mathcal{Q}, \quad \mathbb{Q}\left(X = x_0 + \int_0^T \phi_t \cdot dS_t\right) = 1 \right] \Rightarrow \mu(X) = 0 \quad (6.4.6)$$

- c) Convexity: model uncertainty may not be increased through diversification.

$$\forall X_1, X_2 \in \mathcal{C}, \forall \lambda \in [0, 1] \quad \mu(\lambda X_1 + (1 - \lambda)X_2) \leq \lambda \mu(X_1) + (1 - \lambda)\mu(X_2) \quad (6.4.7)$$

The above property 6.4.4 defines a scale for  $\mu$ : When  $\mu$  verifies the property 6.4.4 then  $\lambda \mu$  may also verifies this property for  $0 < \lambda \leq 1$ , but not necessary for  $\lambda > 1$ . This may allow one to construct a maximal element among all mapping proportional to  $\mu$  which can be defined as the one that saturates the range constraint 6.4.4 (Cont [26]):

$$\mu_{\max} = \lambda_{\max} \mu \quad \lambda_{\max} = \sup\{\lambda > 0, \lambda \mu \text{ verifies } 6.4.4\} \quad (6.4.8)$$

### 6.4.2 A Coherent Measure of Model Uncertainty (Rama Cont [26])

Using the above ingredient, Cont [26] constructs a measure of model uncertainty which verifies the above properties. Let  $X \in \mathcal{C}$  be a payoff which has a well-defined value in

all the pricing models  $\mathbb{Q} \in \mathcal{Q}$ . Cont [26] defines the upper and lower price bounds as follows:

$$\pi_{hi}(X) = \sup_{\mathbb{Q} \in \mathcal{Q}} \mathbb{E}_{\mathbb{Q}}[X] \quad \pi_{lo}(X) = \inf_{\mathbb{Q} \in \mathcal{Q}} \mathbb{E}_{\mathbb{Q}}[X] = -\pi_{hi}(-X).$$

A coherent risk measure is defined when  $X \mapsto \pi_{hi}(-X)$ . Any of the pricing models  $\mathbb{Q} \in \mathcal{Q}$ , will give a value of  $X$  which will fall in the interval  $[\pi_{lo}, \pi_{hi}]$ . If the value of the payoff  $X$  is not influenced by the model uncertainty then we have  $\pi_{hi}(X) = \pi_{lo}(X)$ . Hence, Rama Cont [26] derives a model uncertainty formula by taking the difference between the highest price  $\pi_{hi}$  and lowest price  $\pi_{lo}$  for a payoff  $X$  under a set of risk neutral measures  $\mathcal{Q}$

$$\mu_{\mathbb{Q}}(X) = \pi_{hi}(X) - \pi_{lo}(X). \quad (6.4.9)$$

When one computes the market value of the derivative using the pricing of Lévy models ( $\mathbb{E}_{\mathbb{Q}}[X]$ ), the margin for model uncertainty is given by  $\pi_{hi} - \mathbb{E}_{\mathbb{Q}}[X] \leq \mu_{\mathbb{Q}}(X)$ , which represents an upper bound on the margin for "model risk" (Rama Cont [26]).

In fact, the only problem with the model risk formula 6.4.9 is that the both prices  $\pi_{hi}$  and  $\pi_{lo}$  contain the fitting RMSE error described in chapter 4. In order to remove this bias from the barrier and lookback fixed options, one needs to normalize the above 6.4.9 model risk formula. To do this, we modify the model risk formula obtained by Rama Cont [26] by dividing the expression  $\mu_{\mathbb{Q}}$  by sum of  $\pi_{hi}$  and  $\pi_{lo}$  (model risk ratio) which follows:

$$\bar{\mu}_{\mathbb{Q}}(X) = \frac{\pi_{hi}(X) - \pi_{lo}(X)}{\pi_{hi}(X) + \pi_{lo}(X)}. \quad (6.4.10)$$

Note that if the model risk ratio  $\bar{\mu}_{\mathbb{Q}}(X)$  is high, this indicates that the model risk is a large component of the risk of the portfolio and that ratio can be used like a tool for model validation (model validation takes the models and methods developed by modeling quantitative analyst and determines if these models and methods are valid and correct [2])(Rama Cont [26]). We summary that the model risk ratio helps verify that the models and methods developed by the modeling quantitative analyst are valid and correct ([2]).

#### 6.4.2.1 Remark

To compute the value of  $\pi_{hi}$  and  $\pi_{lo}$ , one can use an approach similar to that introduced by El Karoui and Quenez [36] (the superhedging approach). When using complete market models, all models in  $\mathcal{Q}$  correspond to the complete market models, and  $\pi_{lo}$  is interpreted as the cost of the cheapest strategy dominating  $X$  in the worst-case

model (Rama Cont [26]). However, if using superhedging approach, the value of  $Q$  is considered as the set of all martingale measure equivalent to a given probability measure  $\mathbb{P}$  (Rama Cont [26]). Thus, price intervals produced by the superhedging approach have tendency to be quite large and can sometime coincide with the maximal arbitrage bounds (Eberlein and Jacod [35]) which renders them useless when comparing them with market prices (Rama Cont [26]). Rama Cont [26] states that by using the above approach when  $X$  is that terminal payoff of a trade option, the construction of the interval  $[\pi_{hi}(X), \pi_{lo}(X)]$  is compatible with bid-ask interval for this option. The above remark shows that the calibration condition 6.4.2 is essential for ensuring that the model uncertainty measure is useful and nontrivial (Rama Cont [26]).

## 6.5 The Results of Model Risk Ratio

In this section, we discuss the results of the model risk ratio obtained using the model risk ratio 6.4.10. Below we report the results for the model risk of the exotic options computed with NIG, VG, CGMY and Black-Scholes models using their risk-neutral parameters calibrated to "real world" data obtained with the varying parameters of the CGMY model.

Tables 6.5, 6.5, 6.8 and 6.9 show the results of the model risk ratio for the up-and-in calls, and lookback calls computed with all models. The values of the model risk ratio differ to zero, indicating model risk is present in the pricing of exotic options (see section 6.3). In table 6.5, the values of the model risk ratio for the up-and-in call when the options are in-the-money are large than those that are out-the-money for certain sets of the new parameters. This means, the up-and-in calls are more sensitive to model risk when these options are in-the-money. But, for the lookback options (see the table 6.8), the the values of model risk ratio are small when the options are in-the-money while they are high for the options out-the-money (table 6.9) for certain sets of the new parameters. This implies that the lookback options are more sensitive to model risk when these options are out the money. These results show that even for the common derivative, the model risk ratio is a major risk factor as much as market risk, since it does not represent a small price correction (Rama Cont [26]). When the model risk ratio is high for the lookback call and the option is out-the-money (0.4679), that means the variation of the lookback prices across the models are high. It is important for financial institutions such as the banks to consider which model is uses, given the relevant criteria, to price its lookback option so as to avoid exposure to the risk of using an incorrect or inappropriate model. Thus, knowing the value of the model risk ratio, the financial institutions such



**Table 6.6:** The result of model risk for exotic option with model price computed for all set of model estimated from 9 different call vanilla from CGMY model

The results of model risk  $\bar{\mu}_Q$  of the up-and-in call computed with the NIG, VG, CGMY and BS models using their new parameters calibrated to different sets of the "real world" data obtained with the set of the varying parameters of CGMY model. Strike price  $K = 110$ , spot price  $S_0 = 100$ , interest rate  $r = 19\%$ , dividend  $q = 12\%$  and  $T = 1$

Barrier level	up-and-in with (C, G, M, Y)	up-and-in with (C <sup>-</sup> , G, M, Y)	up-and-in with (C <sup>+</sup> , G, M, Y)	up-and-in with (C <sup>-</sup> , G, M, Y <sup>-</sup> )
100	0.1196	0.1496	0.0614	0.3578

The results of model risk  $\bar{\mu}_Q$  of the up-and-in call computed with the NIG, VG, CGMY and BS models using their new parameters calibrated to different sets of the "real world" data obtained with the set of the varying parameters of CGMY model. Strike price  $K = 110$ , spot price  $S_0 = 100$ , interest rate  $r = 19\%$ , dividend  $q = 12\%$  and  $T = 1$

Barrier level	up-and-in with (C <sup>-</sup> , G, M, Y <sup>+</sup> )	up-and-in with (C <sup>+</sup> , G, M, Y <sup>-</sup> )	up-and-in with (C <sup>+</sup> , G, M, Y <sup>+</sup> )	up-and-in with (C, G, M, Y <sup>-</sup> )	up-and-in with (C, G, M, Y <sup>+</sup> )
100	0.0834	0.1890	0.0732	0.2758	0.1093

as the banks choose the correct model to use for valuing exotic options, thereby avoiding financial loss or minimizing risk, since the model risk ratio can be used as a tool for model validation. In conclusion, lookback options are more sensitive to the model risk than barrier options are (especially up-and-in calls), particularly when the options are out-the-of- money. Therefore, when pricing lookback fixed options instead of up-and-in call when the options are out the money, one is exposed to more risk.

**Table 6.7:** The result model risk for exotic option with model price computed for all set of model estimated from 9 different call vanilla from CGMY model

The results of model risk  $\bar{\mu}_Q$  of the up-and-in call computed with the NIG, VG, CGMY and BS models using their new parameters calibrated to different sets of the "real world" data obtained with the set of the varying parameters of CGMY model. Strike price  $K = 95$ , spot price  $S_0 = 100$ , interest rate  $r = 19\%$ , dividend  $q = 12\%$  and  $T = 1$

Barrier level	up-and-in with (C, G, M, Y)	up-and-in with (C <sup>-</sup> , G, M, Y)	up-and-in with (C <sup>+</sup> , G, M, Y)	up-and-in with (C <sup>-</sup> , G, M, Y <sup>-</sup> )
100	0.1295	0.1619	0.0844	0.1741

The results of model risk  $\bar{\mu}_Q$  of the up-and-in call computed with the NIG, VG, CGMY and BS models using their new parameters calibrated to different sets of the "real world" data obtained with the set of the varying parameters of CGMY model. Strike price  $K = 95$ , spot price  $S_0 = 100$ , interest rate  $r = 19\%$ , dividend  $q = 12\%$  and  $T = 1$

Barrier level	up-and-in with (C <sup>-</sup> , G, M, Y <sup>+</sup> )	up-and-in with (C <sup>+</sup> , G, M, Y <sup>-</sup> )	up-and-in with (C <sup>+</sup> , G, M, Y <sup>+</sup> )	up-and-in with (C, G, M, Y <sup>-</sup> )	up-and-in with (C, G, M, Y <sup>+</sup> )
100	0.1562	0.2019	0.0739	0.1936	0.1170

**Table 6.8:** The results of model risk ratio  $\mu_{\mathbb{Q}}$  for the lookback call computed with the NIG, VG, CGMY and BS models using their new parameters calibrated to different sets of the "real world" data obtained with the set of the varying parameters of CGMY model. Strike price  $K = 95$ , spot price  $S_0 = 100$ , interest rate  $r = 19\%$ , dividend  $q = 12\%$  and  $T = 1$

CGMY, NIG, VG and BS parameters calibrated to "CGMY-world" data obtained with the following set of varying parameters	$\bar{\mu}_{\mathbb{Q}}$
(C, G, M, Y)	0.0836
(C <sup>-</sup> , G, M, Y)	0.0856
(C <sup>+</sup> , G, M, Y)	0.0836
(C <sup>-</sup> , G, M, Y <sup>-</sup> )	0.1274
(C <sup>-</sup> , G, M, Y <sup>+</sup> )	0.0854
(C <sup>+</sup> , G, M, Y <sup>-</sup> )	0.1229
(C <sup>+</sup> , G, M, Y <sup>+</sup> )	0.0839
(C, G, M, Y <sup>-</sup> )	0.1078
(C, G, M, Y <sup>+</sup> )	0.1137

**Table 6.9:** The results of model risk ratio  $\mu_{\mathbb{Q}}$  for the lookback calls obtained with the NIG, VG, CGMY and BS models using their new parameters calibrated to different sets of the "real world" data obtained with the set of the varying parameters of CGMY model. Strike price  $K = 110$ , spot price  $S_0 = 100$ , interest rate  $r = 19\%$ , dividend  $q = 12\%$  and  $T = 1$

CGMY, NIG, VG and BS parameters calibrated to "CGMY-world" data obtained with the following set of varying parameters	$\bar{\mu}_{\mathbb{Q}}$
(C, G, M, Y)	0.3738
(C <sup>-</sup> , G, M, Y)	0.2788
(C <sup>+</sup> , G, M, Y)	0.2025
(C <sup>-</sup> , G, M, Y <sup>-</sup> )	0.4679
(C <sup>-</sup> , G, M, Y <sup>+</sup> )	0.2645
(C <sup>+</sup> , G, M, Y <sup>-</sup> )	0.4030
(C <sup>+</sup> , G, M, Y <sup>+</sup> )	0.2087
(C, G, M, Y <sup>-</sup> )	0.4576
(C, G, M, Y <sup>+</sup> )	0.2457

## Chapter 7

# Conclusion and Future work

This research focused on comparing the performance of a Lévy model in pricing vanilla and exotic options. We first calibrated the model parameters to the S&P 500 index option. We found that the CGMY model fits the S&P 500 index better than the VG, NIG and Black-Scholes models. This was evidenced by the model prices with more degrees of freedom or model parameters fitting the observed market values better than one with a single model parameter (Volatility) as in the Black Schole model. We also showed that the vanilla prices obtained with the NIG, CGMY and VG models are similar, but they differ from prices obtained from the Black-Scholes model. The NIG and VG models give similar prices for the barrier call (Up-in and Up-out) which differed from the prices obtained using the CGMY and Black-Scholes models. Furthermore, the CGMY model fitted the market better than the other models. The pure jump Lévy model priced the European call, and the up-and-in and up-and-out calls options better than Black-Scholes model did. It was noted that the prices of the lookback fixed option obtained from each model differed from one another.

We also calibrated CGMY, NIG, VG and BS models to the "CGMY-world" data (market prices obtained with the varying parameters of CGMY model), and we found that the new parameters of the CGMY model obtained through this calibration differed slightly to the varying parameters, even though the model "CGMY-world" data was computed with varying parameters. A further finding was that the NIG model fits the "CGMY-world" data better than the VG model, despite the fact that VG model is a particularly type of the CGMY model. We then priced the lookback and barrier options, and quantified model risk using the new parameters calibrated to "CGMY-world" data. We noted that the lookback options are more sensitive to model risk when the options are out-the-money while barrier (up-and-in call) options are sensitive to model risk when

options are in-the-money.

In general, it appears that the NIG, VG and CGMY models price the barrier, lookback fixed and vanilla call options better than the Black-Scholes model does. Possible future research stemming from this thesis would be to compare the performance of the pure jump, and Heston and Bate models with the Black-Scholes model when hedging the exotic option (especially the barrier option, lookback option and Asian option).

## Appendix A

# The graphics of hedging performance

### A.1 Table of S&P 500 indexed

The table below has 77 call option prices of the S&P 500 index. The market price closed on 18 April 2002 and that day the spot price of the S&P 500 index closed at 1124.47, the interest rate at  $r = 1.9\%$  and the dividend at  $q = 1.2\%$  per year.

### A.2 The Algorithms for Simulating the Path of the Pure Jump Model

In this section we discuss the procedure to simulate the pure jump models. We discuss the algorithms for each of our given models (VG, NIG and CGMY models). The VG, NIG and CGMY models can be written via a subordinator part, an important factor because it helps us to avoid dealing directly with the jump kernel may hinder the simulation of our models.

#### A.2.1 The Algorithm for Simulating the Path of the VG processes

In order to simulate the path of the VG model we need to consider the subordinator part of the VG model as previously stated. The subordinate part of VG model is the Inverse Gamma process. The following algorithm of the VG model presented below is similar to the one introduced by *Johnk's generator*. First the process generates first the IG

**Table A.1:** Table of 77 call prices of S&P 500 indexed.

Strike	May (2002)	Jun (2002)	Sep. (2002)	Dec (2002)	March (2003)	June (2003)	Dec. 2003
975	0.000	0.000	161.60	173.30	0.000	0.000	0.000
995	0.000	0.000	144.80	157.00	0.000	182.10	0.000
1025	0.000	0.000	0.000	120.10	133.10	146.50	0.000
1050	0.000	84.50	100.70	114.80	0.000	143.00	171.40
1075	0.000	64.30	82.50	97.60	0.000	0.000	0.000
1090	43.10	0.000	0.000	0.000	0.000	0.000	0.000
1100	35.00	0.000	65.50	81.00	96.20	111.30	140.40
1110	0.000	39.50	0.000	0.000	0.000	0.000	0.000
1120	22.90	33.50	0.000	0.000	0.000	0.000	0.000
1125	20.20	30.70	51.00	66.90	81.70	97.00	0.000
1130	0.000	28.00	0.000	0.000	0.000	0.000	0.000
1135	0.000	25.60	45.50	0.000	0.000	0.000	0.000
1140	13.30	23.20	0.000	58.90	0.000	0.000	0.000
1150	0.000	19.10	38.10	53.90	68.30	83.30	112.80
1160	0.000	15.30	0.000	0.000	0.000	0.000	0.000
1170	0.000	12.10	0.000	0.000	0.000	0.000	0.000
1175	0.000	10.90	27.70	42.50	56.60	0.000	99.80
1200	0.000	0.000	19.60	33.00	46.10	60	0.000
1225	0.000	0.000	13.20	24.90	36.90	49.80	0.000
1250	0.000	0.000	0.000	18.30	29.30	41.20	66.90
1275	0.000	0.000	0.000	13.20	22.50	0.000	0.000
1300	0.000	0.000	0.000	0.000	17.20	27.10	49.50
1325	0.000	0.000	0.000	0.000	12.80	0.000	0.000
1350	0.000	0.000	0.000	0.000	0.000	17.10	35.70
1400	0.000	0.000	0.000	0.000	0.000	10.10	25.20
1450	0.000	0.000	0.000	0.000	0.000	0.000	17.00
1500	0.000	0.000	0.000	0.000	0.000	0.000	12.20

process. By adding the IG section to the standard Brownian motion, we are dealt with the following algorithm :

## Appendix A: Table A.2. The Algorithms for Simulating the Path of the Pure Jump Model

**Algorithm: (Johnk's generator of Gamma variables)**

- First procedure: we want to generate the Gamma process  $G(t) \sim \text{gamma}(\frac{t}{\nu}, \nu)$ 
  - i. We must generate the tow i.i.d. uniforms  $[0,1]$  random variables  $U, Z$ .
  - ii. Set  $A = U^{\frac{1}{b}}$  and  $B = Z^{\frac{1}{1-b}}$  with  $b = \frac{1}{\nu}$
  - iii. if  $A + B \leq 1$  pass to the next step otherwise back to the first step (i)
  - iv. Generate an exponential random variable  $\exp$
  - v. Return  $G(t) = (\exp A)/(A + B)$
- Second procedure: Now, we put the  $G(t)$  into a Brownian motion
  - i. Generate  $W$  as a standard Brownian motion
  - ii. Return the  $X_{VG}(t, \sigma, \nu, \theta)$
  - i.e.  $X = \theta G(t) + \sigma \sqrt{G(t)} W$

This algorithm is validated if the following condition is satisfied  $\frac{t}{\nu} < 1$ . Which is in general true for the most cases since we can cut the time line in the smallest segments (see [33? ]). The graph A.2.1 shows the path of VG model simulated with above algorithm:

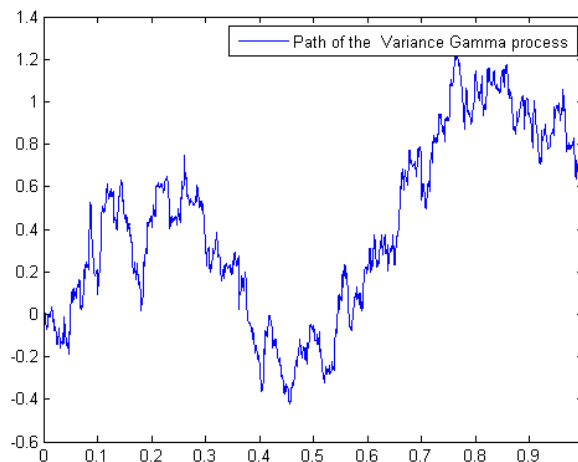


**Figure A.1:** The Path of VG process with  $\nu = 0.0100, \sigma = 0.24, \theta = 0.542$ , the Number of simulation  $N = 1000$ , the time  $T = 1$ .



### A.2.2 The Algorithm for Simulating the Path of NIG processes

The simulation of the path of NIG process is given in the same way as the simulation of the path of VG process. We first need to consider the subordinator part of NIG model which is the Inverse Gaussian process (IG) in order to generate the path of NIG process. The following algorithm gives the process to simulate the path of NIG model. We first generate the path of Inverse Gaussian process and then we plug it into the standard Brownian Motion.

- First procedure: we want to generate the Inverse Gaussian process  
 $(IG)_t \sim NIG(t, \delta \sqrt{\alpha^2 - \beta^2})$ 
  - i. Set  $d = \delta \sqrt{\alpha^2 - \beta^2}$
  - ii. Generate  $V$  as a standard normal random variable
  - iii. Set  $z = V^2$
  - iv. Set  $v = \frac{1}{d}$
  - v. Set  $y = tv + \frac{1}{2}zv^2 - \sqrt{\frac{4tz}{v} + \frac{1}{2}z^2v^2}$
  - iv. Generate  $U$  as a uniform random number
  - ii. if  $U \leq \frac{t}{t+yd}$ , return  $(IG)_t = \frac{t^2}{d^2y}$ , return  $(IG)_t = y$
- Second procedure: Now, we insert  $(IG)_t$  into a Brownian motion
  - i. Generate  $W$  as a  $N(0,1)$  random variable
  - ii. Return the  $X_{NIG}^t$
  - i.e.  $X_{(NIG)}^t = \delta^2 \beta (IG)_t + \delta \sqrt{(IG)_t} W$

The figure A.2.2 below shows the path for NIG processes simulated via the above algorithm: A.2.2.

### A.2.3 The Algorithm for Simulating the Path of the CGMY processes

In general, the density of the CGMY process can not be expressed in a simple form, except for the simple simulation technique. As we said in section 3 the simulation of the path of CGMY model is difficult. Therefore, we need to approximate subordinate part of the CGMY process via the compound Poisson process. Thanks to Dilip and Yor [57], because they were able to calculate the density of the CGMY subordinator and presents it under absolute continuous with  $\alpha$ -stable subordinator. Thus, they apply the rejection technique to approximate the subordinator part of the process.

## Appendix A: Tables. The Algorithms for Simulating the Path of the Pure Jump Model

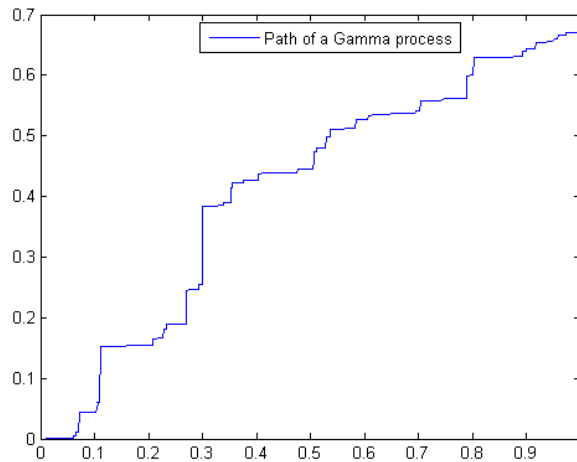


**Figure A.2:** The Path of NIG process with  $\alpha = 12, \beta = 11, \delta = 0.8$ , the Number of simulation  $N = 1000$  and the time  $T = 1$

### A.2.3.1 Key point for the simulation of the CGMY model: The stable process

As said previously, the stable process is a key aspect of simulating the sample paths of the CGMY subordinator. We can define the stable process as follows:

**Definition A.2.1** (Stable process (cont and Tankov [29])). *Let  $X$  be a random variable on  $\mathbb{R}^d$  is said to be stable if it is stable under an addition property: if  $X$  has a stable distribution, means for all  $n > 0, \exists b(n) > 0$  and  $c(n) \in \mathbb{R}^d$  such that:*

$$\Phi_X(y)^n = \Phi_X(yb(n)) \exp\{ic(n)y\}, \quad \forall y \in \mathbb{R}^d. \quad (\text{A.2.1})$$

And when  $X_1, \dots, X_i$  are independent copies of a stable random variable  $X$  and also  $X$  has a stable distribution; therefore,  $\exists c_i > 0$  and a vector  $d \in \mathbb{R}$  such that

$$X_1 + \dots + X_i = c_i X + d. \quad (\text{A.2.2})$$

The above property can only verify at any given time  $t$ , if the distribution of of  $X$  is that of a *selfsimilar Lévy process* ( cont and Tankov [29],pg.105).

It may be shown by (Gennady and Murad [70],corollary 2.1.3), for every stable distribution it exists a constant positive  $\alpha \in ]0,2]$  so that, we can rewrite the value  $b(n)$  in A.2.1 as  $b(n) = n^{1/\alpha}$ . Then, we can refer the stable distribution with index of stability  $\alpha$  as  $\alpha$ -stable distribution ( Cont and Tankov [29],pg.105). If  $X_t$  is a stable Lévy process,

the following equation is evident :

$$X_{at} = \sum_{j=0}^{n-1} X_{(j+1)at/n} - X_{jat/n}. \quad (\text{A.2.3})$$

Using the fact that for every Lévy process, the increments are i.i.d. Therefore, the equation A.2.3 reduces as

$$X_{at} \stackrel{d}{=} \sum_{j=0}^{n-1} X_{jat/n} = X_0 + \dots + X_{(n-1)at/n}, \quad (\text{A.2.4})$$

and applying the stability property A.2.2 to equation A.2.4, it follows:

$$X_{at} \stackrel{d}{=} mX_{at/n} + r, \quad \forall m > 0, \quad \text{and } r \text{ is a vector.} \quad (\text{A.2.5})$$

In general, an  $\alpha$ -stable Lévy process can satisfy this relation up to translation [ [29], pg.106]:

$$(X_{at})_{t \geq 0} \stackrel{d}{=} (a^{1/\alpha} X_t + ct)_{t \geq 0} \quad (\text{A.2.6})$$

where  $a > 0$  and  $c \in \mathbb{R}^d$ . We can say that the family of the stable distribution is defined by a stable Lévy process. And conversely we can say that: the stable distribution is the distribution at any given time of a stable Lévy process and it is also infinitely divisible (Cont and Tankov [29], section 3.7). In the following result we present the characteristic triplet of stable distribution and for all stable Lévy processes:

$$\mu(x) = \frac{a}{x^{1+\alpha}} 1_{x>0} + \frac{b}{|x|^{1+\alpha}} 1_{x<0}, \quad (\text{A.2.7})$$

where the constants  $a > 0$  and  $b > 0$ . We can derive the characteristic function of stable Lévy process using Lévy-Khinchin representation:

$$\phi_X(y) = \begin{cases} \exp \left\{ -\sigma |y| \left( 1 + (i\beta \frac{2}{\pi}) \text{sgn}(y) \log |y| \right) + ivy \right\}, & \text{if } \alpha = 1, \\ \exp \left\{ -\sigma^\alpha |y|^\alpha \left( 1 - (i\beta) \text{sgn}(y) \tan \frac{\pi\alpha}{2} \right) + ivy \right\}, & \text{if } \alpha \neq 1, \end{cases}$$

where  $0 < \alpha \leq 2$ ,  $\mu \in \mathbb{R}$  and

$$\sigma = \frac{a + b}{2} \frac{\Gamma(\frac{\alpha}{2}) + \Gamma(1 - \frac{\alpha}{2})}{\Gamma(1 + \alpha)} \quad (\text{A.2.8})$$

$$\text{and} \quad (\text{A.2.9})$$

$$\beta = \frac{a - b}{a + b}. \quad (\text{A.2.10})$$

## Appendix A: Tables. The Algorithms for Simulating the Path of the Pure Jump Model

The scale parameter  $\beta$  determines the Skewness of the distribution and  $\alpha$  its shape. When we give the specific values to scale parameters  $\beta$  and  $\alpha$ , therefore the  $\alpha$ -stable distribution can be characterised as follows:

- 1 For  $\beta = 0$ , the Gaussian distribution which is symmetric around its mean .
- 2 For  $\beta = 1$ , the Lévy distribution which is concentrated on  $(\mu, \infty)$ .
- 3 For  $\alpha = 1$ , the Cauchy distribution which is symmetric around its mean .
- 4 For  $\alpha = 2$ , the Wiener process.

### A.2.4 Describing the algorithm of CGMY subordinator

First, we need to see that the CGMY process can satisfy all the conditions given in the proposition 2.7.1, in order to relate the two Lévy densities of the CGMY process and a one-sided stable subordinator.

- i The  $\nu_{CGMY}$  Lévy density is absolutely continuous with respect to a density  $\nu(dy)$  (i.e.  $\nu_{CGMY}(0^-) = \nu_{CGMY}(0^+)$ ) and then it can be given by :

$$\nu_{CGMY}(y) = C \frac{e^{Ay-B|y|}}{|y|^{1+Y}} \quad \text{where} \quad A = \frac{G-M}{2}, B = \frac{G+M}{2}. \quad (\text{A.2.11})$$

- ii if we set  $\mu = \frac{G-M}{2}$  we then show  $\nu_{CGMY}(-y)e^{\mu y} = \nu_{CGMY}(y)e^{-\mu y}$ :

$$\begin{aligned} \nu_{CGMY}(-y)e^{\mu y} &= \left\{ \frac{Ce^{My}}{|y|^{1+Y}} 1_{y<0} + \frac{Ce^{-Gy}}{|y|^{1+Y}} 1_{y>0} \right\} \exp\left(\frac{G-M}{2}y\right) \\ &= \frac{Ce^{\frac{G+M}{2}y}}{|y|^{1+Y}} 1_{y<0} + \frac{Ce^{-\frac{G+M}{2}y}}{|y|^{1+Y}} 1_{y>0} \\ &= \frac{Ce^{Gy+\frac{M-G}{2}y}}{|y|^{1+Y}} 1_{y<0} + \frac{Ce^{-My+\frac{M-G}{2}y}}{|y|^{1+Y}} 1_{y>0} \\ &= \left\{ \frac{Ce^{\frac{G}{2}y}}{|y|^{1+Y}} 1_{y<0} + \frac{Ce^{-\frac{M}{2}y}}{|y|^{1+Y}} 1_{y>0} \right\} \exp\left(\frac{M-G}{2}y\right) \\ &= \nu_{CGMY}(y)e^{-\mu y} \end{aligned} \quad (\text{A.2.12})$$

- iii if  $\mu = -M$

$$\begin{aligned} \nu_{CGMY}(\sqrt{u})e^{-\mu\sqrt{u}} &= C \frac{e^{-M\sqrt{u}}}{u^{(1+Y)/2}} e^{M\sqrt{u}} \\ &= \frac{C}{u^{(1+Y)/2}} \end{aligned}$$

is completely monotonic if  $Y > -1$ .

Dilip and Yor [57] were able to give an exact form of the CGMY subordinator by applying the proposition 2.7.2 and related the two Lévy densities of CGMY model and for the one-sided stable subordinator. Thus, we can express a Lévy density of CGMY model in the following proposition.

**Proposition A.2.2.** *Given a subordinator  $(Z_t)_{t \geq 0}$  with its Lévy density expresses as follows :*

$$\nu_{Z_t}(x) = \frac{e^{\frac{x}{2}A^2 - \frac{x}{4}B^2}}{|x|^{1+Y/2}} D_{-Y}(\lambda\sqrt{x}), \quad (\text{A.2.13})$$

where  $D_{-Y}$  represents the parabolic function with index  $\alpha$  and  $A = \frac{G-M}{2}$ ,  $B = \frac{G+M}{2}$ . Thus, the subordinator process  $X_t$  may be expressed as:

$$X_t = aZ_t + W(Z_t) \quad (\text{A.2.14})$$

where  $(W_t)_{t \geq 0}$  is standard Brownian motion and a CGMY process.

This above form A.2.13 is just a simple one, and the original of this form has been produced by (Jérémy and Tankov [64]). The outline of the proof can be found on the paper of Dilip and Yor [57]. On other hand, Dilip and Yor [57] have related a Lévy density of the subordinator with Lévy process of a  $\frac{\alpha}{2}$ -stable subordinator. Which is shown in the following theorem.

**Theorem A.2.3** (Linking between the Lévy density of CGMY subordinator and of  $\frac{\alpha}{2}$ -stable process). *Given a Lévy density of CGMY subordinator  $\nu_{Z_t}$  and  $\nu_{\frac{\alpha}{2}}$  of  $\frac{\alpha}{2}$ -stable process; hence the both densities are linked as follows :*

$$\nu_{z_t}(y) = g(y)\nu_{\frac{\alpha}{2}}(y), \quad (\text{A.2.15})$$

with the continuous function  $g$  is expressed as

$$g(x) = \frac{2^{\frac{Y}{2}} \Gamma(\frac{Y+1}{2}) e^{\frac{x}{2}(A^2 - B^2/2)}}{\sqrt{\pi}} D_{-Y}(B\sqrt{x}), \quad (\text{A.2.16})$$

where  $A = \frac{G-M}{2}$ ,  $B = \frac{G+M}{2}$  and

$$\nu_{\frac{\alpha}{2}}(x) = \frac{C\sqrt{\pi}}{2^{\frac{Y}{2}} \Gamma(\frac{Y+1}{2})} \frac{1_{x>0}}{x^{1+Y/2}} \equiv \frac{K}{x^{1+Y/2}} 1_{x>0}, \quad (\text{A.2.17})$$

where  $g(x) \leq 1$ .

## Appendix A: Tables. The Algorithms for Simulating the Path of the Pure Jump Model

The outline of the proof can be found on the paper of ( Dilip and Yor [57]).

Based in the above result, we can say that the CGMY subordinator is absolutely continuous with  $\frac{\alpha}{2}$ –stable subordinator. Since Dilip and Yor [57] derived the exact form of a Lévy density for CGMY subordinator A.2.15, therefore we only need a technique that will allow us to simulate that exact form. Hence, we can apply the rejection method which has been developed by (Jan Rosinski [67]).

### A.2.4.1 Rosinski Rejection method

The Rejection method can simplify the simulation of the paths of  $\alpha$ –stable subordinator see [67], as the exact form A.2.15 has been written in term of stable subordinator.

**Theorem A.2.4** (Rejection method). *Given a Lévy process  $(X_0(t))_{0 \leq t \leq 1}$  on  $\mathbb{R}^d$  and  $Q_0$  its Lévy measure, which satisfies to the following condition:*

$$\frac{dQ}{dQ_0} \leq 1, \quad (\text{A.2.18})$$

where  $Q$  is related Lévy measure of a Lévy process  $X(t)_{0 \leq t \leq 1}$ . Let  $Z_0$  be a jump process of  $X_0$ , which is represented as

$$Z_0 \stackrel{d}{=} \sum_{k=0}^{\infty} \delta(U_k, J_k^0), \quad (\text{A.2.19})$$

where  $(U_k)_{k \in [1, \infty)}$  is an i.i.d sequence of uniform  $\mathcal{U}[0, 1]$  random variable and  $J_k^0$  is non zeros jumps. Let  $\{B_k\}_{k \geq 0}$  be also an i.i.d. sequence  $\mathcal{U}[0, 1]$  random variable which does not dependent to a couple  $\{U_k, J_k^0\}$ . Then, we can define

$$J_k = \begin{cases} J_k^0 & \text{if } \frac{dQ}{dQ_0} \geq B_k, \\ 0 & \text{otherwise,} \end{cases}$$

Then

$$Z^* \stackrel{d}{=} \sum_{k=0}^{\infty} \delta(U_k, J_k), \quad (\text{A.2.20})$$

where  $Z^*$  represents the market Poisson point process.

The outline of the proof can be found on the papaer of (Jan Rosinski [67]).

The central idea of that theorem is to find a simple way to generate a Lévy process  $X_0$  such that the small number of jumps can be removed in order to find the jumps of  $X$  (Jan Rosinski [67]). Now, we have a clear idea about the rejection method. We only need to approximate the stable subordinator in order to apply the rejection method as a Compound Poisson process.

### A.2.4.2 Application of rejection technique as Compound Poisson process

There are many techniques which can be used to directly simulate the stable process. Moreover, the process can have an infinite number of jumps, therefore to use the rejection method to generate the CGMY subordinator, one needs to approximate the stable subordinator via a compound Poisson process with drift. To achieve this, we would neglect all jumps smaller than  $\epsilon$  with  $\epsilon > 0$  (Jérémy and Tankov [64]). In section 2.5, we express a Lévy density of a compound Poisson process by  $\lambda f(y)$  with  $\lambda$  its intensity and  $f(y)$  the jumps size distribution. We need to make the correct choice of the size distribution  $f$  and intensity  $\lambda$  such that we can link the truncated Lévy measure of the stable process with the approximating compound Poisson process (Jérémy and Tankov [64]). We can then express a truncated Lévy density in the following form:

$$v_\epsilon(y) = \frac{C\sqrt{\pi}}{2^{\frac{Y}{2}}\Gamma(\frac{Y}{2} + \frac{1}{2})} \frac{1_{y>\epsilon}}{|y|^{1+\frac{Y}{2}}} \equiv \frac{K}{y^{1+Y/2}} 1_{y>0}. \quad (\text{A.2.21})$$

We can normalise the above density A.2.21 in order to obtain  $f$ :

$$\begin{aligned} \int_{-\infty}^{\infty} v_\epsilon(x) dx &= \int_{\epsilon}^{\infty} \frac{K}{x^{1+Y/2}} dx = \left[ -\frac{2K}{Yx^{\frac{Y}{2}}} \right]_{\epsilon}^{\infty} \\ &= \frac{2K}{Y\epsilon^{Y/2}} \quad (Y > 0), \end{aligned} \quad (\text{A.2.22})$$

And  $f$  can be expressed as follows:

$$f(y) = \frac{v_\epsilon(y)}{\int_{-\infty}^{\infty} v_x dx} = \frac{Y\epsilon^{Y/2}}{2y^{1+\frac{Y}{2}}} 1_{y>\epsilon}. \quad (\text{A.2.23})$$

Its cumulative density is given by  $F(y)$  :

$$\begin{aligned} F(y) &= \int_{-\infty}^y f(x) dx = \int_{\epsilon}^y \frac{Y\epsilon^{Y/2}}{2x^{1+\frac{Y}{2}}} dx \\ &= \left[ -\frac{\epsilon^{\frac{Y}{2}}}{x^{\frac{Y}{2}}} \right]_{\epsilon}^y = 1 - \frac{\epsilon^{\frac{Y}{2}}}{y^{\frac{Y}{2}}}, \end{aligned} \quad (\text{A.2.24})$$

and  $F^{-1}$  is given

$$F^{-1}(y) = \frac{\epsilon}{(1-y)^{\frac{2}{Y}}} \quad (y > \epsilon > 0). \quad (\text{A.2.25})$$

Thus, we can generate the jump sizes of the approximating using  $\epsilon/U^{\frac{Y}{2}}$  (inverse of the cumulative distribution) where  $U$  is a sequence of uniform distribution and  $\epsilon$  (it is a

## Appendix A: Tables. The Algorithms for Simulating the Path of the Pure Jump Model

very small value). We can choose the expected arrival rate of jumps  $\lambda$  such that  $v_\epsilon(y) = \lambda f(y)$ :

$$\lambda = \frac{2K}{Y\epsilon^{\frac{Y}{2}}}. \quad (\text{A.2.26})$$

In order to improve the precision of the approximation, we have to replace the small jumps which have been lost during the truncated by expected value at a rate :

$$\begin{aligned} \int_0^\epsilon x v_{\frac{Y}{2}}(x) dx &= \int_0^\epsilon \frac{K}{x^{\frac{Y}{2}}} dx \\ &= \left[ \frac{Kx^{1-\frac{Y}{2}}}{1-\frac{Y}{2}} \right]_0^\epsilon = \frac{K\epsilon^{1-\frac{Y}{2}}}{1-\frac{Y}{2}} \equiv d \quad (Y < 2). \end{aligned} \quad (\text{A.2.27})$$

It may be seen that, the truncated can insert the error into the approximation when the  $Y \rightarrow 2$ . Therefore, it may be difficult to quantify such error when it implies on the final process (Jérémy and Tankov [64]). Therefore, we advise that for the value of the  $\epsilon$  to be very smaller or  $10^{-4}$ .

### A.2.4.3 Algorithm to simulate the path of the CGMY processes

Summarising the precedent section A.2.4.2, we could build the algorithm of CGMY processes as follows:

- Setting a time step  $t = C$ , and we take

$$B = \frac{G + M}{2} \quad (\text{A.2.28})$$

$$A = \frac{G - M}{2}. \quad (\text{A.2.29})$$

- Next simulate the one-side stable subordinator at time  $t$ , with a Lévy measure

$$\frac{K}{x^{1+Y/2}} dx.$$

Thus, we take  $\epsilon = 10^{-4}$  and then truncated jump below  $\epsilon$  and replacing them by their expected value :

$$\begin{aligned} d &= \int_0^\epsilon \frac{K}{x^{\frac{Y}{2}}} dx \\ &= \frac{K\epsilon^{1-\frac{Y}{2}}}{1-\frac{Y}{2}} \end{aligned}$$

where  $K$  is defined in A.2.21.



- Next, we determine the arrival rate  $\lambda$  in term of small value  $\epsilon$

$$\begin{aligned}\lambda &= \int_{\epsilon}^{\infty} \frac{K}{x^{\frac{Y}{2}}} dx \\ &= \frac{2K}{Y\epsilon^{\frac{Y}{2}}}.\end{aligned}$$

- The exponential interval jumps times are simulated by

$$t_j = -\frac{1}{\lambda} \log(1 - u_{2j}),$$

where  $u_{2j}$  is an independent uniform sequence.

- The actual jumps sizes are given by

$$\Gamma_i = \sum_{j=1}^i t_j.$$

- The jumps sizes  $y_i$  are given by

$$y_i = \frac{\epsilon}{(1 - u_{1i})^{\frac{2}{Y}}}, \quad (\text{A.2.30})$$

with an independent uniform sequence  $u_{1i}$ .

- Let  $S(t)$  be a process of the stable subordinator defines by:

$$S(t) = dt + \sum_{i=1}^{\infty} y_i 1_{\Gamma_i < t}.$$

- Therefore, we can simulate the CGMY subordinator  $Z_t$  by

$$Z_t = dt + \sum_{i=1}^{\infty} y_i 1_{\Gamma_i < t} 1_{h(y) > u_{3i}}$$

with  $u_{3i}$  representing an independent uniform sequence and  $h(y)$  is a truncated function given by

$$h(y) = e^{-\frac{B^2 y}{2}} \frac{\Gamma(\frac{Y}{2} + 0.5)}{\Gamma(Y)\Gamma(1/2)} 2^Y \left(\frac{B^2 y}{2}\right)^{Y/2} I(Y, B^2 y, \frac{B^2 y}{2}), \quad (\text{A.2.31})$$

where

$$I(Y, 2\lambda, \lambda) = \frac{H_Y(\sqrt{2\lambda})\Gamma(Y)}{(2\lambda)^{Y/2}}.$$

### Appendix A: Tables A.3. Trajectories of pure jump Lévy model via Monte Carlo Method

The function  $H_\beta$  is Hermite function is defined in term of the Confluent Hypergeometric function  $1G_1$ :

$$H_\beta(x) = 2^\beta \left[ \frac{1}{\Gamma(\frac{1-\beta}{2})\Gamma(\frac{1}{2})} 1G_1 \left( \frac{-\beta}{2}, \frac{1}{2}, \frac{x^2}{2} \right) \right] - 2^{\beta/2} \left[ \frac{x}{\sqrt{2}\Gamma(\frac{-\beta}{2})\Gamma(\frac{3}{2})} 1G_1 \left( \frac{1-\beta}{2}, \frac{3}{2}, \frac{x^2}{2} \right) \right].$$

- Finally, the CGMY process is given

$$X = AZ_t + \sqrt{Z_t}W,$$

where  $W$  is standard Brownian motion. The above expression is similar to one given here (Jérémy and Tankov [64]).

In the following figures A.2.4.3 we simulate the paths of CGMY model using the above algorithm. .

### A.3 Trajectories of pure jump Lévy model via Monte Carlo Method

In appendix A we simulated the sample trajectories of the VG, NIG and CGMY models using their algorithms for each model with the random values of the model parameters. Here We want to simulate the trajectories for those models via the Monte Carlo method using the model parameters obtained with the calibration of the S&P 500 indexed options. The figures A.4 and A.5 show the trajectories for each models.

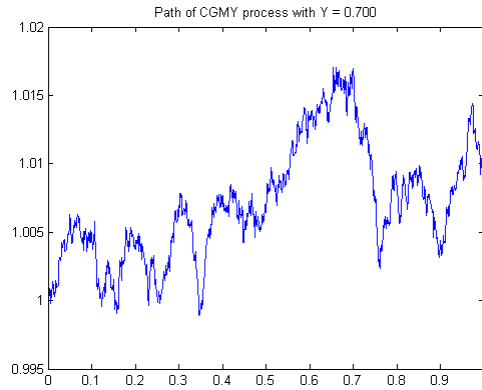
Looking at the figures above, we observe that the trajectories for each model simulate via Monte Carlo method look similar with their trajectories simulated in appendix A based on their algorithms. In the next we present the results of the exotic options computed via Monte Carlo method.

### A.4 Compute the Call Price using the Fast Fourier Transform

In this section, we discuss the method for computing the integral A.4.1 using the FFT algorithm. We want to write the integral 4.4.9 in the form of summation. Carr and Madan[24], and Schoutens [73] describe the method of computing the option prices based on FFT.

The integral of option price below

$$C(k; T) = \frac{\exp(-\alpha k)}{2\pi} \int_{\mathbb{R}} e^{-ivk} \psi(T; v) dv. \quad (\text{A.4.1})$$



The Path of CGMY process with  $Y = 0.7$  the Number of simulation  $N = 1000$ , the time  $T = 1$ .

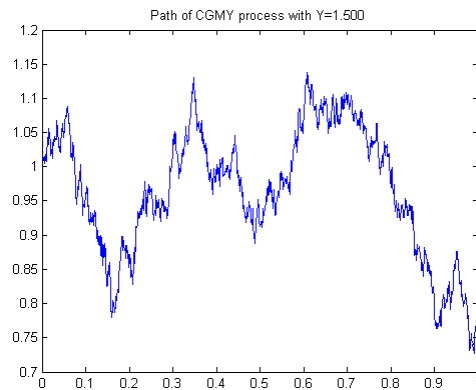


**Figure A.3:** The Path of CGMY process with  $Y = 1.5$  the Number of simulation  $N = 1000$ , the time  $T = 1$

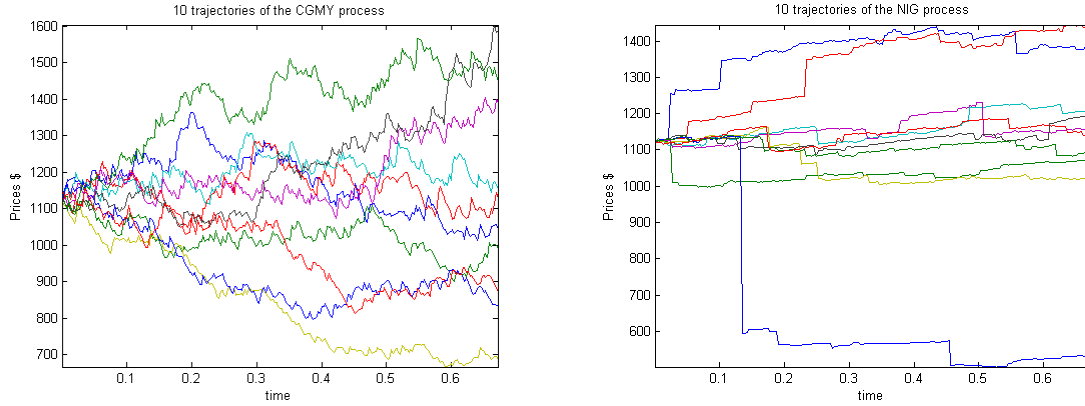
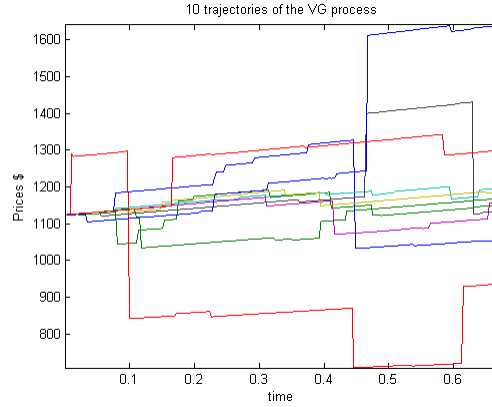
can be computed numerically using Trapezoid rule. To do this, Carr and Madan [24] used the Trapezoid rule for an integral in order to approximate the integral in terms of the summation. Thus, they approximated the integral

$$C(k; T) = \frac{\exp(-\alpha k)}{\pi} \int_0^{\infty} e^{-ivk} \psi(C; v) dv, \quad (\text{A.4.2})$$

on the  $N$  point-grid  $(0, \eta, 2\eta, \dots, (N-1)\eta)$  using the Trapezoid rule as:

$$C(k; T) \simeq \frac{\exp(-\alpha k)}{\pi} \sum_{n=1}^N e^{-iv_n k} \psi(C, v_n) \eta \quad \text{where } v_n = \eta(n-1). \quad (\text{A.4.3})$$

We can compute the value of the above vanilla call formula A.4.3 for  $N$  log-strikes in the


**Figure A.4:** Trajectories of the CGMY and NIG models

**Figure A.5:** Trajectories of the VG model

range of  $-b$  to  $b$  (Schoutens [73], pg.37). We notice that  $b = 0$  if the initial price  $S_0 = 1$ :

$$k_j = -b + \lambda(j-1) \quad \text{where, } j = 1, \dots, N \quad \text{and} \quad \lambda = \frac{2b}{N}.$$

Thus, we can rewrite the summation 4.1 as follows:

$$C(k_j; T) \simeq \frac{\exp(-\alpha k_j)}{\pi} \sum_{n=1}^N e^{-iv_n(-b+\lambda(j-1))} \psi(v_n) \eta, \quad (\text{A.4.4})$$

$$\simeq \frac{\exp(-\alpha k_j)}{\pi} \sum_{n=1}^N e^{(-i\eta\lambda(n-1)(j-1))} e^{iv_n b} \psi(v_n) \eta. \quad (\text{A.4.5})$$

When the values of  $\eta$  and  $\lambda$  are chosen such that  $\eta\lambda = \frac{2\pi}{N}$ , we obtain

$$C(k_j; T) \simeq \frac{\exp(-\alpha k_j)}{\pi} \sum_{n=1}^N e^{(-i\frac{2\pi(n-1)(j-1)}{N})} e^{iv_n b} \psi(v_n) \eta. \quad (\text{A.4.6})$$

The above summation A.4.6 is an exact application of FFT on the vector  $(\exp(iv_nb)\Psi(v_n)\eta, n = 1, \dots, N)$ . When we set  $\eta\lambda = \frac{2\pi}{N}$ , and also consider the smaller value of  $\eta$ . We observe that the grid-size  $\lambda$  for the log-strike grid are become larger [Carr and Madan [73],pg.37].

Carr and Madan [24] proposed that Simpson's rule weightings can be applied in the summation A.4.6 on the  $N$  grid-space  $(0, \eta, 2\eta, \dots, (N-1)\eta)$ . In order to obtain an accurate integration on a large value of  $\eta$ . Applying the Simpson's rule weightings and the summation A.4.6 can be approximated by:

$$C(k_j; T) \simeq \frac{\exp(-\alpha k_j)}{\pi} \sum_{n=1}^N e^{iv_nb} \psi(v_n) \eta \left( \frac{3 + (-1)^n - \delta_{n-1}}{3} \right) \quad (\text{A.4.7})$$

where the value  $\delta_n$  represents an indicator function whose the value is 1 for  $n = 0$  and zero otherwise.

## List of references

- [1] <http://www.global-derivatives.com/index.php/component/content/32?task=view>.
- [2] [http://en.wikipedia.org/wiki/Quantitative\\_analyst](http://en.wikipedia.org/wiki/Quantitative_analyst).
- [3] <http://ocw.mit.edu/courses/mathematics/18-443-statistics-for-applications-fall-2006/lecture-notes/lecture14.pdf>.
- [4] [http://www.mathwave.com/articles/goodness\\_of\\_fit.html](http://www.mathwave.com/articles/goodness_of_fit.html).
- [5] [http://www.riskglossary.com/link/path\\_dependence.htm](http://www.riskglossary.com/link/path_dependence.htm).
- [6] <http://www.springerreference.com/docs/html/chapterdbid/205395.html>.
- [7] John Aldrich et al. Ra fisher and the making of maximum likelihood 1912-1922. *Statistical Science*, 12(3):162–176, 1997.
- [8] Theodore W Anderson and Donald A Darling. A test of goodness of fit. *Journal of the American Statistical Association*, 49(268):765–769, 1954.
- [9] David Applebaum. Lévy processes: From probability to finance and quantum groups. *Notices of the AMS*, 51(11):1336–1347, 2004.
- [10] Mikosch Bandoff-Nielsen, O and Resnick. Lévy processes; theory and applications, 2001.
- [11] Karl F Bannör and Matthias Scherer. Model risk and uncertainty-illustrated with examples from mathematical finance. In *Risk-A Multidisciplinary Introduction*, pages 279–306. Springer, 2014.
- [12] Ole E Barndorff-Nielsen. Processes of Normal Inverse Gaussian type. *Finance and stochastics*, 2(1):41–68, 1997.

- 
- [13] Jean Bertoin. *Lévy Processes*, volume 121. Cambridge university press, 1998.
- [14] Erik Bølviken and Fred Espen Benth. Quantification of risk in Norwegian stocks via the normal inverse Gaussian distribution. February 01, date, 2000.
- [15] Jean-Philippe Bouchaud and Marc Potters. *Theory of financial risk and derivative pricing: from statistical physics to risk management*. Cambridge university press, 2003.
- [16] George EP Box and Norman R Draper. *Empirical model-building and response surfaces*. John Wiley & Sons, 1987.
- [17] George EP Box, Gwilym M Jenkins, and Gregory C Reinsel. *Time series analysis: forecasting and control*. John Wiley & Sons, 2013.
- [18] Svetlana I Boyarchenko and SERGEI Z LEVENDORSKII. Option pricing for truncated Lévy processes. *International Journal of Theoretical and Applied Finance*, 3(03):549–552, 2000.
- [19] Svetlana I Boyarchenko and Sergei Z Levendorskii. *Non-Gaussian Merton-Black-Scholes Theory*, volume 9. World Scientific, 2002.
- [20] Svetlana I Boyarchenko and SZ Levendorskii. Generalizations of the Black-Scholes equation for truncated Lévy processes. *Working paper Boyarchenko Generalizations of the Black-Scholes equation for truncated Lévy processes* 1999, 1999.
- [21] Douglas T Breeden and Robert H Litzenberger. Prices of state-contingent claims implicit in option prices. *Journal of business*, pages 621–651, 1978.
- [22] Peter J Brockwell and Richard A Davis. *Introduction to time series and forecasting*, volume 1. Taylor & Francis, 2002.
- [23] Peter Carr, Hélyette Geman, Dilip B Madan, and Marc Yor. Stochastic volatility for Lévy processes. *Mathematical Finance*, 13(3):345–382, 2003.
- [24] Peter Carr and Dilip Madan. Option valuation using the fast Fourier transform. *Journal of computational finance*, 2(4):61–73, 1999.
- [25] Carr.P, Hélyette Geman, Madan.Dilip B, and Marc Yor. The Fine Structure of Asset Returns: An Empirical Investigation\*. *The Journal of Business*, 75(2):305–333, 2002.
- [26] Rama Cont. Model uncertainty and its impact on the pricing of derivative instruments. *Mathematical finance*, 16(3):519–547, 2006.

- 
- [27] Rama Cont, Jose da Fonseca, and Valdo Durrleman. Stochastic models of implied volatility surfaces. *Economic Notes*, 31(2):361–377, 2002.
- [28] Rama Cont, Marc Potters, and Jean-Philippe Bouchaud. Scaling in stock market data: stable laws and beyond. In *Scale invariance and beyond*, pages 75–85. Springer, 1997.
- [29] Rama Cont and Peter Tankov. *Financial modelling with jump processes*, volume 133. Chapman & Hall/CRC Boca Raton, 2004.
- [30] Rama Cont, Peter Tankov, et al. Non-parametric calibration of jump-diffusion option pricing models. *Journal of computational finance*, 7(3):1–50, 2004.
- [31] Rama Cont, Peter Tankov, et al. Non-parametric calibration of jump-diffusion option pricing models. *Journal of computational finance*, 7(3):1–50, 2004.
- [32] Emanuel Derman and Paul Wilmott. Perfect models, imperfect world. *Business Week*, 59, 2009.
- [33] Damien Deville. On Lévy Processes for Option Pricing: Numerical Methods and Calibration to Index Options. 2007.
- [34] Bruno Dupire. *Pricing and hedging with smiles*. Mathematics of derivative securities. Dempster and Pliska eds., Cambridge Uni. Press, 1997.
- [35] Ernst Eberlein and Jean Jacod. On the range of options prices. *Finance and Stochastics*, 1(2):131–140, 1997.
- [36] Nicole El Karoui and Marie-Claire Quenez. Dynamic programming and pricing of contingent claims in an incomplete market. *SIAM journal on Control and Optimization*, 33(1):29–66, 1995.
- [37] Sergio M Focardi and Frank J Fabozzi. *The mathematics of financial modeling and investment management*, volume 138. John Wiley & Sons, 2004.
- [38] Hélyette Geman. Pure Jump Lévy Processes for Asset Price Modelling. *Journal of Banking & Finance*, 26(7):1297–1316, 2002.
- [39] Helyette Geman, Dilip Madan, and Marc Yor. Asset prices are Brownian motion: only in business time. *Quantitative analysis in financial markets*, 2:103–146, 2001.
- [40] Iosif Il'ich Gikhman and Anatoliï Skorokhod. *Introduction to the theory of random processes*.



- 
- [41] Paul Glasserman. *Monte Carlo methods in financial engineering*, volume 53. Springer, 2004.
- [42] Alok Gupta, Christoph Reisinger, and Alan Whitley. Model uncertainty and its impact on derivative pricing. *Rethinking Risk Management and Reporting: Uncertainty, Bayesian Analysis and Expert Judgement*. Risk Books, 2010.
- [43] Patrick S Hagan, Deep Kumar, Andrew S Lesniewski, and Diana E Woodward. Managing smile risk. *The Best of Wilmott*, page 249, 2002.
- [44] Andrew G Haldane and Vasileios Madouros. The dog and the frisbee. In *Speech presented at the Federal Reserve Bank of Kansas City—Jackson Hole economic policy symposium*, 2012.
- [45] J Michael Harrison and Stanley R Pliska. Martingales and stochastic integrals in the theory of continuous trading. *Stochastic processes and their applications*, 11(3):215–260, 1981.
- [46] John Hull. *Options, futures and other derivatives*. Pearson education, 2009.
- [47] Albyn Jones. Math 141: Quantile-Quantile Plots.
- [48] Jeroen Kerkhof, JM Schumacher, and Bertrand Melenberg. Model risk and regulatory capital. *Available at SSRN 301531*, 2002.
- [49] Joerg Kienitz and Daniel Wetterau. *Financial Modelling: Theory, Implementation and Practice with MATLAB Source*. John Wiley & Sons, 2012.
- [50] Frank H Knight. Risk, uncertainty and profit. *New York: Hart, Schaffner and Marx*, 1921.
- [51] Ismo Koponen. Analytic approach to the problem of convergence of truncated Lévy flights towards the gaussian stochastic process. *Physical Review E*, 52(1):1197, 1995.
- [52] Andreas Kyprianou. *Introductory Lectures on Fluctuations of Lévy processes with Applications (Universitext)*. Springer, 2006.
- [53] Andreas Kyprianou, Wim Schoutens, and Paul Wilmott. *Exotic option pricing and advanced Lévy models*. John Wiley & Sons, 2006.
- [54] STEVEN P. LALLEY. Lévy processes, Stable processes, and Subordinators. <http://galton.uchicago.edu/~lalley/Courses/385/LevyProcesses.pdf>.

- 
- [55] Paul Lévy. Sur les intégrales dont les éléments sont des variables aléatoires indépendantes. *Annali della Scuola Normale Superiore di Pisa-Classe di Scienze*, 3(3-4):337–366, 1934.
- [56] Dilip B Madan, Peter P Carr, and Eric C Chang. The Variance Gamma process and option pricing. *European finance review*, 2(1):79–105, 1998.
- [57] Dilip B Madan and Marc Yor. Representing the CGMY and Meixner Lévy processes as time changed Brownian motions. *Journal of Computational Finance*, 12(1):27, 2008.
- [58] Andrew Matacz. Financial modeling and option theory with the truncated Lévy process. *International Journal of Theoretical and Applied Finance*, 3(01):143–160, 2000.
- [59] Yoshio Miyahara. A note on Esscher transformed martingale measures for geometric Lévy processes. *Discussion Papers in Economics, Nagoya City University*, 379:1–14, 2004.
- [60] In Jae Myung. Tutorial on maximum likelihood estimation. *Journal of Mathematical Psychology*, 47(1):90–100, 2003.
- [61] Laurent Nguyen-Ngoc. Exotic options in general exponential Lévy models. *Prépublication, Universités Paris*, 6, 2003.
- [62] B Otto. *Linear algebra with applications*. Third Eddition, 1995.
- [63] Antonis Papapantoleon. An introduction to Lévy processes with applications in finance. *arXiv preprint arXiv:0804.0482*, 2008.
- [64] Jérémy Poirot and Peter Tankov. Monte Carlo option pricing for tempered stable (CGMY) processes. *Asia-Pacific Financial Markets*, 13(4):327–344, 2006.
- [65] Narahari U Prabhu. *Stochastic storage processes: queues, insurance risk, and dams, and data communication*, volume :15. Springer, 1998.
- [66] Riccardo Rebonato. *Volatility and Correlation in the Pricing of Equity, FX, and Interest-rate Options*. John Wiley, 1999.
- [67] Jan Rosiński. Series representations of Lévy processes from the perspective of point processes. In *Lévy processes*, pages 401–415. Springer, 2001.
- [68] Tina Hviid Rydberg. The normal inverse Gaussian Lévy process: simulation and approximation. *Communications in statistics. Stochastic models*, 13(4):887–910, 1997.

- 
- [69] Tina Hviid Rydberg. Generalized hyperbolic diffusion processes with applications in finance. *Mathematical Finance*, 9(2):183–201, 1999.
- [70] Gennady Samorodnitsky and Murad S Taqqu. Stable NON-GAUSSIAN RANDOM PROCESSES. *Econometric Theory*, 13:133–142, 1997.
- [71] Ken-Iti Sato. *Lévy processes and infinitely divisible distributions*. Cambridge university press, 1999.
- [72] Wim Schoutens. *Lévy Processes in Finance: Pricing financial derivatives*. 2003.
- [73] Wim Schoutens. The World of VG. In M. Vanmaele, D. Deelstra, A. De Schepper, J. Dhaene, en P. Van Goethem, editors, *Handelingen Contactforum Actuarial and Financial Mathematics Conference, pagina's*, pages 3–54, 2008.
- [74] Wim Schoutens, Erwin Simons, and Jurgen Tistaert. A perfect calibration! now what? *70+ DVD's FOR SALE & EXCHANGE*, page 281, 2003.
- [75] Wim Schoutens, Erwin Simons, and Jurgen Tistaert. Model risk for exotic and moment derivatives. *Exotic Option Pricing and Advanced Lévy Models*, (Wiley), to appear, 2005.
- [76] Steven E Shreve. *Stochastic calculus for finance II: Continuous-time models*, volume 11. Springer, 2004.
- [77] Mike Tso. Multivariate Statistical Methods. [http://www.maths.manchester.ac.uk/~mkt/MT3732\(MVA\)/Notes/MVA\\_Section3.pdf](http://www.maths.manchester.ac.uk/~mkt/MT3732(MVA)/Notes/MVA_Section3.pdf). [Online; accessed January 28,2015].
- [78] Jianwei Zhu. *Applications of Fourier transform to smile modeling: Theory and implementation*. Springer Science & Business Media, 2009.